

178

NASA CONTRACTOR REPORT



NASA CR-120

NASA CR-120

FACILITY FORM 602

164 32434
(ACCESSION NUMBER)
122
(PAGES)
(NASA CR OR TNA OR AD NUMBER)

(THRU)
1
(CODE)
27
(CATEGORY)

SELF-SEALING STRUCTURES FOR CONTROL OF THE METEOROID HAZARD TO SPACE VEHICLES

*by Philip J. D'Anna, Roger M. Heitz,
and James J. Piechocki*

Prepared under Contract No. NASr-102 by
NORTHROP SPACE LABORATORIES
Hawthorne, Calif.
for

NATIONAL AERONAUTICS AND SPACE ADMINISTRATION • WASHINGTON, D. C. • OCTOBER 1964

SELF-SEALING STRUCTURES FOR CONTROL OF THE
METEOROID HAZARD TO SPACE VEHICLES

By Philip J. D'Anna , Roger M. Heitz, and James J. Piechocki

Distribution of this report is provided in the interest of
information exchange. Responsibility for the contents
resides in the author or organization that prepared it.

Prepared under Contract No. NASr-102 by
NORTHROP SPACE LABORATORIES
Hawthorne, California

for

NATIONAL AERONAUTICS AND SPACE ADMINISTRATION

For sale by the Office of Technical Services, Department of Commerce,
Washington, D.C. 20230 -- Price \$2.75

FOREWORD

This Summary Report was prepared by Northrop Space Laboratories, Hawthorne, California, under NASA Contract NASr-102. The contract is administered by the Office of Advanced Research and Technology, Structures Research Group, Space Vehicle Division, with Mr. Norman Mayer as Project Monitor.

Principal authors of this report are P. J. D'Anna and Dr. R. M. Heitz, Co-Principal Investigators, and J. J. Piechocki, all of Space Materials Laboratory; Dr. R. D. Johnson, Laboratory Head. Other contributors to this program include R. K. Jenkins, R. W. Hunter, J. K. Magill, Dr. B. Arden, Dr. A. Caron and T. W. Brown of the Space Materials Laboratory, R. Hornung of NSL Structural Analysis Branch, M. Garman of Northrop's Nortronics Division and Prof. G. V. Bull of McGill University.

This summary report, written in two parts, describes performance of the period from 1 April 1963 through 31 March 1964. Part I reports the results of the program related to self-sealing panels and their evaluation. Shock wave damage control was found to be essential to obtaining effective sealing, particularly in the chemically activated self-sealing panel configurations. Part II reports the results from an investigation and development of shock wave damage control techniques under conditions resulting from high velocity particle penetration into liquid-filled compartments. In addition, Part II includes the results of an investigation of the mechanical and chemical phenomena associated with high velocity particle penetration into fluid-filled compartments. Part II has been classified Confidential.

This report is documented at Northrop Space Laboratories as NSL 62-132-7 (Part I).

TABLE OF CONTENTS

<u>SECTION</u>	<u>PAGE</u>
1.0 INTRODUCTION AND SUMMARY.....	1
2.0 COMPARATIVE EVALUATION OF SELF-SEALING CONCEPTS.....	6
2.1 Summary of Test Results.....	6
2.2 Conclusions and Recommendations.....	16
3.0 TECHNICAL DISCUSSION AND ANALYSIS.....	20
3.1 High Velocity Particle Penetration Into Compartments Containing Nearly Incompressible Medium....	20
3.2 Perforation of Composite Structures.....	25
3.3 Material Selection and Evaluation.....	29
3.4 Temperature Dependence of Self-Sealing Capability	56
4.0 EXPERIMENTAL PROGRAM.....	60
4.1 Equipment and Testing Procedure.....	60
4.2 Mechanical Self-Sealing Concepts.....	65
4.2.1 Elastomer Sphere Concept.....	65
4.2.2 Fiber Mat Concept.....	71
4.3 Combined Mechanical and Chemical Self-Sealing Concepts.....	73
4.3.1 RTV Silicone Elastomer/Fiber Mat or Rubber Spheres or Air Gap Concept.....	73
4.3.2 Rigid Silicone Foam/Fiber Mat or Rubber Spheres Concept.....	81
4.3.3 Flexible Silicone Foam/Fiber Mat or Rubber Spheres Concept.....	89
4.3.4 Silicone Foam/Balsa Wood Concept.....	93
4.3.5 Elastomeric Spheres/Viscous Face Concept..	100
4.3.6 Rigid Silicone Foam/Air Gaps Concept.....	102
4.3.7 Rigid Silicone Foam/Rubber Spheres/Air Gap Concept.....	105

TABLE OF CONTENTS

<u>SECTION</u>	<u>PAGE</u>
5.0 REFERENCES.....	107
APPENDIX A - STATE OF MATERIAL SUBJECTED TO IMPACT SHOCK.....	A-1

LIST OF ILLUSTRATIONS

<u>FIGURE</u>		<u>PAGE</u>
3-1	Ruptured Honeycomb Core-Elastomer Panel	21
3-2	Ruptured Aluminum Panel (Water-Filled Tank)	22
3-3	Approximate Solution of Shock Pressure in Chemical Compartment	24
3-4	Combined Concept-Rigid Silicone Foam or RTV 60 Silicone Elastomer/Fiber Mat or Rubber Spheres Concept - Configuration	33
3-5	Polyurethane Foam + Fiber Mat Concepts Combined - Configuration	47
3-6	Combined Concept - Rigid Silicone Foam/Fiber Mat Concept - Configuration	52
3-7	Balsa Wood/Silicone Foam Concept	53
3-8	Rigid Silicone Foam/Air Gaps Concept - Configuration	54
4-1	Northrop Particle Accelerator	61
4-2A	Northrop Corporation-Light Gas Gun Facility (Vacuum Chamber)	63
4-2B	Northrop Corporation-Light Gas Gun Facility	64
4-3	Gun Facility for Ballistic Testing of Heated and Cooled Targets in a High Vacuum	66
4-4	Self-Sealing Panel-Elastomer Sphere Concept	68
4-5	Punctured Elastomer Sphere Self-Sealing Panel Configuration	69
4-6	Fiber Mat Panel Configuration	72
4-7	Combined Concept-RTV Silicone Elastomer/Fiber Mat Concept Configuration	74
4-8	Combined Concept-RTV Silicone Elastomer/Rubber Spheres Concept-Configuration	77
4-9	RTV Silicone Elastomer/Air Gap Concept	79
4-10	Ruptured Aluminum Faced Self-Sealing Panel (RTV Silicone Elastomer/Air Gap Concept)	80
4-11	Self-Sealing Mechanism-Rigid Silicone Foam/Fiber Mat Concept	84
4-12	Combined Concept-Rigid Silicone Foam/Fiber Mat Concept	85

LIST OF ILLUSTRATIONS

<u>FIGURE</u>		<u>PAGE</u>
4-13	Combined Concept-Rigid Silicone Foam/Rubber Spheres Concept-Configuration	87
4-14	Combined Concept-Flexible Silicone Foam/Rubber Spheres Concept Configuration	90
4-15	Self-Sealing Mechanism-Flexible Silicone Foam/Rubber Spheres Concept	91
4-16	Combined Concept-Flexible Silicone Foam/Fiber Mat Concept-Configuration	92
4-17	Balsa Wood/Silicone Foam Concept	94
4-18	Internal Foaming in Panel B-1	95
4-19	Internal Foaming in Panel B-4	98
4-20	Elastomer Spheres/Viscous Face Concept-Configuration I	101
4-21	Elastomer Spheres/Viscous Face Concept-Configuration II	103
4-22	Rigid Silicone Foam/Air Gaps Concept-Configuration	104
4-23	Combined Concept-Rigid Silicone Foam/Rubber Spheres/ Air Gap-Configuration	106

LIST OF TABLES

<u>TABLE</u>		<u>PAGE</u>
2-1	Comparative Evaluation of Self-Sealing Panel Concepts	7
4-1	Summary of Calculations	99

LIST OF ILLUSTRATIONS FOR APPENDIX A

<u>FIGURE</u>		<u>PAGE</u>
A-1	Analytical Model of One-Dimensional Impact Conditions	A-2
A-2	Graphical Solution to Impact Problems	A-6
A-3	Shock Solution: Two-Layered Target	A-6

1.0 INTRODUCTION AND SUMMARY

The recent limited findings from satellite experiments, although confirming the existence of a "meteoroid environment," have not as yet resolved the various conflicting opinions concerning the exact nature of the environment or the magnitude of its hazard to space vehicles. However, it is generally agreed by most investigators that, due to their extremely high velocities, meteoroids do present a real hazard to manned space vehicles, particularly those destined for long duration missions.

Among techniques proposed for minimizing this hazard, the bumper shield or spaced sheet structure concept has been the one most frequently proposed by space vehicle designers. In this concept, the bumper fragments the meteoroid while the resulting spray of particles is hopefully stopped by the inner shell. However, although it has been shown that this configuration can be highly effective in preventing the spray of impact induced particles into the interior of a space vehicle compartment, damage to the inner shell by the more energetic meteoroids may be severe enough to cause fluid leakage from pressurized compartments. Therefore, although the bumper shield concept may provide adequate protection for limited short duration missions, our proposed self-sealing structures guarantee the sealed integrity of a pressurized compartment, and provide the "fail-safe" capability required for the more ambitious space missions.

The implications, therefore, appear obvious--that, for long duration space missions, more reliable techniques than those currently proposed need to be evaluated.

With this objective in mind, Northrop has been proposing the philosophy of the self-sealing structure. In pursuance of this approach, various structural concepts have been developed and experimentally evaluated in

which the best features of the bumper shield concept have been combined with a self-sealing inner shell to give a system possessing high penetration resistance, shock wave damage control and self-sealing capability.

During the first year of effort on this two year program, as summarized in Reference 1, various self-sealing structure concepts were investigated. Out of this initial program, five successful self-sealing panel configurations were fabricated and their self-sealing capabilities experimentally demonstrated by puncturing with 1/8-inch diameter steel and glass spheres at impact velocities to 7,000 fps.

Both mechanical and chemically activated self-sealing concepts were evaluated. The principle of operation of the mechanical concepts depends upon either the mechanical response of elastomer materials in rebounding upon being punctured and sealing the hole, or on the forces generated by the pressure differential across a puncture in a pressurized compartment in drawing a rubber sphere or other sealing element into the hole and effecting a seal. The working principle of the chemically activated concepts depends on the penetrating particle causing the intermixing of two initially separated chemical constituents so that the ensuing chemical reaction will cause one of the constituents (an easy flowing elastomer) to cure and form a solid mass along the pellet entry path and to effect a seal.

During the latter part of the first year's program, some limiting hypervelocity testing of these initial self-sealing panel configurations was conducted at NASA Ames Research Center in an attempt to verify results obtained at 7,000 fps. Detailed results of these tests, which were conducted with 1/8-inch diameter glass spheres at impact velocities to 23,000 fps, are given in Reference 1. Initial results from these tests were not completely conclusive in that only two of the five panels tested were perforated. However, examination of the impacted panels indicated

that shock wave effects at these higher velocities increase panel damage and material removal along the pellet entry path, thereby making it more difficult to achieve self-sealing action.

Based on these initial high velocity tests, it was concluded that those concepts where sealing capability was dependent solely upon the mechanical response of elastomeric materials would not seal at the higher puncturing velocities and, for the other concepts, shock wave damage control would be a primary prerequisite for obtaining successful self-sealing action. In view of this, the second year's program was oriented towards obtaining shock wave damage control in those concepts where initial results indicated promise of successful self-sealing action at impact velocities above 7,000 fps.

During the past year, the major effort has been directed to the following tasks:

1. Ballistic testing and concept evaluation at impact velocities from 10,000 to 26,000 fps.
2. Investigation of techniques for control of shock wave damage and material removal during high velocity puncturing. The following techniques were investigated:
 - Using composite non-metallic face sheets.
 - Isolating the chemical compartments of the chemically activated configurations from the panel face sheets or interposing a highly compressible material between the chemical compartment wall and the face sheets.
 - Incorporating a volume increasing mechanism (e.g., foaming reaction) in those configurations sensitive to material removal.

- Combining the best features of two or more concepts to give greater effective sealing action against the more severe type of high velocity impact damage.

The incorporation of one or more of these techniques has resulted in the development of nine basic panel configurations that have successfully maintained their self-sealing capability when punctured with 1/8-inch diameter steel spheres at impact velocities from 10,000 fps to 26,000 fps. The techniques used for self-sealing the panels are either mechanical (elastomer spheres), chemical (uncured elastomers or foaming resins) or combined mechanical and chemical (elastomer spheres or asbestos fibers plus a chemical system). The mechanical elastomer sphere concept, although not giving complete sealing action (air leakage rate of 1.3 lbs/day for a $\Delta p = 14.7$ psi), added the lowest weight to a double wall panel (0.31 lbs/ft²). The chemical or combined mechanical-chemical concepts, with the exception of one configuration (see panel configuration I, Table 2-1), gave complete sealing action (zero leakage rate) when tested at impact velocities of 10,000 fps and above. The weight for these concepts varied from 1.24 lbs/ft for the Elastomer Sphere-Viscous Face Concept to 3.44 lbs/ft² for the Rigid Foam-Balsa Wood concept. A comparative evaluation of the various self-sealing panel configurations tested is given in Section 2.0 while panel construction details and other phases of the program are given in the subsequent sections.

As an additional task during this year's program, some exploratory experiments were conducted in which water-filled tanks were penetrated with high velocity particles. The purpose of this investigation was to evaluate techniques for preventing explosive rupturing of the penetrated tank wall under ballistic conditions normally creating such failures. Certain techniques have been developed whereby explosive rupturing of water-filled tanks may be prevented for ballistic conditions creating

failure without the incorporation of these techniques. Details of these techniques and a summary of test results may be found in Part II of this report, which has been classified CONFIDENTIAL.

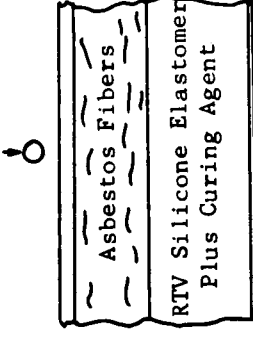
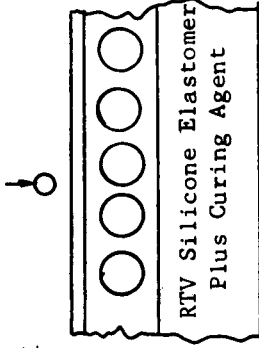
2.0 COMPARATIVE EVALUATION OF SELF-SEALING CONCEPTS

2.1 SUMMARY OF TEST RESULTS

Subject to the limitations imposed by the absence of test data above 20,000 fps for some of the concepts listed, Table 2-1 presents a preliminary comparative evaluation of the most successful self-sealing panel configurations resulting from this program. Experience with those configurations for which test data above 20,000 fps exist, indicates that it is reasonable to assume that panel configurations which successfully seal at impact velocities between 10,000 and 15,000 fps will retain their sealing capability at velocities in the range of 20,000 fps.

The ballistic conditions listed are the most severe, to date, under which each concept has been tested. For those concepts which successfully sealed at 7,000 fps, but failed at higher impact velocities, both velocities are recorded. The sealability or self-sealing effectiveness of each configuration was determined by checking for air leakage, across the puncture, against a pressure differential of one atmosphere (14.7 psi). The unit weight which was added to a basic double wall panel in order to give it self-sealing capability is given in Column 4 of Table 2-1 while the total panel unit weight is given in Column 5. In reference to these weights, it must be noted that the configurations tested during this program were basically "breadboard models" in which the primary purpose was to evaluate the various self-sealing concepts, and to experimentally demonstrate their feasibility with no serious attempts made to optimize the panels for minimum weight. However, examinations of the results from the test program indicates that the panel configurations, as currently fabricated, can be substantially reduced in weight without sacrificing their self-sealing capability. The chemically activated concepts in particular have consistently demonstrated an amount of chemical activity, upon panel puncture, in excess of that required to obtain effective sealing. Consequently, it

TABLE 2-1 - COMPARATIVE EVALUATION OF SELF-SEALING PANEL CONCEPT

Panel Configuration	Ballistic Test Conditions @ T = 70-75°F and ΔP = ~14.7 psi	Air Leakage Rate thru Punctured Panel @ ΔP = ~14.7 psi (lbs/day)	Panel Unit Wt. Less Face Sheets (lbs/ft ²)	Panel Unit Wt. With Face Sheets (lbs/ft ²)	Remarks
<p>I</p>  <p>RTV Silicone Elastomer/ Fibermat Concept See Section 4.3.1 for panel details</p>	1/8" Dia. Steel @ 26,000 fps	3	3.02	4.14	<p>1. Extensive cracks in pellet exit face resulted in slight air leakage around the sealing plug of cured elastomer</p> <p>2. Test conducted at McGill University</p>
<p>II</p>  <p>RTV Silicone Elastomer/ Rubber Sphere Concept See Section 4.3.1 for panel details</p>	1/8" Dia. Steel @ 19,000 fps*	Panel not completely penetrated	3.07	4.19	<p>1. Panel weight based on using four 3/8 inch dia. spheres per square inch of panel.</p> <p>2. Test conducted at McGill University</p>

*Velocity estimated from crater formed in blast shield by sabot.

TABLE 2-1 - COMPARATIVE EVALUATION OF SELF-SEALING PANEL CONCEPTS

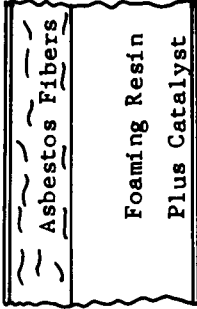
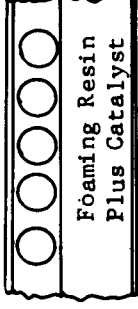
Panel Configuration	Ballistic Test Conditions @ T = 70-75°F and ΔP = ~ 14.7 psi	Air Leakage Rate thru Punctured Panel @ ΔP = ~ 14.7 psi (lbs/day)	Panel Unit Wt. Less Face Sheets (lbs/ft ²)	Panel Unit Wt. With Face Sheets (lbs/ft ²)	Remarks
III 	1/8" Dia. Steel @ 23,000 fps	0	2.74	3.86	1. Test conducted at McGill University
Rigid Silicone Foam/Fibermat Concept See Section 4.3.2 for panel details					
IV 	1/8" Dia. Steel @ 12,000 fps	0	2.79	3.91	1. Panel weight based on using four 3/8-inch dia. spheres per square inch of panel 2. Test conducted at Northrop
Rigid Silicone Foam/Rubber Sphere Concept See Section 4.3.2 for panel details					

TABLE 2-1 - COMPARATIVE EVALUATION OF SELF-SEALING PANEL CONCEPTS

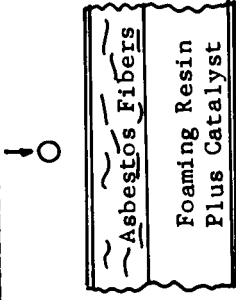
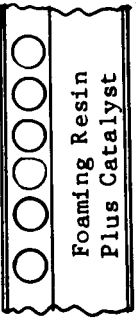
Panel Configuration	Ballistic Test Conditions @ T = 70-75°F and ΔP = ~14.7 psi	Air Leakage Rate thru Punctured Panel @ ΔP = 14.7 psi (lbs/day)	Panel Unit Wt. Less Face Sheets (lbs/ft ²)	Panel Unit Wt. With Face Sheets (lbs/ft ²)	Remarks
<p>V</p>  <p>Flexible Silicone Foam/Fiber Mat Concept</p> <p>See Section 4.3.3 for panel details</p>	1/8" Dia. Steel @ 7,000 fps	0	2.74	3.86	1. Test conducted at Northrop
<p>VI</p>  <p>Flexible Silicone Foam/ Rubber Sphere Concept</p> <p>See Section 4.3.3 for panel details</p>	1/8" Dia. Steel @ 12,000 fps	0	2.79	3.91	1. Panel weight based on using four 3/8-inch diameter spheres per square inch of panel 2. Test conducted at Northrop

TABLE 2-1 - COMPARATIVE EVALUATION OF SELF-SEALING PANEL CONCEPTS

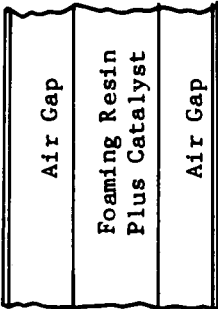
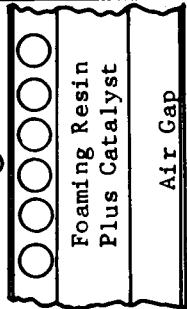
Panel Configuration	Ballistic Test Conditions @ T = 70-75°F and ΔP = ~ 14.7 psi	Air Leakage Rate thru Punctured Panel @ ΔP ≈ 14.7 psi (lbs/day)	Panel Unit Wt. Less Face Sheets (lbs/ft ²)	Panel Unit Wt. With Face Sheets (lbs/ft ²)	Remarks
<p>VII</p>  <p>Rigid Silicone Foam/Air Gaps Concept</p> <p>See Section 4.3.6 for panel details</p>	1/8" Dia. Steel @ 13,500 fps	0	2.74	3.86	1. Test conducted at Northrop
<p>VIII</p>  <p>Rigid Silicone Foam/Rubber Spheres/Air Gap Concept</p> <p>See Section 4.3.7 for panel details</p>	1/8" Dia. Steel @ 26,000 fps*	0	2.99	4.11	1. Panel weight based on using four 3/8-inch dia. spheres per square inch of panel 2. Test conducted at McGill University

TABLE 2-1 - COMPARATIVE EVALUATION OF SELF-SEALING PANEL CONCEPTS

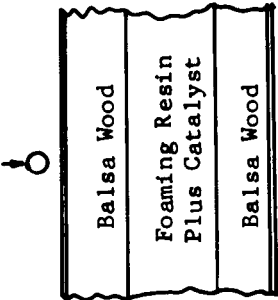
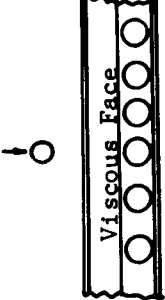
Panel Configuration	Ballistic Test Conditions @ T = 70-75°F and $\Delta P \approx 14.7$ psi	Air Leakage Rate thru Punctured Panel @ $\Delta P \approx 14.7$ psi (lbs/day)	Panel Unit Wt. Less Face Sheets (lbs/ft ²)	Panel Unit Wt. With Face Sheets (lbs/ft ²)	Remarks
<p>IX</p>  <p>Rigid Silicone Foam/Balsa Wood Concept See Section 4.3.4 for panel details</p>	1/8" Dia. Steel @ 10,000 fps	0	3.44	4.30	1. Test conducted at Northrop
<p>X</p>  <p>Elastomeric Spheres/Viscous Face Concept See Section 4.3.5 for panel details</p>	1/8" Dia. Steel @ 18,000 fps	0	1.29	2.41	1. Test conducted at Northrop 2. Panel weight based on using four 3/8-inch diameter spheres per square inch of panel

TABLE 2-1 - COMPARATIVE EVALUATION OF SELF-SEALING PANEL CONCEPTS

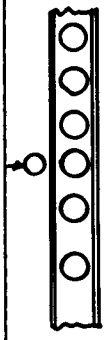
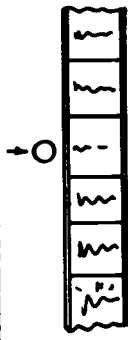
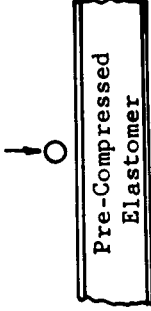
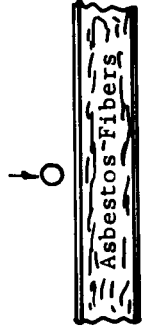
Panel Configuration	Ballistic Test Conditions @ T = 70-75°F & ΔP ≈ 14.7 psi	Air Leakage Rate thru Punctured Panel @ ΔP ≈ 14.7 psi (lbs/day)	Panel Unit Wt. Less Face Sheets (lbs/ft ²)	Panel Unit Wt. With Face Sheets (lbs/ft ²)	Remarks
<p>XI</p>  <p>Elastomer Spheres Concept</p> <p>See Section 4.2.1 for panel details</p>	1/8" Dia. Steel @ 24,700 fps	1.3	0.31	1.43	<p>1. Without the spheres to seal the 3/16-inch dia. hole in the pellet entry face, the leakage rate would have been 595 lbs/day (calculated)</p> <p>2. Panel weight based on using four 3/8-inch diameter spheres per square inch of panel</p> <p>3. Test conducted at McGill University</p>
<p>XII</p>  <p>Honeycomb Core-Elastomer (not pre-compressed) Concept</p> <p>See Figure 4-7, page 45 of Reference 1 for panel details</p>	<p>1/8" Dia. Steel @ 7,000 fps</p> <p>1/8" Dia. Glass @ 7,000 fps</p> <p>1/8" Dia. Glass @ 20,950 fps</p>	<p>0</p> <p>0 - 1.5</p> <p>Failure No sealing action</p>	0.99	2.16	<p>1. At impact velocities > 7,000 fps, excessive material removal along pellet entry face reduces self-sealing capability</p> <p>2. 20,950 fps test conducted at NASA Ames Research Center</p> <p>Low velocity tests conducted at Northrop.</p>

TABLE 2-1 - COMPARATIVE EVALUATION OF SELF-SEALING PANEL CONCEPTS

Panel Configuration	Ballistic Test Conditions @ T = 70-75°F & ΔP ≈ 14.7 psi	Air Leakage Rate thru Punctured Panel @ ΔP ≈ 14.7 psi (lbs/day)	Panel Unit Wt. Less Face Sheets (lbs/ft ²)	Panel Unit Wt. With Face Sheets (lbs/ft ²)	Remarks
XIII  Pre-Compressed Elastomer Concept See Figure 4-16, Page 69 of Reference 1 for panel details	1/8" Dia. Steel @ 7,000 fps 1/8" Dia. Glass @ 7,000 fps 1/8" Dia. Glass @ 19,700 fps	0 0 Failure No sealing action	2.02	2.98	1. At impact velocities > 7,000 fps excessive material removal along pellet entry face reduces self-sealing capability 2. High residual pre-stress (~ 35 psi) requires rigid panel construction 3. 19,700 fps test conducted at NASA Ames Research Center. Low velocity tests conducted at Northrop.
XIV  Fiber Mat Concept A Mixture of fibers and water B Dry fibers	1/8" Dia. Steel @ 7,000 fps 1/8" Dia. Steel @ 7,000 fps 1/8" Dia. Steel @ 21,000 fps	0 - 4 4 - 5 Failure No sealing action	1.30 0.67 1.30	2.15 1.79 2.15	1. At velocities > 7,000 fps "Tank Effect" induces excessive damage to face sheets of Config. A while shock wave effects disperse dry fibers from puncture in Config. B so that self-sealing capability of panels is reduced. 2. Tests conducted at Northrop

See Table 2-2, Page 17 of Reference 2 for panel details

appears reasonable to assume that a panel optimization program will result in panel unit weights more competitive with non-self-sealing structures. It should also be noted that, in addition to the self-sealing capability of the panels, some of the components of the combined mechanical-chemical concepts possess multi-functional properties in that they make structural and insulative contributions to the panel configurations. Therefore, within the qualifications imposed by the above considerations and the limited scope of the test program, the following statements may be made about the listed self-sealing concepts.

- All of the panel configurations presented in Table 2-1, with the exception of Configurations XII, XIII and XIV possess the capability for self-sealing air pressurized (14.7 psig) compartments, after puncturing by 1/8-inch diameter steel spheres at impact velocities to 20,000 fps and above.
- Weightwise, the Elastomer Sphere Concept (XI) is the lightest panel configuration (1.43 lb/ft^2), while the Rigid Silicone Foam/Balsa Wood Concept (IX) is the heaviest (4.30 lb/ft^2).
- The chemical and combined chemical-mechanical concepts are the most reliable for obtaining complete sealing action (zero leakage rate) while the mechanical concept (Elastomer Spheres) may result in small residual leakage rates (3 lbs/day).
- The self-sealing capability of the listed concepts was evaluated under standard room temperature conditions. At extreme temperatures, particularly at sub-zero temperatures, the reaction rates of the chemical concepts and their sealing capability could be adversely affected. The temperature limitations for the successful working of each concept have not yet been established. However, it can be qualitatively stated that the Elastomer Sphere Concept

(XI) where the working principle does not depend on chemical reactions, would be the least sensitive to extreme temperatures. A more detailed discussion on the environmental dependence of self-sealing capability is given in Section 3.4.

- The self-sealing concepts, as conceived, possess potential application for use in the wall construction of pressurized manned modules or other pressurized compartments containing fluids which would be compatible with the sealing materials used in the panel configuration.

2.2 CONCLUSIONS AND RECOMMENDATIONS

The feasibility of constructing a self-sealing structure has been experimentally demonstrated by puncturing panel specimens with 1/8-inch diameter steel spheres at impact velocities to 26,000 fps. Both mechanically and chemically activated techniques have been employed in the panel configurations with the most successful using combined mechanical-chemical techniques. Based on the results of this program, and evaluation of self-sealing panel specimens, the following concluding statements are made:

- The combined mechanical-chemical concept in which rubber spheres are used as one of the sealing elements, possess the best "fail-safe" features of all concepts evaluated, since either the spheres or the chemical reaction could effect a seal.
- In all self-sealing panel concepts, the outer face sheet acts as a meteoroid bumper shield, thereby resulting in an over-all panel configuration possessing high penetration resistance, shock wave damage control and self-sealing capability.
- The evaluation of the self-sealing configurations was limited to demonstrating their capability (at room temperature) for sealing air-filled compartments pressurized to one atmosphere. From these results, it can be said that these self-sealing concepts possess potential applications for use in the wall construction of manned space vehicles or other air pressurized compartments (up to one atmosphere pressure differential). Further evaluation will be required to determine the feasibility of these concepts for sealing punctured fluid-filled (both air and other fluids) compartments under more severe environmental conditions of pressure and temperature.
- For the present state of panel development, the weight that would have to be added to a double wall panel in order to give

it self-sealing capability may vary from 0.31 lbs/ft² for the Elastomer Sphere Concept to 3.44 lbs/ft² for one of the Rigid Silicone Foam/Balsa Wood configurations. However, as previously stated, these are non-optimized weights which could be substantially reduced if the panels would be subjected to a weight optimization program.

- Some of the components of the combined mechanical-chemical concepts possess multi-functional properties in that they may make structural and insulative contributions to the panel configurations.
- Damage control to the face sheets of punctured panels has been accomplished by use of nonmetallic laminates, and by isolating the pellet entry face from nearly incompressible materials (liquid chemicals) by air gaps or the interposition of low density highly compressible materials. Material loss, along the projectile entry path, has been mitigated by use of volume addition techniques (e.g., rapid foaming and curing polymers, with a volume expansion ratio of about 10 to 1).
- Impact induced damage to the pellet exit face of punctured chemical concept panels has not been severe enough (at impact velocities to 26,000 fps) to necessitate isolating it from the chemical compartment. However, at impact velocities above 26,000 fps, the transmitted shock in the chemical compartment may be sufficiently high to severely damage the pellet exit face and, thereby necessitate its isolation from the chemical compartment.

In order to enhance the further development and evaluation of self-sealing structures, the following recommendations are made:

- Optimize, for minimum weight, the panel configurations of the most promising self-sealing concepts developed during this

program. Evaluation of panel configurations should be conducted with particle sizes more representative of the greater majority of meteoritic particles expected to impact a space vehicle (1/16-inch diameter and smaller). Particle velocities should be in excess of 25,000 fps.

- The most promising weight optimized self-sealing structure concepts should be integrated into lightweight space vehicle structural panel configurations. Consideration should be given to the following factors:
 1. Fabrication problems associated with incorporating panel designs into practical space vehicle structural configurations.
 2. Lightweight construction consistent with structural integrity and self-sealing capability.
 3. Potential areas of space vehicle applications.
- The self-sealing panel configurations resulting from the above task should be subjected to analysis and a comparative evaluation with the armor plate and meteoroid bumper techniques. Some of the factors and parameters that should be considered in evaluating non-self-sealing structures with those possessing self-sealing capability should include, but not be limited to the following:
 1. Ballistic limit for equivalent panel weight (lbs/ft^2) configurations.
 2. Panel weights (lbs/ft^2) for equivalent ballistic limits.
 3. Panel weight (lbs/ft^2) for various probabilities of zero to "n" punctures and for various values of the mission parameter $(A\tau)^*$.

* A = Area exposed to meteoroid environment.

τ = Mission time in meteoroid environment.

4. Air leakage rate (across a pressure differential of one atmosphere) for each panel configuration punctured at impact velocities equal to their ballistic limit.
 5. Structural compatibility.
 6. Multifunctional properties of panel components.
 7. Reliability and "fail-safe" capability of each configuration.
- For each successful self-sealing panel configuration, determine their environmental limitations to extreme temperature exposures and various compartment pressure differentials. This evaluation should be conducted for both air and other fluid-filled compartments applicable to space vehicle mission requirements.

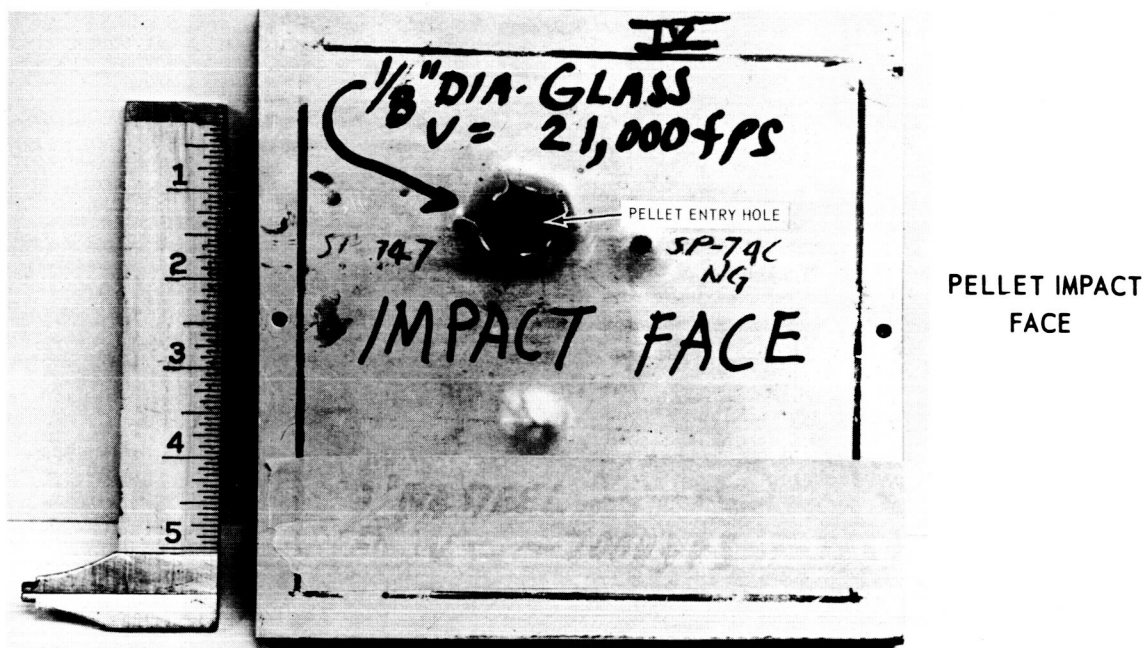
3.0 TECHNICAL DISCUSSION AND ANALYSIS

3.1 HIGH VELOCITY PARTICLE PENETRATION INTO COMPARTMENTS CONTAINING A NEARLY INCOMPRESSIBLE MEDIUM

When a high velocity particle penetrates a compartment containing a nearly incompressible material (liquid or solid), the incident shock wave induces extremely high pressures at the compartment wall interface which may exceed the dynamic rupture strength of the penetrated wall. If the penetrated wall material is metallic or prone to rapid crack propagation, when loaded at high strain rates, then, the consequence may be petalling and/or explosive rupturing of the penetrated face sheets. This was dramatically demonstrated during the ballistic testing of one of the earlier panel configurations. The panel construction was basically a honeycomb core sandwich, with the core cells filled with a nearly incompressible elastomer. The pellet entry face of the panel was an 0.032-inch aluminum sheet while the pellet exit face was a 1/16-inch asbestos cloth (wire reinforced) neoprene sheet. The aluminum face sheet petalled while the neoprene sheet did not (see Figure 3-1).

The chemical compartments used in the chemical self-sealing panel configurations are in essence liquid-filled tanks and, as a consequence, are also subject to such failures. An example of the explosive rupturing of an aluminum face sheet used as the penetrated wall of a liquid (water) filled tank is shown in Figure 3-2.

In order to obtain a better understanding of the magnitude of the pressures that may be generated by a high velocity particle penetrating the chemical compartments of a chemical self-sealing panel, the method of analysis described in Appendix A is used to determine the pertinent interface pressures. The required Hugoniot shock data for the chemicals and face sheet materials used in the self-sealing panels were not available. Therefore, existing shock data of materials with densities approximately equal to those of interest were selected for this analysis. This approach, although yielding an approximate solution, is sufficiently accurate to indicate the pertinent pressures within a factor of two or less. For this analysis, an aluminum



1/8" DIA. GLASS SPHERE
V = 21,000 FPS

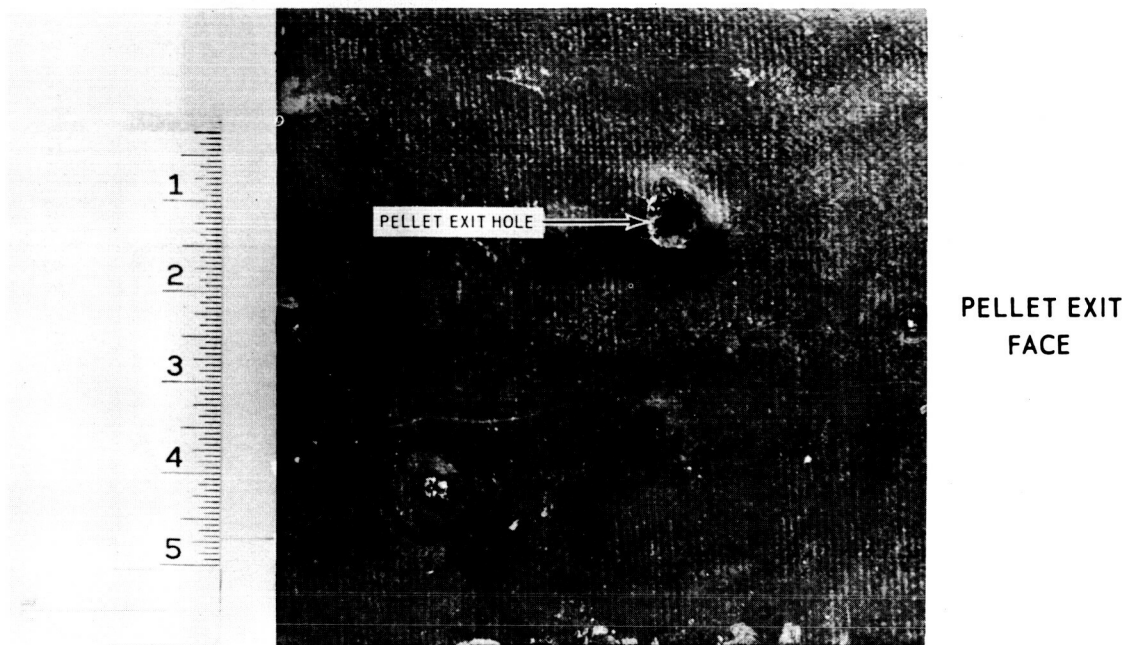


FIGURE 3-1 RUPTURED HONEYCOMB CORE-ELASTOMER PANEL



FIGURE 3-2 RUPTURED ALUMINUM PANEL (WATER FILLED TANK)

projectile was assumed to impact a water-filled nylon wall compartment at an impact velocity of 20,000 fps. The graphical solution for the interface pressures is illustrated in Figure 3-3.

An aluminum projectile impacting a nylon compartment wall at 20,000 fps will result in an Al/nylon interface pressure of 425 kilobars (Pt.A) while the Nylon/H₂O interface pressure would be 370 kilobars ($\sim 5.44 \times 10^6$ psi) (Pt.B).

It is this latter pressure then that loads up the compartment wall. This pressure, when combined with initial impact induced damage to the wall, results in rupture of the penetrated face sheet. It is interesting to note that, for the ballistic conditions cited, an aluminum compartment wall gives an Al/H₂O interface pressure of 360 kilobars (Pt.C) or 10 kilobars lower than when a lower density (Nylon) material is used for the compartment wall. On the other hand, the initial impact pressure of the aluminum projectile on the aluminum wall (Al/Al) is about twice that of the aluminum projectile on the nylon wall (Al/Nylon). This apparent anomaly can be explained by the fact that the impedance* mismatch between the aluminum and water is greater than between nylon and water. This results in a smaller percentage of the incident pressure being transmitted to the water for the Al/Al/H₂O impact conditions. However, it should not be concluded that an aluminum wall compartment would be more effective, for damage control, than an appropriate structural non-metallic wall. Metals in general are more sensitive than non-metals to rapid crack propagation when subjected to loading conditions under high strain rates (e.g., hypervelocity impact conditions). They would be expected to sustain more extensive damage than non-metals when tested under similar ballistic conditions. Therefore in order to mitigate the hazard of explosive rupturing of the self-sealing panels, non-metallic structural laminate face sheets were used and the chemical compartment, of the chemical self-sealing configurations, was isolated from the pellet entry

*Impedance = $(\rho_o C_o + \rho_o \lambda Up)$ where ρ_o = unshocked mass density, C_o = bulk acoustic velocity, λ = empirical compressibility factor and Up = material particle velocity

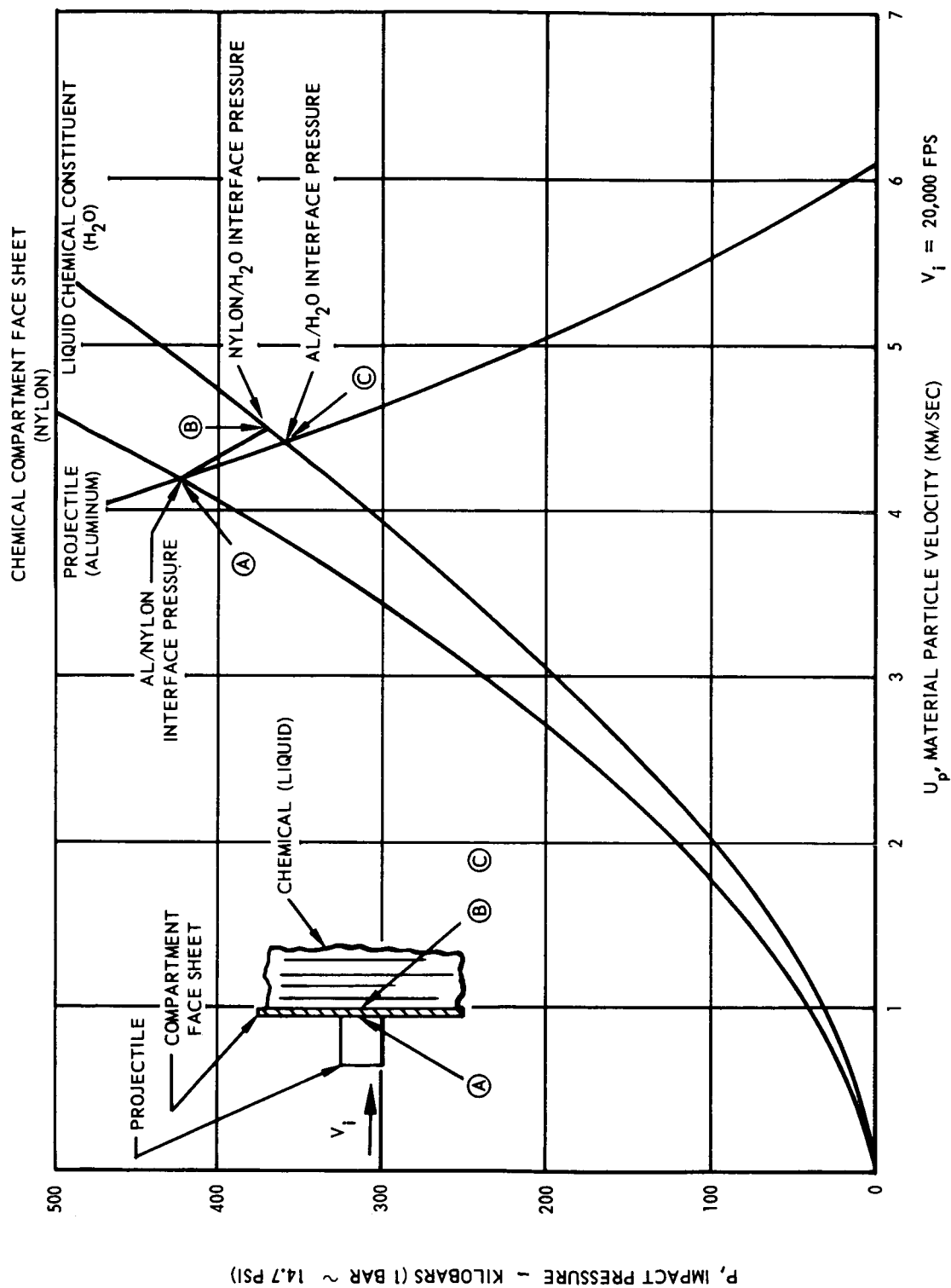


FIGURE 3-3 APPROXIMATE SOLUTION OF SHOCK PRESSURE IN CHEMICAL COMPARTMENT

face of the panel.

3.2 PERFORATION OF COMPOSITE STRUCTURES

In general, candidate self-sealing geometries consist of composite assemblies of metallic or non-metallic face sheets and a softer, polymeric interior whose function is to close the perforation. The sealant layers proposed and tested may be in liquid or solid form, depending on the mode of activation of the self-sealing mechanism. In addition, low-density interlayers have been used to isolate the sealant layer from the structural face sheets of the panels to prevent excessive damage to the latter by shock wave transmission. The presence of discontinuities in the panels complicates analysis of penetration and hole size. For this reason, an approach using semi-empirical penetration mechanics, modified to the case of layered media, has been implemented. It was the purpose of this analysis to establish the relationship between penetration resistance and hole size in targets of stratified media.

3.2.1 A Semi-Empirical Theory of Perforation of Composite Targets. In Reference 3, Watson presents an analysis pertinent to the case of plate perforation. This analysis has features which merit study for application to composite or layered panel perforation. It is summarized in the following paragraph.

A so-called resistance to penetration is postulated in the form

$$p = \frac{1}{2} \rho_t \dot{z}^2 + K \quad (3-1)$$

where the first term on the right is a stagnation pressure in the target medium and the K-factor is an empirical target strength term. The target space coordinate is z measured in the direction of target thickness. Only normal impact is considered. Considering the projectile to be traversing the target medium, the summation of forces acting on the projectile mass, m_p , yields

$$-m_p \ddot{z} = \frac{1}{2} \rho_t \dot{z}^2 A_p + K A_p \quad (3-2)$$

where dot symbols define differentiation with respect to time, subscripts p and t refer to projectile and target properties, respectively, and A represents area. Upon the substitution

$$\ddot{z} = \dot{z} \frac{d\dot{z}}{dz} \quad (3-3)$$

and the boundary condition

$$\dot{z} = V_i, z = 0 \quad (3-4)$$

the solution to equation (3-2) is

$$\dot{z} = V_i^2 e^{-\rho_t A_p z/m_p} + \frac{2K}{\rho_t} (e^{-\rho_t A_p z/m_p} - 1) \quad (3-5)$$

where \dot{z} is the residual velocity of the projectile mass after perforating a thickness, Z . A thick-target penetration formula may be obtained from equation (3-5) by imposing

$$z = \bar{P}; \dot{z} = 0 \quad (3-6)$$

and solving

$$\bar{P} = \frac{m_p}{\rho_t A_p} \ln \left[1 + \frac{\rho_t}{2K} V_i^2 \right] \quad (3-7)$$

Equation (3-7) is similar to the familiar Herrmann-Jones penetration relation

$$\bar{P} = 0.6 \left(\frac{6}{\pi} \right)^{1/3} \left(\frac{\rho_p m_p}{\rho_t^{2/3}} \right)^{1/3} \ln \left[1 + \left(\frac{\rho_p}{\rho_t} \right)^{2/3} \frac{\rho_t}{4H_t} V_i^2 \right] \quad (3-8)$$

where H_t , the Brinell hardness of the target material, assumes the significance of the K-factor from Watson's equation. The utility of the Herrmann-Jones equation is known.

The limitations of the Watson equation arise from the observation that no single value of K-factor suffices over a moderate range of impact velocities. This is highly suggestive of \dot{z} - dependence, and forms the basis for a

slightly modified analysis pertinent to the case of composite panel perforation.

3.2.2 Modified Analysis. It is proposed that equation (3-2) be modified to read

$$-m_p \ddot{z} = \frac{1}{2} \rho_t \dot{z}^2 A_p + K A_t(z) \quad (3-9)$$

where the target hole area term, $A_t(z)$ has been introduced. It is obvious that we are concerned with the situation where the target hole area (or damaged area) varies with depth, particularly for the composite targets of concern here. The solution to equation (3-9) is complicated by the z -dependence of the target density. A step-wise solution to each layer is suggested. As an approximation, the effects of density gradients will be neglected and a solution of the following form is suggested;

$$\dot{z} = e^{-\overline{\rho_t z} A_p / m_p} \left[\text{const} - \frac{2K}{m_p} \int_0^h A_t e^{\rho_t A_p z / m_p} dz \right] \quad (3-10)$$

where

$$\overline{\rho_t z} = \int_0^h \rho_t dz \quad (3-11)$$

and h is the overall target thickness. Now, applying the boundary condition of equation (3-4) to preserve the identity of the K -factor for purposes of comparison, yields,

$$\dot{z} = v_i^2 e^{-\overline{\rho_t z} A_p / m_p} + \frac{2K}{m_p} e^{-\overline{\rho_t z} A_p / m_p} \left[\int_0^h A_t dz - \int_0^h e^{\rho_t z A_p / m_p} A_t dz \right] \quad (3-12)$$

In order to determine the value of the target strength factor, K , from experiment, one must record the impact and residual velocities, and the target hole profile. However, the residual velocity is a somewhat arbitrary term, especially at speeds where projectile fragmentation and spray cloud formation occur upon perforation. Since this is the rule rather

than the exception, one alternative is to perform experiments at the target ballistic limit, thereby eliminating the residual velocity term. The ballistic limit is defined as the threshold impact velocity at which the target stops the projectile. In this case, $\dot{z} = 0$ and

$$K = \frac{m_p}{2} v_i^2 \left[\int_0^h e^{\rho_t A_p z / m_p} A_t dz - \int_0^h A_t dz \right]^{-1} \quad (3-13)$$

The integrals may be evaluated by post-shot inspection of expended targets. Test panel interiors of materials which "trap" the damage pattern are required. For this reason balsa wood or rigid foam interlayers were suggested for test configurations. Other factors, dictating a requirement for low density interlayers, made this requirement compatible with the overall test program.

A series of test shots involving the use of balsa wood interlayers is described in Section 4.3.4. The target strength term, K, was calculated for one configuration representing the ballistic limit.

A number of conclusions may be drawn from the analysis and the limited test results. A comparison with the original analysis can be made by assuming an average density of the panel and neglecting hole size variation. A comparison of calculated strength factors for one test case (Panel B-4, see Section 4.3.4) was made.

Watson's original method: $K = 1.66 \times 10^6 \text{ psf} = 7.96 \times 10^8 \text{ dynes/cm}^2$

Modified composite panel method: $K = 1.12 \times 10^6 \text{ psf} = 5.363 \times 10^8 \text{ dynes/cm}^2$

The agreement of terms is deemed gratifying in view of the difference in methods of calculation, and the inclusion of hole dependence in the latter. At present, no significance can be attached to the lower value of the latter except the absence of the contribution from the backup sheet which was not perforated. It can be stated that the calculated values of strength factor are depressed two orders of magnitude below values for continuous metallic targets.³

The exponential term

$$e^{-\frac{\rho_t Z}{m_p} A_p}$$

in equation (3-12) brings into the analysis of composite panel perforation the influence of target area density and projectile size effects. The precise definition of K-factor permits the delineation of scaling effects which would be extremely important to practical design considerations. Unfortunately, additional data are not available, from tests to be conducted at McGill University at this writing, to confirm initial conclusions about the target strength term.

The complete calculation of the modified strength factor for a composite panel is presented in Section 4.3.4, Table 4-1.

3.3 MATERIAL SELECTION AND EVALUATION

The effectiveness of a self-sealing structure to control the meteoroid hazard to space vehicles will depend to a great extent upon the selection and use of suitable materials. To establish more realistically the feasibility and space area applicability, the selection and evaluation of materials should be performed under combined simulated space environments. To simulate true space missions, the dependence of self-sealing capability upon combined temperature extremes, vacuum and radiations should be established. However, due to the necessity to investigate self-sealing concepts giving effective sealing at higher velocities (up to 26,000 fps) and in the interest of simplification and efficiency, the major effort during this year's research program was concentrated on the selection and evaluation of materials to be incorporated in self-sealing techniques for minimizing the detrimental high velocity shock wave effects on the sealing capability of our self-sealing concepts under one standard environment.

The tests which were performed consisted of impacting self sealing structures with 1/8-inch steel pellets at velocities from 7,000 fps to 26,000 fps. The environment under which these tests were performed was ambient temperature (≈ 70 to 80°F.) and a pressure differential of one atmosphere (14.7 psi.) existing across the self-sealing structure faces at the time of impact.

The weight factor was considered as secondary in order that more emphasis could be placed upon the evaluation of various self-sealing concepts. Although the weight factor was considered as secondary, the non-optimized weights for all the self-sealing structures investigated during this program varied from 0.31 lb/ft² to 3.44 lbs/ft². Also, since we have reached the point in this last quarter of the program where we are now able to seal at higher velocities (up to 26,000 fps), a weight optimization program has been initiated for some of our most successful self-sealing structures.

During this task, the big step in the selection and evaluation of materials was to improve the sealing at velocities from 15,000 fps to 25,000 fps and up. In the previous year's program, the feasibility of fabricating successful self-sealing structures at impacting velocities to 7,000 fps was demonstrated. However, by using similar self-sealing structures at impact velocities to 23,000 fps, tests had revealed that, due to increased shock wave effects, greater damage to the structure face sheets and material removal along the pellet entry path would make it more difficult to achieve effective sealing at these higher velocities.

To alleviate these shock wave effects at higher velocities, the following techniques were investigated:

- (a) The utilization of nonmetallic face sheets.
- (b) The separation of the liquid chemical constituents, in particular from the entry face sheet of the self-sealing structure, by inserting between the chemical compartment and the entry face sheet, a highly compressible and energy absorbing material.
- (c) New self-sealing concepts using foaming systems to introduce in the self-sealing structure, a volume expanding system.
- (d) The combination of the best mechanical concepts with the best chemical concepts to accomplish a greater self-sealing capability at higher velocity impact.

The incorporation of these new techniques required an extensive study of a wide range of materials.

The degree of damage provoked to the face sheets, and, particularly to the entry face sheet, upon impact by a 1/8-inch projectile is one of the major determining factors of the self-sealing capability of the self-sealing structure. Thus, the selection of the proper materials for the fabrication of the self-sealing structure face sheets was of great importance. Particularly, at high velocities (15,000 to 25,000 fps and up) this selection was crucial due to the shock wave effects.

For example, the efficiency of the concepts whereby elastomeric spheres are used as the highly compressible material and energy absorber will depend on the regularity of "cleanliness" of the puncture in the sealing face. Ideally, this puncture should be circular with no radial cracking around it and no delamination of the sealing surface or fraying of its edges. This would enable an elastomeric sphere with only a small pressure differential activating it to seat firmly in the puncture and seal it partially or effectively with the chemical system completing the seal or reinforcing it.

Similarly, in the case of the concept whereby fibers are used as the highly compressible material and energy absorber, the damage to the sealing surface should be minimal so that the fibers can partially plug the hole more readily and enable the chemical system to effect the final seal.

3.3.1 Selection of Materials for the Self-Sealing Structure Face Sheets

In the search for a suitable sealing surface configuration which had to meet the above mentioned requirements, a large variety of materials were investigated. The configuration which proves to be, as of to date, the most suitable is a 3-ply laminate of 181 fiberglass cloth impregnated with a 55% Versamide 125 and 45% Epoxy 828 resin combination and a 1/32-inch thick sheet of AMS 3212 J nitrile rubber bonded to the epoxy laminate with a polysulfide sealant.

This type of sealing surface configuration gave excellent results with all the self-sealing concepts evaluated as well at low velocities (7,000 fps)

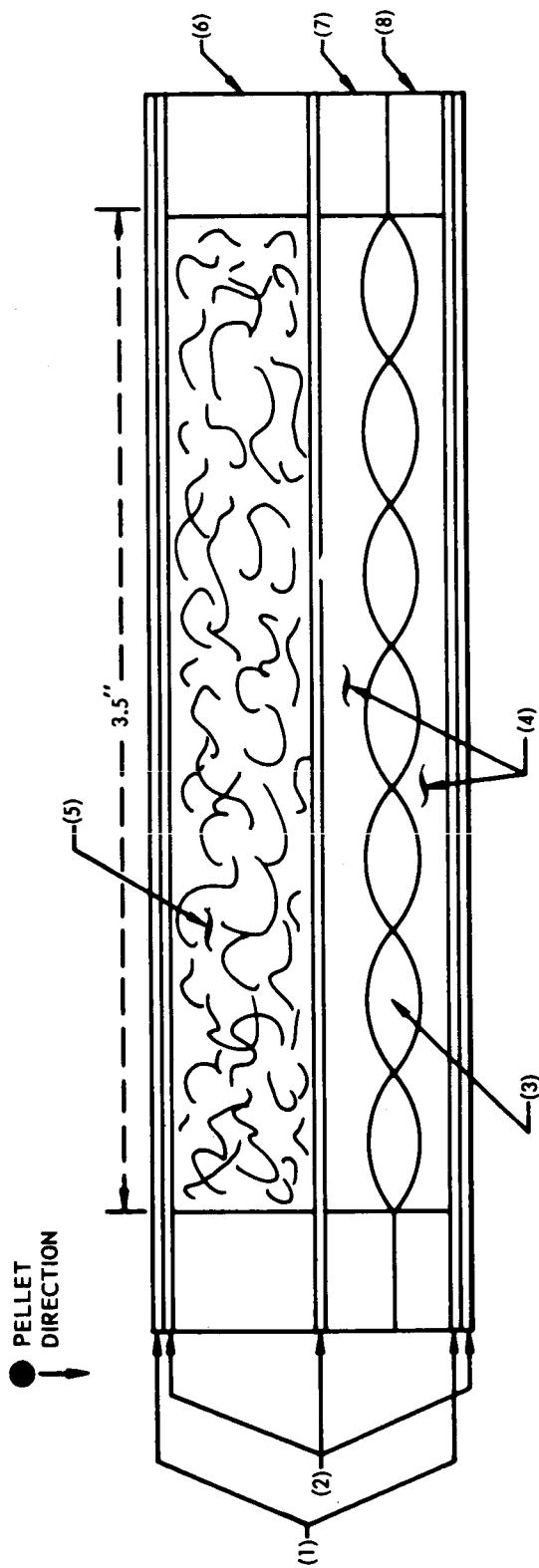
as at higher velocities (up to 26,000 fps). In this velocity range, the hole diameter of the self-sealing structure entry face varies normally from 1/8-inch to 1/4-inch and in fewer cases to 5/16-inch as the velocity increases. This large increase in hole area is caused by the dynamic response of the face sheet material at the high strain rates resulting from the higher impact velocities. At high strain rates the material behaves as if it were glass-like with no damping mechanisms and responds to impact loading as a "brittle" material in that it suffers greater damage than at the lower strain rates.

The structural damage to both the entry and exit faces will vary with the velocity, the type of compressible material used, the type of chemical components, the thickness of the self-sealing structure, and, the type of projectile used. For example, two self-sealing panels having the same structural configuration (see Figure 3-4), were impacted at approximately the same velocity (24,000 fps) by 1/8-inch diameter steel pellets. In one case, the chemical constituent was fluid RTV 60 silicone rubber and, in the other case, rigid foam silicone resin. After penetration, the structure which contained the liquid RTV 60 silicone rubber showed a 1/4-inch diameter hole and no cracking in the entry face. However, the exit face showed heavy cracking of the epoxy laminate. But, due to the presence of the nitrile rubber sheet outside the exit face, the damage was kept to a minimum and allowed the hole to seal. On the other hand, the self-sealing structure which contained the rigid foam silicone resin showed, after impact, a 1/4-inch diameter hole and no cracking in the entry face and a 5/16-inch diameter hole and no cracking in the exit face.

The different results obtained with these self-sealing structures are probably due to the large variance in density and viscosity of the two types of chemical components.

3.3.2 Selection of Compressible Materials for Shock Wave Attenuation.

The approach to minimize excessive self-sealing structure damage and material removal local to the pellet entry path by interposing highly compressible material, necessitated a thorough study of various materials.



- (1) EPOXY LAMINATE (3 PLY FIBERGLASS; 55% VERSAMIDE 125, 45% EPON RESIN 828)
- (2) NITRILE RUBBER SHEET (AMS2312J, 1/32" THICK)
- (3) CHAIN OF PLASTIC BAGS (MYLAR PLASTIC FILM) CONTAINING NUOCURE 28 OR UNSTABILIZED STANNOUS OCTOATE AND BONDED TO THE HONEYCOMB STRUCTURE SIDES TO AVOID SLIPPAGE OF THE BAGS WHEN PANEL IS TESTED.
- (4) XR-6-3700 RIGID SILICONE FOAM RESIN OR RTV60 UNCURED ELASTOMER
- (5) ASBESTOS FIBERS (3R 12) OR ELASTOMERIC SPHERES
- (6) HONEYCOMB STRUCTURE, 1/2" THICK
- (7) HONEYCOMB STRUCTURE, 1/4" THICK
- (8) HONEYCOMB STRUCTURE, 3/16" THICK

FIGURE 3-4 COMBINED CONCEPT - RIGID SILICONE FOAM OR RTV60 SILICONE ELASTOMER/FIBER MAT OR RUBBER SPHERES CONCEPT - CONFIGURATION

Especially, two types of materials were retained: (1) low density asbestos fibers, and (2) elastomeric spheres made of various types of rubbers.

This technique encourages the expansion of the shock wave in a compressible material and permits some lateral dispersion of the incident energy. It is conceivable that sufficient energy is dissipated in this manner so that any puncturing of the sealing constituents will be accomplished at a lower residual velocity, thereby resulting in minimum material removal and successful sealing.

The asbestos fibers 3R12 from Canadian Johns-Manville Co., Ltd., used as a compressible material, demonstrated very successful results. When used in the "Fiber Mat Concept," that is, used as the sole sealing element, the fibers demonstrated good self-sealing effectiveness at low velocities (up to 7,000 fps). However, at velocities of 12,000 fps and higher (up to 23,000 fps), the self-sealing capability decreased. At the higher puncturing velocities, the shock waves, although attenuated by the fibers, dispersed the fibers sufficiently afar from the pellet entry path to prevent their being drawn to the hole in sufficient quantity to effect a seal.

The self-sealing effectiveness of the asbestos fibers at higher velocities (up to 26,000 fps) when combined with a chemical system is increased drastically. As a matter of fact, one of the best self-sealing structures to date consists of a combination of fibers and rigid foam. This combination was tested at 23,500 fps at McGill University using 1/8-inch diameter steel pellets and giving an immediate and complete seal. The fibers, when used in combination with the chemical concepts, were found to improve the sealing action by reducing the efflux of the chemical sealing constituents through the puncture before the chemical sealing process is completed.

The elastomeric spheres which were retained as the other compressible material demonstrated excellent results too, as well at low velocities as at higher velocities (up to 25,000 fps). The physical parameters controlling the elastomeric spheres sealing capability were studied. The parameters included sphere diameter, impact hole diameter or slope of

hole, sphere material, and pressure differential across the hole.

Three different materials were selected for the fabrication of these elastomeric spheres, RTV 11 silicone rubber and RTV 60 silicone rubber (both from General Electric) and EC 1828 expanded natural rubber foam (from 3 M Company). The sizes ranged from 1/2-inch to 1/8-inch in diameter.

Upon completion of these studies, the following conclusions were derived:

- The elastomeric spheres should be selected so as to be larger than the largest anticipated puncture. The amount of oversize depends on the peripheral damage anticipated around the puncture.
- The spheres should be soft enough to conform to irregularities in the puncture, and trapped fragments of sealing surface and/or damaged spheres, and still effect a seal.
- Spheres which seal satisfactorily against damage when the pressure differential is 14.7 psi will continue to seal against lesser pressure differential if the pressure is reduced on the "cabin" side.

When used in the "Elastomeric Spheres Concept," that is, as the sole sealing element, the elastomeric spheres demonstrated excellent self-sealing capabilities at low velocities as well as at higher velocities (up to 25,000 fps). This is in contrast to the asbestos fibers self-sealing capability which is lower at higher velocities.

It was shown that elastomeric spheres were capable of effectively sealing punctures caused by 1/8-inch diameter lead, glass and steel pellets at velocities of approximately 7,000 fps. In addition, it was also shown that the elastomeric spheres had good potential for sealing punctures made by 1/8-inch diameter glass spheres at an impact velocity of 23,000 fps and demonstrated successfully an almost complete seal of a puncture made by 1/8-inch diameter steel pellet at an impact velocity of 24,700 fps.

It was found that the sealing could be accomplished with 3/16-inch diameter or smaller spheres when the self-sealing structures were impacted at the lower velocities. Increasing the velocity to 24,700 fps increased the hole size to the point where larger diameter spheres were required to effect a seal. In this case, 3/8-inch diameter spheres were large enough to effect a seal as it was demonstrated during tests.

By combining the elastomeric spheres with the chemical concepts, tests have shown highly successful results in self-sealing structure configurations upon impact at velocities to 26,000 fps with 1/8-inch steel pellets. Particularly successful was a self-sealing structure in which elastomeric spheres were combined with the rigid foam chemical system. The impact velocity was 26,000 fps and the projectile used was a 1/8-inch diameter steel pellet.

This combination gives an ideal self-sealing mechanism whereby, upon impact, the elastomeric spheres (as the compressible material) attenuate the shock wave effects by dissipating the incident energy and, due to the existing pressure differential, one of the spheres is pulled into the punctured hole, thus effecting a partial or complete seal. At the same time, the penetrating pellet initiates a chemical reaction which effectuates a complete seal of the self-sealing structure whereby the entry hole is completely sealed by the permanently adhering sphere and the cured material. The exit hole is completely sealed by the cured material. Thus, the elastomeric spheres improve the sealing action of the chemical systems by reducing the efflux of the sealing constituents through the puncture before the sealing process is completed.

A more sophisticated and simpler combined mechanical-chemical concept was investigated for the purpose of simplification and of reducing the weight of the self-sealing structure. Because of the large quantities of curing agent used in their preparation, the silicone elastomeric spheres were found to cause local contact curing of other room temperature silicone

elastomers. The principle of this simplified concept, which is called the "Viscous Face Concept," involves the following mechanism. Upon penetration of the self-sealing structure, one of the silicone spheres will set itself in the punctured hole to effect a partial or complete seal. Simultaneously, an uncured RTV silicone fluid is released from a thick (1/8- or 1/16-inch thick) viscous face located either behind the entry face or in front of the exit face. This fluid contacts the silicone sphere which initiates a curing action and completes the seal. It also allows the sphere to permanently adhere to the sealing surface once it has set itself in the punctured hole. This prevents the sphere from being shaken loose (due to vibration or other mechanical loads) from the sealing surface and unsealing the hole.

To speed up the curing action, and to render this concept more effective, additional refinements were introduced, such as coating the spheres with the catalyst and using a silicone foam resin as the viscous face. This new system gave excellent results.

More data and discussion are given in Section 4.0 "Experimental Program" regarding the application of asbestos fibers and elastomeric spheres as the compressible and energy absorbing material.

3.3.3 Selection of the Chemical Constituents

With the help of either the fibers or elastomeric spheres as the compressible and energy dissipating materials, the chemical concepts acquire an excellent feasibility and their self-sealing capabilities increased tremendously, particularly for the higher impact velocities (up to 26,000 fps). These large improvements were mostly due to the combination of the proper materials making up the self-sealing structure. Particularly, the selection of the chemical constituents played a big part of this success. Most of the effort on the development of the now successful mechanical-chemical concepts was expended on the search of suitable chemical components.

Four different areas were explored: (1) RTV silicone elastomers, (2) polyurethane elastomers and foams, (3) silicone foams, and (4) the corresponding catalysts.

The principal guiding factors in the selection of these fluids were:

(1) selection of reactive materials which cure very rapidly upon mixing in order to avoid total expulsion of the components through the puncture during the reaction, (2) selection of reactive fluids which have a viscosity that will allow proper flow and mixing inside the self-sealing structure once penetrated, (3) selection of reactive fluids which form expanding materials, such as foams, (4) selection of reactive fluids which form an elastomeric or foam material of sufficient strength and adhesion to the self-sealing structure walls to withstand the pressure differential of 14.7 psi across the structure surfaces, and (5) selection of reactive fluids which are the least toxic or nontoxic and do not undergo explosive reactions or highly exothermic reactions with the formation of highly volatile and toxic products.

Most of the effort expended on evaluating and selecting the most suitable RTV silicone was spent during last year's research program (see Reference 1). A variety of RTV silicones, using Nuocure 28 (Stannous 2-Ethylhexoate, Tin Octoate) as a catalyst, were investigated. Results of tests indicated that among the silicone elastomers evaluated, RTV 60 gave the most successful sealings. RTV 60 was chosen because of its ideal viscosity range, its fast cure with Nuocure 28 and the excellent properties of the cured elastomer.

Other reactive components were tested such as Adiprene L-315 (polyurethane elastomer) as the resin and diethylene triamine-DETA (with or without filler), or triethylene tetramine-TETA (with or without filler), or Versamid and/or mixtures of Versamid and DETA, as the catalysts. However, because of viscosity conditions and curing rates, the cured mass obtained did not conform with the necessary requirements to accomplish a

successful sealing action. Thus, this material was eliminated.

The above described materials, silicone and polyurethane elastomers, had been evaluated for application to strictly chemical concepts, that is, without combination with either of the mechanical concepts. By contrast, this year's research program was mostly concentrated around the combined mechanical-chemical self-sealing concepts and for the reasons explained earlier in this report.

When using the chemical concept strictly by itself, the degree and rate of mixing and the viscosity of the two reactive fluids were of great importance. These factors dictated the amount of material being extruded from the self-sealing structure hole without having time to cure and effect a seal. The curing rate depends upon the degree and rate of mixing which in turn is directly dependent upon the viscosity range of the reactive fluids, the temperature of the reactive fluids (in this case ambient temperature) and the pressure differential existing across the structure surfaces.

In the case of the combined concepts, these factors are still very important, particularly the degree and rate of mixing, but not as important as in the above case due to the fact that the compressible materials (fibers or elastomeric spheres) will reduce the efflux of the chemical sealing constituents through the puncture before the sealing process is completed. This of course gave us a little more flexibility in the search for suitable reactive fluids.

Initially in the evaluation of the combined mechanical-chemical self-sealing concepts, the RTV 60 Silicone-Nuocure 28 chemical system was investigated. A series of tests at low ($\sim 7,000$ fps), medium (10,000 to 15,000 fps) and higher (up to 26,000 fps) velocities indicated excellent self-sealing capabilities. However, for weight considerations and to increase the self-sealing capability, other reactive fluids were

investigated such as foaming materials. Two types of foams were studied: (a) polyurethane foams both rigid and flexible, and, (b) silicone foams both rigid and flexible.

3.3.3.1 Evaluation of Polyurethane Foams

The foaming materials are among the fastest growing segments of organic polymer families and one of the leaders is the urethanes. The recent advances in the development of polyurethane foams, and their generally attractive properties and characteristics suggested a possible application to self-sealing structures. The polyurethane foams are diisocyanate-linked condensation polymers which involve, in their preparation, a device for the formation of high polymeric molecules of predetermined structure. This device is a two-step reaction in which primary polymer chains terminating in reactive groups are treated with a bifunctional reagent adapted to react with these terminal groups and, thus, by uniting the primary chains, lead to molecules of a higher molecular weight. The material of the first step consists primarily of polyester or polyether resins and the material for the second step is a diisocyanate which reacts with the terminal group and, in presence of a blowing agent, forms the polyurethane foam.

The polyester resins are produced by the reaction of a dibasic acid and a polyol with the elimination of water. These resins, when used for polyurethane foam systems, have a number of unreacted alcohol groups which remain to react with the polyisocyanate in converting the low molecular weight-liquid polymer into a high molecular weight elastomer. Simultaneously, the excess of polyisocyanate reacts with water to generate the carbon dioxide (CO_2), the foaming agent. The reaction of the polyisocyanate and water also contributes to the cross-linkage of the structure and its final chemical composition. Less cross-linkage or less branching produces a flexible foam. More cross-linkage or more branching produces a less elastic structure, semi-rigid or rigid foam.

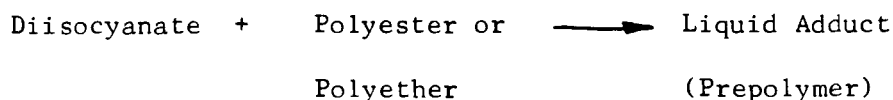
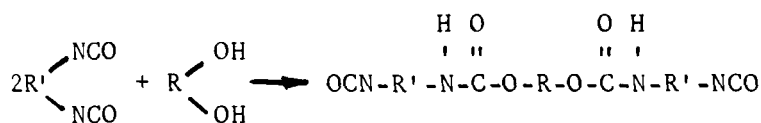
The polyester resins are produced by the catalyzed addition of propylene oxide to an alcohol by a reaction similar to the curing of epoxy resin systems. In the case of rigid foams, a few molecules of propylene oxide are added to the basic alcohol, while in flexible foam, many hundreds are added.

The polyisocyanates are chemicals derived from basic raw materials. Being very active and able to react readily with compounds containing active hydrogen atoms, as for example polyesters and polyethers, they permit combinations leading to many new synthetics. Differences in reactivity with other chemical groups enable control of the formulation and characteristics of the resulting synthetic foams with an infinite range of physical, thermal and chemical properties. These reactions usually take place quite readily at room temperature or with only moderate heating and the absence of catalysts. However, most of the reactions are greatly accelerated by small amounts of catalyst. The reactivity is usually more pronounced with aromatic diisocyanates than with the aliphatic derivatives. By choosing the right catalyst, the reaction can take place within 5 to 30 seconds. The diisocyanates have a tendency to form the dimers (the product of the first step in the reaction of two monomers) at room temperature when stored for long periods of time and, particularly, when exposed to the moisture in air. The addition of small amounts of phosphorous chlorides and acyl chlorides have been recommended to prevent any loss in reactivity.

In the original foaming method for polyurethanes, carbon dioxide is used as the blowing agent. In the new method, a low boiling chlorofluorinated hydrocarbon (Freon) is introduced into the catalyst portion of the components. When the catalyst is added to the polyurethane resin, an exothermic reaction takes place, raising the temperature of the mass above the boiling point of the Freon, causing it to expand and fill the cells. Freon blown foams are, in general, considered more stable than the carbon dioxide blown foams.

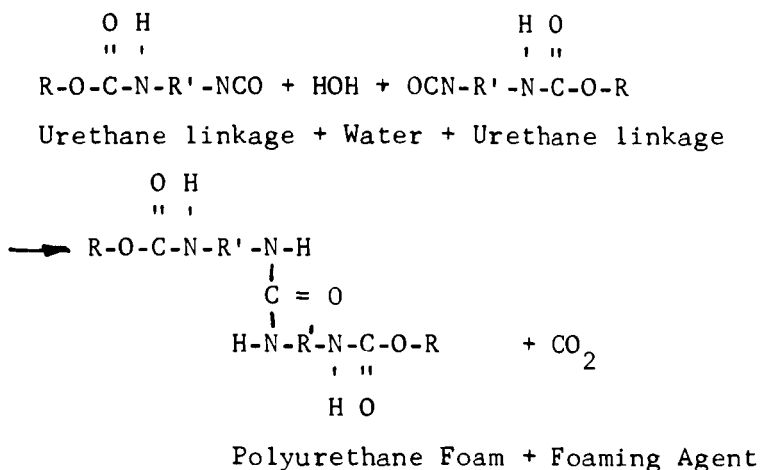
Because a basic understanding of the polyurethane foams chemistry is helpful in realizing the limitations of the application to the self-sealing panels, a brief description will be given here. Below, two of the most important primary reactions involved in the polyurethane formation are given:

In a first step, the polyfunctional compounds, diisocyanate (in excess) and polyester resin (or polyether resin), having unreacted alcohol groups react to form molecular chains terminated with isocyanate groups:



The obtained liquid adduct contains both active hydrogens and reactive isocyanate groups which continue to react with hydroxyl groups to form long chains. This reaction frequently has an induction period of from 5 to 10 minutes followed by a rapid evolution of heat. The rate of this reaction can be increased. The degree of increase will depend upon the base used. Strong bases can cause the reaction to become violent. Generally, when a base is used, a mildly basic tertiary amine is recommended. The reaction time of the polyurethane foam systems which is required for our chemical self-sealing systems is between 5 and 10 seconds. This is accomplished by adding small amounts of stannous octoate catalyst.

In the second step, the foaming reaction takes place. The free isocyanate groups react very readily with water in the following manner:



The carbon dioxide (foaming agent) is controlled by the quantity of water or amine present in the reaction mixture.

Among the polyurethane foam systems studied, concentrated effort was placed upon one obtained from Western Plastic Chemicals, Inc. in Santa Monica, California. This foam is Freon blown, thus, no excess diisocyanate is necessary as is the case in the CO₂ blown foams. As indicated previously, a small amount of stannous octoate is added to obtain a faster reaction (5 to 10 seconds). In preliminary tests to study the polyurethane foam application to self-sealing concepts, it was noted that a careful control of the rise time property was important.

The rise time is a measure of the time elapsed between initial mixing of the foam ingredients and the completion of the rapid expansion of the foam sample. Rise time is a function of the generated heat (amount and rate) and the Freon and stannous octoate concentrations. More precisely, the rise time will depend upon: (1) the mixing ratio resin

to diisocyanate, and (2) the degree and rate of mixing action. This will dictate the amount and rate of the generated heat which, in turn, will determine the very important parameter, namely, ratio of the rate of curing to the rate of blowing. If this latter ratio is too low, the foam will blow itself apart, that is, the formed cell ribs and membranes will not have sufficient strength and surface tension during the rise to withstand the forces caused by the gas evolution. Conversely, if the ratio is high, the polymer is rigidizing prior to sufficient foaming or rising, resulting in inadequate volume expansion. From this simple description, it can be seen that the reaction kinetics of any formulation are extremely sensitive to the chemical composition. Successful systems usually employ numerous additives whose quantity and function are determined mainly by experiment.

During a series of tests whereby several self-sealing structures using a polyurethane system, were impacted with 1/8-inch steel pellets at the lower velocities ($\sim 7,000$ fps), the following disadvantages were noted:

- (1) The high reactivity of the diisocyanate with compounds containing active hydrogen atoms. As mentioned above, it polymerizes at room temperature when exposed to the air moisture, which makes it fairly unstable, and it becomes less reactive. However, this can be remedied by using small amounts of specific chemicals.
- (2) The impracticability of most of the polyurethane foams being blown by either carbon dioxide or by Freon which will affect the shelf-life of the material and the self-sealing effectiveness of the self-sealing structures.

In the case where carbon dioxide is used as the blowing agent, an excess of diisocyanate is necessary in order to have free isocyanate groups to react with water and form the carbon

dioxide. However, upon impact of the self-sealing structure containing such a foaming system, the proportion of diisocyanate to resin cannot be controlled, and therefore, in some cases, no excess of diisocyanate is present and no blowing agent is formed.

In the case where Freon is used as the blowing agent, the problem is the escape or degassing of the Freon from the foaming ingredients. The degree of escape of the Freon will depend upon the environment in which the foaming ingredients will be before or during the foaming activity. Most severe degassing takes place when the Freon containing ingredients are exposed to vacuum and to temperature variation, particularly to high temperatures for a long period of time. The loss of the Freon blowing agent under such conditions, prior to or during the foaming action, could create a serious problem to the point where no foaming action could take place upon mixing of the two reactive fluids (resin and diisocyanate). However, this problem of degassing of the blowing agent could be prevented to some extent by encapsulating the Freon-containing liquid. For higher temperature exposure, a higher boiling Freon could be used. Upon foaming reaction, the Freon would then either be expanded by the heat surrounding the foaming ingredients at the time of the foaming activity, or by the heat generated from the chemical reaction, depending on which of the heat sources would give the temperature at or above the Freon boiling point.

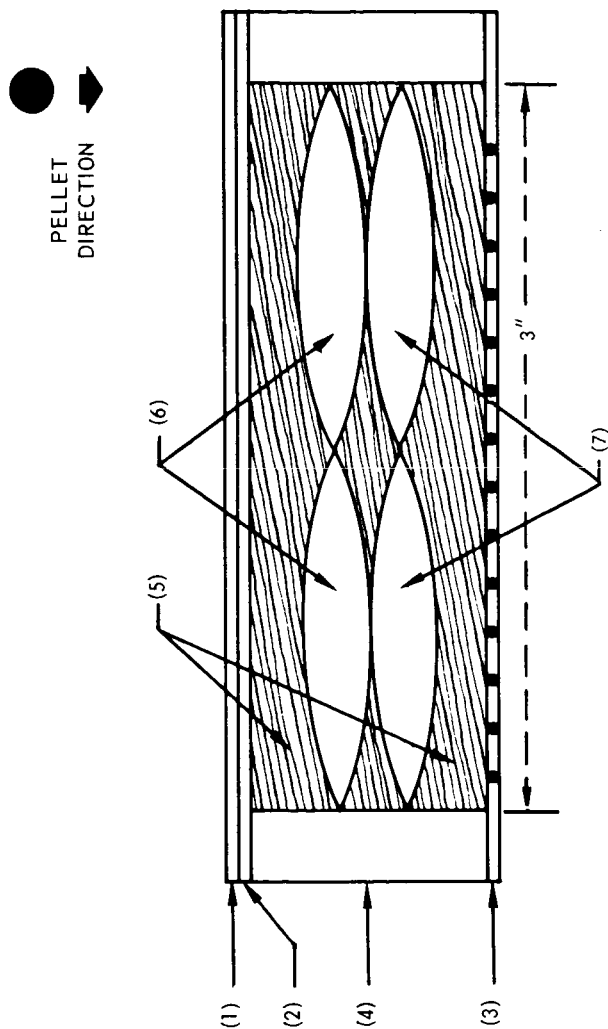
- (3) The collapsing of the formed foam due to the reaction between, for example, the polyether and diisocyanate which had not proceeded far enough for the foam to support its own weight in the case where carbon dioxide is used as the blowing agent. However, today a remedy exists to correct this. A number of

copolymers of polyethers and silicones can be used. These retain the surface activity of the silicones (low surface tension, low internal energy, low polarity) and play the role of stabilizers in polyether urethane foams because of their stability and solubility in water, alcohols and other organic solvents. Once the foam is formed, they stabilize the foam and prevent the collapsing.

To check the feasibility of the use of some of the above discussed polyurethane foams as self-sealing materials, a number of tests were performed with combined mechanical-chemical self-sealing structures (Rigid Polyurethane Foam/Fiber Mat or Elastomeric Spheres Concept) at impact velocities of approximately 7,000 fps. An attempt was made to test a similar configuration at higher velocities (up to 20,000 fps) using the Northrop Light Gas Gun Facility. However, because the sabot and stripper debris hit the structure, an evaluation of the shot was impossible. Nevertheless, tests at 7,000 fps allowed us to screen several self-sealing configurations and come up with a configuration giving us good results. The geometry of this last configuration (see Figure 3-5) was designed so that all the polyurethane foam ingredients could be encapsulated in order to prevent the Freon from escaping and the diisocyanate from polymerizing before puncture.

Based on these tests, the following conclusions were drawn:

- The foaming activity should be confined to the interior of the panel.
- By choosing the proper amount of foaming ingredients and an appropriate structure configuration, one can cause the foam product to completely fill all interior interfaces of the self-sealing structure.
- The presence of an energy absorber (or compressible material) surrounding the foam chemicals assists in damage localization and self-sealing capability.



- (1) EPOXY LAMINATE (2 PLY FIBERGLASS; 60% VERSAMIDE 125 + 40% EPON RESIN 828)
- (2) NITRILE RUBBER SHEET (AMS 3212 J, 1/16" THICK)
- (3) EPOXY LAMINATE PERFORATED (2 PLY FIBERGLASS; 60% VERSAMIDE 125 + 40% EPON RESIN 828)
- (4) HONEYCOMB CORE STRUCTURE 15/16" THICK
- (5) ASBESTOS FIBERS (3R12)
- (6) PLASTIC BAGS (MYLAR FILM) CONTAINING WESTERN PLASTIC'S CATALYST
- (7) PLASTIC BAGS (MYLAR FILM) CONTAINING WESTERN PLASTIC'S RESIN + NUOCURE 28 (10:1)

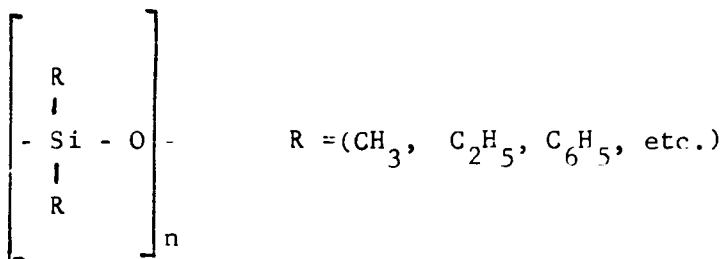
**FIGURE 3-5 POLYURETHANE FOAM + FIBER MAT
CONCEPTS COMBINED - CONFIGURATION**

- Encapsulation of all the polyurethane foam ingredients will prevent leakage problems, that is, retain the Freon within the system and prevent the diisocyanate from polymerizing.
- With the most successful configuration whereby the chemical ingredients were all encapsulated, the mixing ratio resin to diisocyanate was always in the proper range so that an appropriate ratio of the rate of curing to the rate of blowing could be obtained.

3.3.3.2 Evaluation of Silicone Foams

A brief discussion of the chemistry of the silicone polymers in general is presented here in order to convey a better understanding of the type of material used and its applicability to the chemical self-sealing structures.

The silicones are a class of polymers of considerable commercial importance. They are based on a linear, cyclic, or cross-linked arrangement of alternating silicon and oxygen atoms, where the silicon is substituted by organic radicals or hydrogen. This class of polymers is formulated as follows:



Organopolysiloxanes

The usual procedure for preparing silicone polymers is to hydrolyze compounds of the type: R_3SiCl , R_2SiCl_2 , RSiCl_3 , SiCl_4 . The intermediates in the reaction are believed to be the corresponding silanols

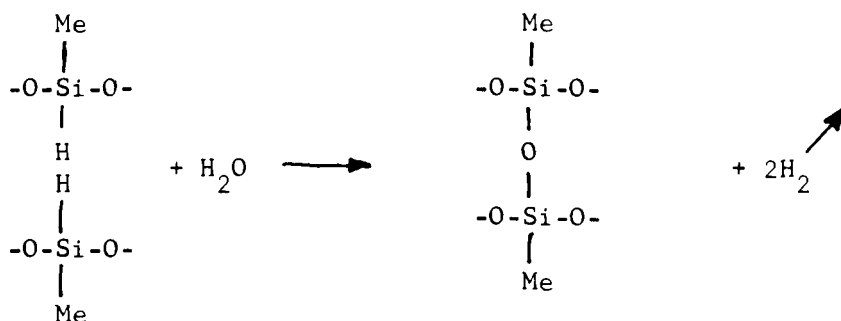
$\text{R}_2\text{Si}(\text{OH})_2$ which condense very rapidly with elimination of water and formation of the $-\text{Si}-\text{O}-\text{Si}-$ link. If (n) ranges from 3 to 9, cyclic systems

are obtained which in the presence of alkaline catalysts open and give high molecular weight, linear silicone gum and, subsequently, elastomers. Various curing techniques are available for converting linear and cyclic materials to cross-linked elastomers and resins.

The manufacture of silicone elastomers is divided essentially into two steps, compounding and cross-linking. The first step consists of the intimate mixing under high shear or milling of the polysiloxane gum, a filler, and usually a cross-linking agent, together with miscellaneous additives for obtaining desired physical properties. The second step involves the cross-linking and curing processes that connect the polymer molecules with one another into an elastomeric mass of the desired properties. It is this second step which was of importance to us in the evaluation of elastomeric ingredients to be incorporated in our self-sealing structures.

In the first step, the compounded stock may be cross-linked by the action of organic peroxide such as benzoyl peroxide. The number of cross-links can be controlled by varying the amount of peroxide (catalyst) used.

In the materials evaluation studies, the silicone foams were of particular interest. These are obtained by catalyzing either a fluid silicone rubber or a fluid silicone resin, either containing a hydrogen foaming source and giving, respectively, a flexible silicone foam and a rigid silicone foam. In this foaming system, the foaming agent (hydrogen) is released upon mixing of either of these two fluids with the appropriate catalyst. A large variety of hydrogen sources exist, but the most interesting one has a releasing mechanism that is initiated at room temperature and is accelerated with the exothermic chemical reaction taking place when the silicone base fluid and catalyst are mixed. Such a hydrogen foaming source could be obtained by the following chemical system:



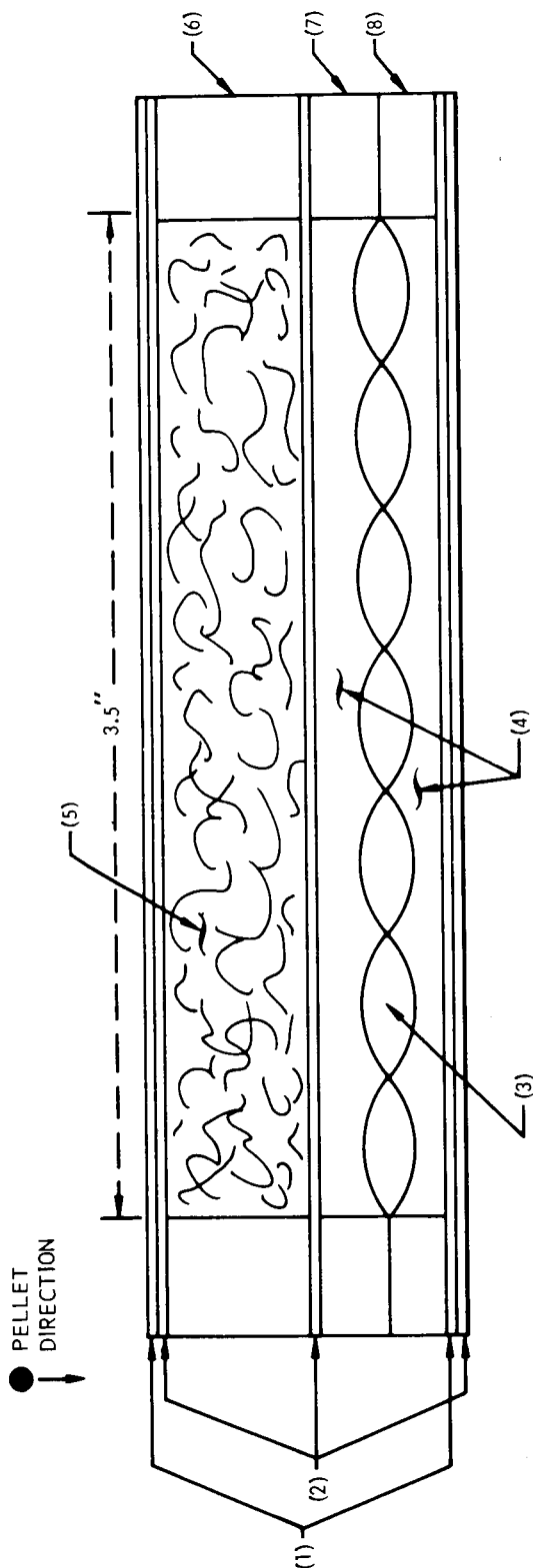
This reaction is very feasible due to the sensitivity of the silicone-hydrogen bond to acid and especially to base catalysts.

In our investigation for such a silicone foaming system, we came across a system which yielded excellent results as self-sealing material when incorporated in our chemical self-sealing concepts. It is a two-phase system (fluid silicone rubber or resin plus catalyst) where no excess of one of the foaming ingredients is necessary for the formation of the blowing agent and where the blowing agent is chemically formed upon mixing of the fluid foaming base and a catalyst. Because of the proprietary nature of this material, the nature of the hydrogen source and the release mechanisms are unknown.

This foaming system was located at Dow Corning Corporation, Midland, Michigan. The material is a RTV (Room Temperature Vulcanizing) silicone foam, either flexible or rigid. The flexible silicone foam is a low-density resilient rubber over a temperature range of -100 to +500°F. and it cures at room temperature. It is supplied as a fluid silicone rubber base (D.C. S-5370) with a separate catalyst (D.C. S-5370). When base and catalyst are mixed together in the proper proportions, expansion and curing begin immediately. When the foaming activity is not confined to a restricted area, the foam will expand approximately seven times its original volume. During the expansion period, a small amount of hydrogen gas (blowing agent) is evolved from the reacting material.

The rigid silicone foam is a low-density foam which is supplied as a fluid silicone resin (D.C X R6-3700) with a separate catalyst (D.C. X R6-3700). Here, too, if the two-phases are mixed properly, expansion and curing begin immediately. Similar to the flexible foam, the blowing agent (hydrogen) is generated from the reacting material. By substituting the Nuocure 28 catalyst for the DC X R6-3700 catalyst, the expansion is accelerated appreciably, the curing time is shortened, and the reactions take place within seconds. However, by making this same substitution for the flexible foam, the expansion and cure was accelerated only slightly and was below the rate of expansion and cure of the rigid foam. Particularly, at the higher velocity shots, the type of catalyst used depends upon the chemical system used and the self-sealing structure configuration. As, for example, when comparing the structure configurations "Rigid Silicone Foam/Fibers or Spheres" (see Figure 3-6) and "Rigid Silicone Foam/Balsa Wood or Air Gaps" (see Figures 3-7 and 3-8) the type of catalyst used will not have to respond as fast in the first configuration as it will have to in the second concept. The obvious reason for that is, that, in the first case we are in the presence of spheres or fibers which will, upon impact, perform a partial or complete seal and thus prevent efflux of the foaming materials. However, in the second case, the balsa wood or air gaps will attenuate the shock wave effect and absorb the energy, but will not seal partially or completely the puncture and, thus, prevent heavy losses of materials.

In the search for the proper agent to be used for the curing and foaming of the fluid silicone base giving, on impact, either a flexible or rigid foam, a catalyst was found which gave significant improvement in higher curing and foaming rates making the chemical self-sealing systems even more effective. With this curing agent, the rates are almost identical for the flexible and rigid foams. This new catalyst was found to be more uniform in its activity and possessing superior performance to the other stannous octoate catalysts in "one-shot" foams. It also maintains its activity for a longer period of time.



- (1) EPOXY LAMINATE (3 PLY FIBERGLASS; 55% VERSAMIDE 125, 45% EPON RESIN 828)
- (2) NITRILE RUBBER SHEET (AMS2312J, 1/32" THICK)
- (3) CHAIN OF PLASTIC BAGS (MYLAR PLASTIC FILM) CONTAINING NUOCURE 28 AND BONDED TO THE HONEYCOMB STRUCTURE SIDES TO AVOID SLIPPAGE OF THE BAGS WHEN PANEL IS TESTED.
- (4) XR-6-3700 RIGID SILICONE FOAM RESIN
- (5) ASBESTOS FIBERS (3 R 12) OR RUBBER SPHERES (3/8" DIA.)
- (6) HONEYCOMB STRUCTURE, 1/2" THICK
- (7) HONEYCOMB STRUCTURE, 1/4" THICK
- (8) HONEYCOMB STRUCTURE, 3/16" THICK

**FIGURE 3-6 COMBINED CONCEPT - RIGID SILICONE FOAM/ FIBER MAT
OR RUBBER SPHERES CONCEPT - CONFIGURATION**

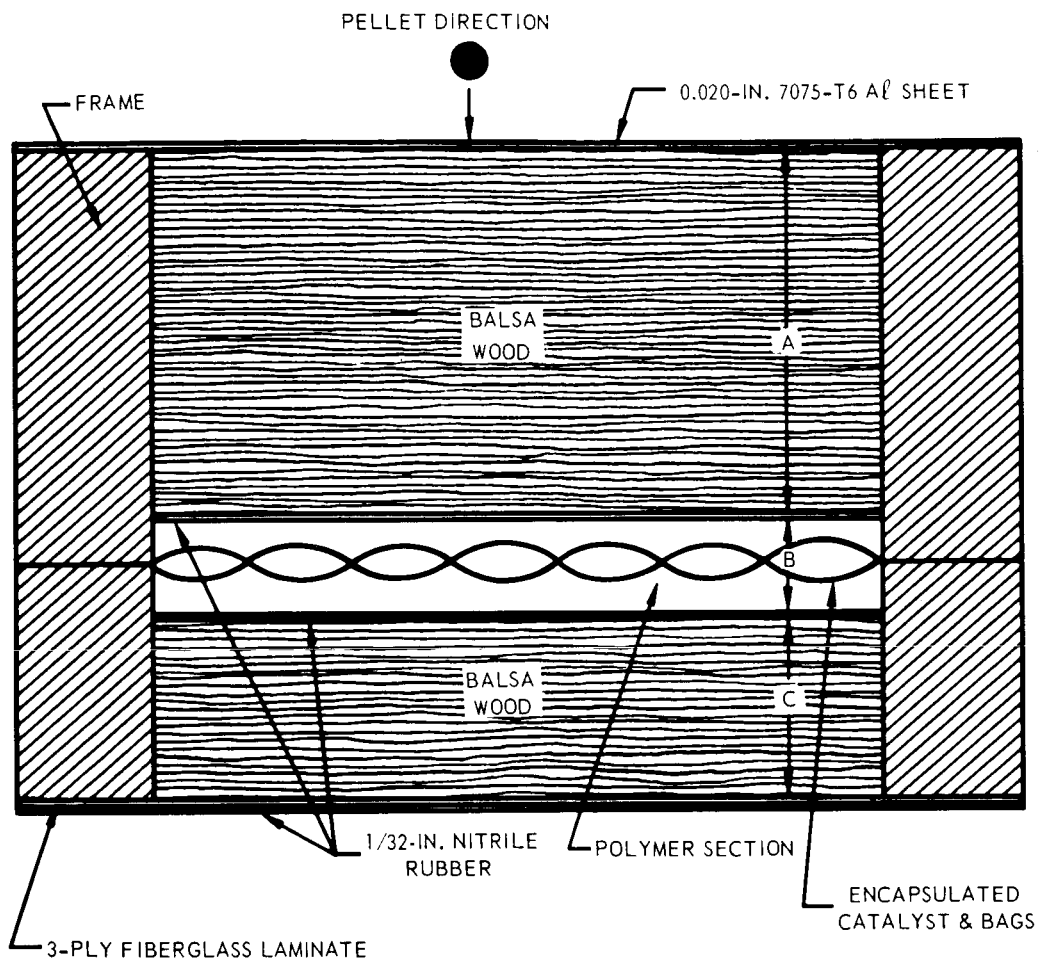


FIGURE 3-7 BALSA WOOD/SILICONE FOAM CONCEPT

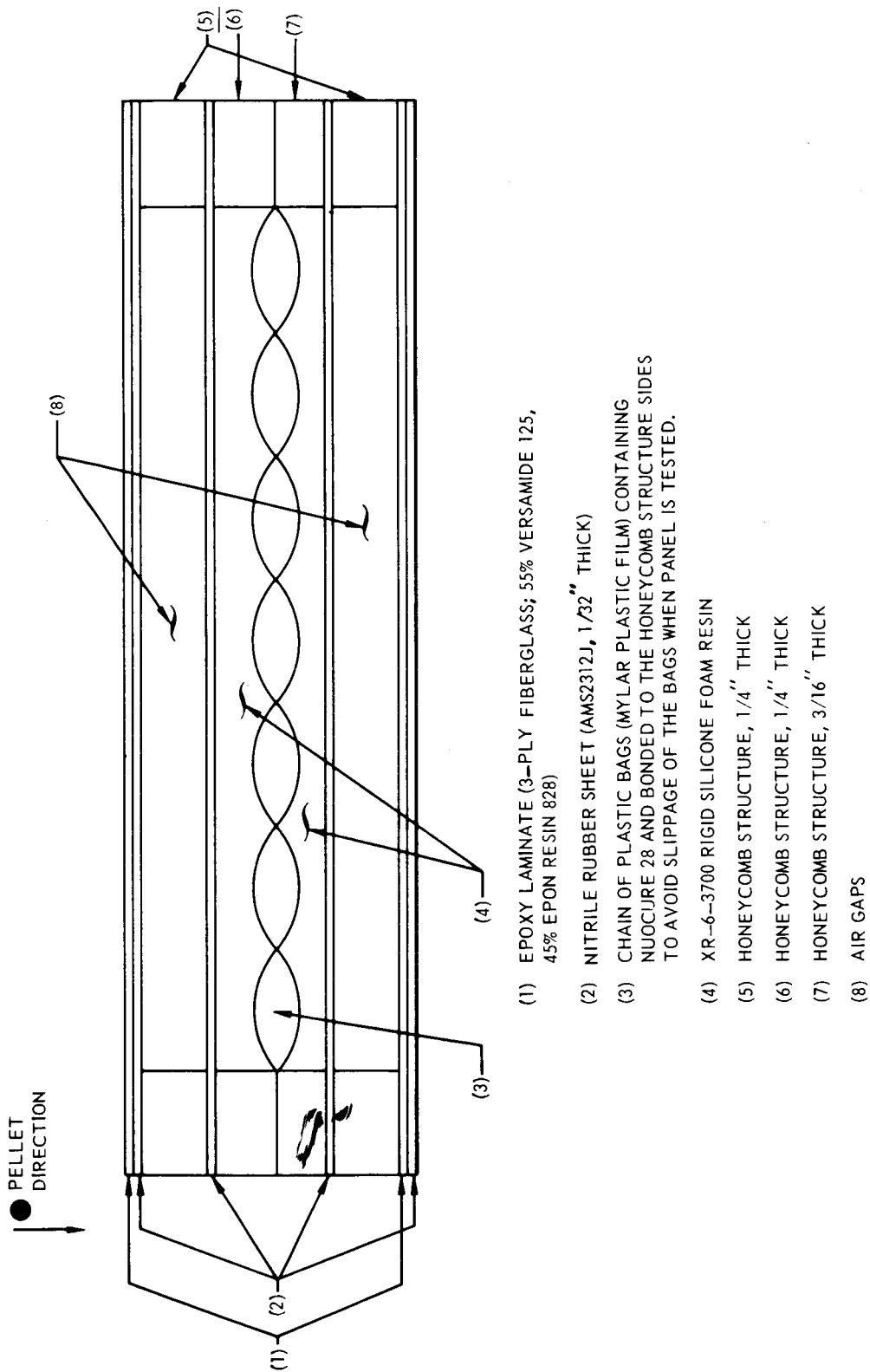


FIGURE 3-8 RIGID SILICONE FOAM/AIR GAPS CONCEPT - CONFIGURATION

Within the chemical reactions taking place for the formation of the silicone foams, two actions occur: (1) a curing action and (2) a foaming action. In order that the formation of these foams can be used in the most effective way in chemical self-sealing concepts, the ratio of curing rate/foaming rate should be kept within a reasonable range. This ratio will vary drastically depending upon: (1) the type of catalyst used, (2) the mixing proportion of the fluid silicone base and catalyst, (3) the degree of mixing (or dispersion) of these two components, (4) the heat generated upon mixing, and (5) the size of the puncture obtained in the self-sealing structure after impact. The ratio should always be lower than one, but not excessively lower, because too low a value will cause heavier losses of foaming materials through the punctured hole. Such cases were experienced with some panels using the "Rigid Silicone Foam/Balsa Wood or Air Gaps Concept". By using a faster curing agent, this situation can be overcome.

In the case where the ratio is too high, the silicone foam will set itself prior to sufficient foaming, resulting in inadequate volume expansion. Such a case was never experienced in the development of the present silicone foam concepts.

From the above, one can say, that the closer the ratio approaches one without exceeding it, the more effective the self-sealing action will be at higher velocities.

During most of this year's research program, tests were performed to demonstrate the feasibility of foaming materials and help to improve the self-sealing capabilities of the self-sealing structures. A variety of self-sealing structures were prepared which contained a foaming system either combined with the fibers, the elastomeric balls, the balsa wood or air gaps. All these structures were combined systems for the reason explained earlier; namely, trying to alleviate the shock wave effects and minimizing excessive structure damage and material removal. This was done by isolating the chemical components from the face sheet(s) (either metallic

or nonmetallic) of the self-sealing structure by interposing a highly compressible material (fibers, balls, etc.) between the chemical compartment walls and the face sheet(s).

These materials were incorporated into the following self-structure configurations which were evaluated at low velocity - 7,000 fps (for preliminary tests), medium velocities - 10,000 to 15,000 fps and higher velocities up to 26,000 fps, using primarily 1/8-inch diameter steel pellets:

- Rigid Silicone Foam/Fiber Mat or Rubber Spheres Concept
- Flexible Silicone Foam/Fiber Mat or Rubber Spheres Concept
- Rigid or Flexible Foam/Balsa Wood Concept
- Elastomeric Spheres/Viscous Face Concept
- Rigid Silicone Foam/Air Gaps Concept
- Rigid Silicone Foam/Rubber Spheres/Air Gap Concept

During these tests, very promising results were obtained to indicate that the techniques used for attenuating the shock wave effects are proving effective in minimizing structure damage and giving highly successful sealing capability at the higher velocities.

Results of all the tests mentioned above and other phases of the evaluation program of the self-sealing structure configurations are presented in Section 4.0 "Experimental Program."

3.4 TEMPERATURE DEPENDENCE OF SELF-SEALING CAPABILITY

The heat input to a vehicle in space is determined by the intensity and spectral distribution of the thermal radiation incident upon its surface and the absorptivity of the surface for such radiation. For a vehicle operating within the solar system, such radiation is predominantly solar radiation. For moon vehicles, the reflected and emitted radiation from the earth is normally not considered. For interplanetary missions, the reflected and emitted radiation from the destination planet will have to be

considered. The heat dissipation likewise occurs by radiation.

During space missions to the moon or interplanetary missions, the temperature outside the spacecraft may fluctuate between $+200^{\circ}\text{F}$ and -270°F . These temperature extremes will affect the self-sealing capability of the self-sealing structures. The high temperature alone will not affect the self-sealing capability of the selected materials, but combined with the hard vacuum of outer space (down to 10^{-14} mm Hg.) it will present a problem of stability particularly in the vicinity of the impact area where base polymeric materials will be exposed to the total space environment. The larger the entry hole, the more area will be exposed. Polymeric materials exposed to such environment will be affected by the volatilization process which includes such properties as weight loss, changing composition due to fractional distillation and variation of permeability due to internal changes in structure.

According to the Langmuir equation (with which the rate of weight loss can be obtained for a pure material), the weight loss would be immeasurably small for periods of years at moderate temperature for any of the cross-linked polymeric material of current engineering importance. However, most polymers undergo thermal and oxidative degradation into lower molecular weight fractions which are considerably more volatile than the base polymer. Other polymer ingredients can be volatilized under these environmental conditions such as the plasticizers which have relatively high vapor pressures.

The low temperature range which will exist in outer space will affect seriously the self-sealing capabilities of the self-sealing structures. Particularly, the polymeric materials may be greatly affected. The extent will vary depending upon the selection of materials used in the self-sealing structures.

Regarding the chemically activated self-sealing concepts, the speed of the sealing action will decrease to the point where there will be no self-sealing action left, particularly for the extremely low temperatures. The self-sealing process at low temperature will be limited and will depend upon the temperature range existing at the time of puncture and upon the materials and self-sealing concept used. Among the mechanically activated concepts, the elastomeric spheres concept will probably offer the best possibilities to self-seal at the very low temperatures. In the case of the chemically activated concepts, the self-sealing action may be improved, for the lower portion of the subzero temperature range, by initiating an exothermic reaction on puncturing or by using new improved elastomeric materials for cryogenic application.

The high temperature range existing in outer space will improve the speed of the sealing action. The degree of improvement will depend upon the polymeric materials selected and the type of self-sealing configuration used. In the case of the elastomeric spheres concept, the sealing is not going to be necessarily faster, but it should be more effective. Regarding the chemically activated concepts, the chemical reaction rates will increase with increasing temperature, subject to the limitations of degradation of the component materials. In a fluctuation from high to cryogenic temperatures, hermetically and mechanically sealed punctures will probably be affected if the proper material is not chosen. With respect to the chemically activated concepts, this problem will be less accentuated.

In addition to the temperature and vacuum effect on the self-sealing structures, radiation will be another important environmental exposure condition to affect the self-sealing structures' materials and their self-sealing capabilities. However, the effects of this third environmental condition will not be extensively discussed here, or just enough to say that the polymeric materials inside the self-sealing structure exposed to the type of radiation existing in space will undergo varying amounts of

change either by cross-linking or scission processes or by molecular rearrangement. The degree of change will depend upon the type of polymeric material used, the shielding of the material against radiation and the portion of the spaceship trajectory in space through which the vehicle will be traveling at the time (which directly dictates the self-sealing structure temperature, the intensity and the duration of environmental exposure).

We have recently initiated a task whereby the more successful self-sealing structures configurations are being evaluated by determining their environmental limitations to extreme temperature exposures. Test results were not available for inclusion in this report but will be reported at a later date.

4.0 EXPERIMENTAL PROGRAM

4.1 EQUIPMENT AND TESTING PROCEDURE

The major apparatus used during this year's research program were: (1) the Northrop Space Laboratories' Particle Accelerator combined with the leak detector, (2) the Northrop Light Gas Gun combined with the leak detector, (3) the McGill University Light Gas Gun, and (4) a new gun facility for ballistic testing of heated and cooled targets in a high vacuum.

4.1.1 The Northrop Space Laboratories' Particle Accelerator. This particle accelerator (Figure 4-1) can propel 1/8-inch diameter projectiles down a 2-foot long barrel by an explosive gun powder discharge from a modified 25-calibre rifle cartridge. Smaller than 1/8-inch projectiles can be propelled if one uses an appropriate sabot-pellet separation technique. Projectile velocity measurements are obtained by means of a velocity measuring trigger break screen circuit for use with a Tektronix 545 oscilloscope. The gun barrel is enclosed in one end of a transparent plexiglass chamber while the other end has an opening for mounting of the test structure. The test structure is mounted to form an air tight seal with the chamber. The chamber is then evacuated to between 0.4 and 0.5 Torr to give a pressure differential across the specimen of approximately one atmosphere. Upon impact of the self-sealing structure, the sealability of the structure can be checked by means of a leak detection apparatus. This apparatus is attached to the vacuum chamber of the particle accelerator as illustrated in Figure 4-1. A method of air flow analysis was developed that permits the calculation of mass loss rate of air through punctured structures at various differential or driving pressures across the puncture.

The leak detection or air flow apparatus may be used as a separate unit or attached to the vacuum chamber of the particle accelerator. In this latter setup, the self-sealing structure can be tested under simulated

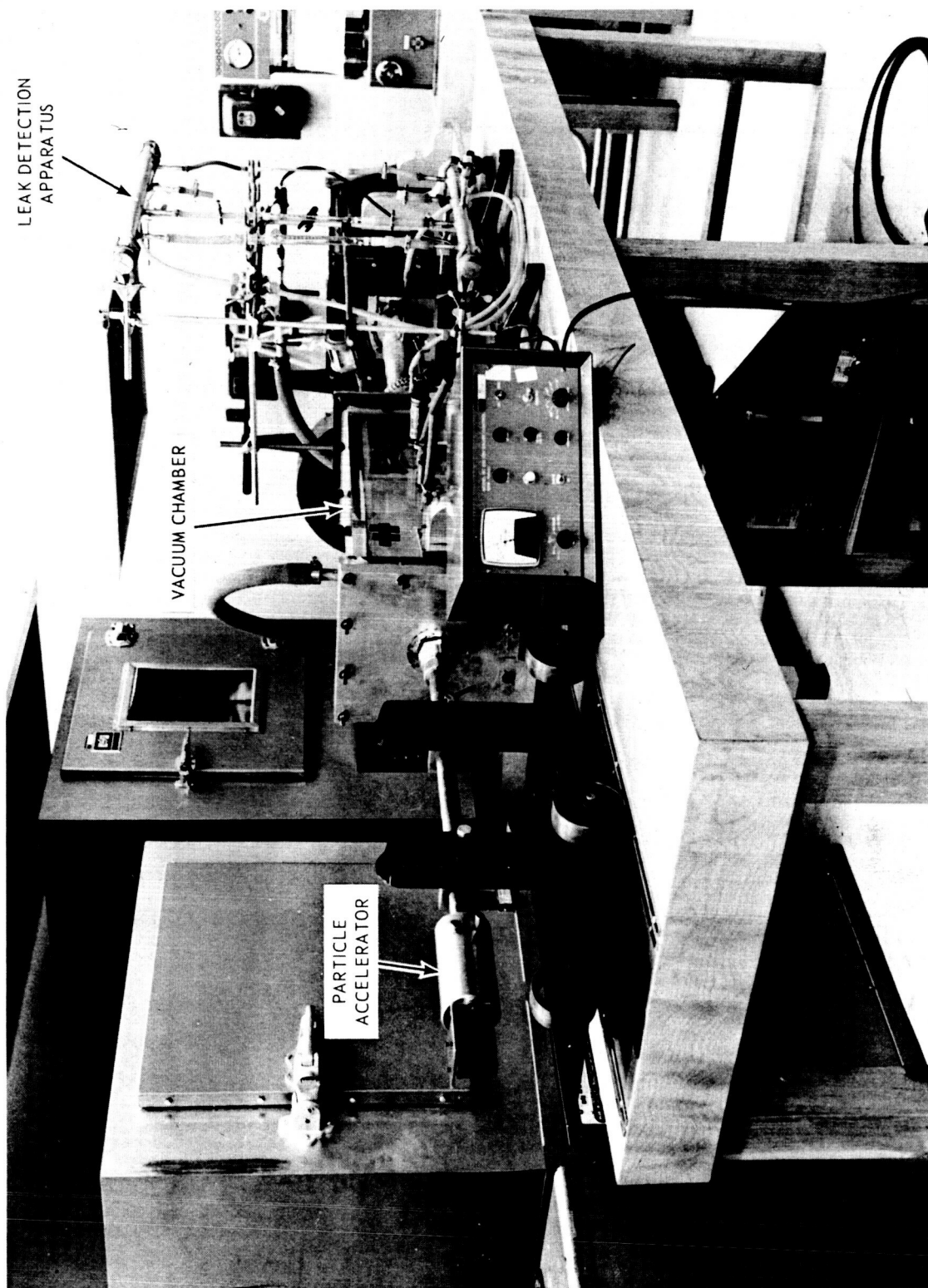


FIGURE 4-1 NORTHROP PARTICLE ACCELERATOR

space vacuum conditions and air flow rates generated immediately following puncture by a projectile.

4.1.2 The Northrop Light Gas Gun Facility. Northrop's Nortronics Division has designed and built a light gas gun of the ARO type which is shown in Figures 4-2A and 4-2B. The gas gun is approximately 21-feet in length, and is constructed from 4340 steel with most of the parts being constructed from standard tubing.

Also shown in Figures 4-2A and 4-2B is the Nortronics 41-cubic foot combination explosion-vacuum chamber used with the light gas gun for evaluation of simulated meteoroid impacts to various space structures.

The design of both gun and vacuum chamber has been predicated on versatile usage. For example, provisions exist for extending the gun launch tube length and for changing launch tubes to provide various bore diameters. Likewise, the vacuum chamber may be used as an explosion chamber as well as a vacuum chamber.

The current hypervelocity program at the Nortronics Division was initiated to study cratering and damage evaluation of high speed particles impacting targets in the atmosphere at ambient pressures. This program was explored until velocities of 12,500 fps were achieved with a 5 gram aluminum projectile. The program produced impact data for design of ordnance items. To date, solid steel, aluminum and Lexan projectiles have been fired against steel and aluminum targets of varying thickness. Composite projectiles composed of: (1) polyurethane sabots carrying steel, lead, or glass particles, (2) aluminum capsules containing tetryl (explosive), and (3) Lexan plastic capsules containing mercury have also been fired against steel and aluminum.

The 41-cubic foot vacuum chamber is capable of achieving a vacuum to 0.5 mm of Hg with mechanical pumps after one-half hour of pumping time. The

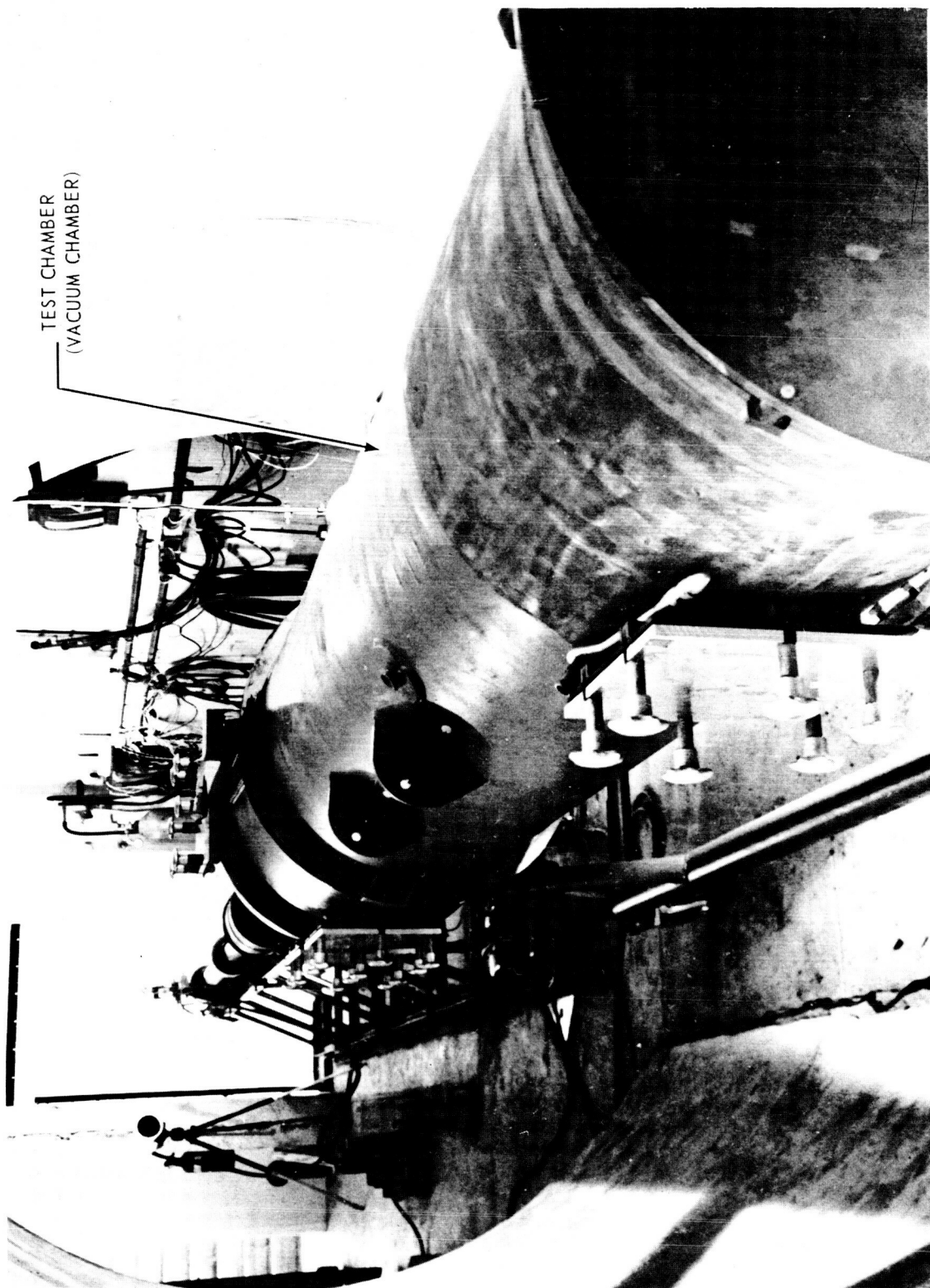


FIGURE 4-2A NORTHROP CORPORATION - LIGHT GAS GUN FACILITY (VACUUM CHAMBER)



FIGURE 4-2B NORTHROP CORPORATION - LIGHT GAS GUN FACILITY

increased velocity and impact phenomena dictated that a flash X-ray would be desirable to record velocity and the actual orientation of projectile both during flight and at impact.

The Northrop light gas gun now utilizes a Flexitron 720 three-channel flash X-ray unit. In addition, a velocity measuring trigger break screen circuit for use with a Tektronix 545 oscilloscope has been incorporated. During firings, stress data are also recorded on strain gauges mounted on the gun's high pressure section and combustion tube. The light gas gun to date has achieved velocities in excess of 22,000 fps for a 1/8-inch diameter steel projectile.

4.1.3 The McGill University Light Gas Gun Facility. The principle of this gun is very similar to the Northrop Light Gas Gun with the only difference that here a three-stage system is used and hydrogen gas is employed instead of helium as the compressed gas. The effectiveness of this gun is particularly due to the use of a very ingenious sabot-pellet separation technique and to the effective utilization of the gas compressing forces with the help of the proper propellant selection. This gun has propelled a large variety of projectiles (Mg, Al, Lexan, Steel, etc.) with diameters varying from 1/32-inch to 1/2-inch and at velocities up to 35,000 fps. Just recently in a hypervelocity test, a 1/8-inch diameter magnesium particle was accelerated to a velocity of 39,500 fps.

4.1.4 New Gun Facility for Ballistic Testing of Heated and Cooled Targets in a High Vacuum. Figure 4-3 shows this facility which is being used in a research program just recently started, whereby some of our most successful self-sealing structures are being tested for their temperature dependence (elevated and cryogenic) of self-sealing capability.

4.2 MECHANICAL SELF-SEALING CONFIGURATIONS

4.2.1 Elastomer Sphere Concept. Basic details of the panel configura-



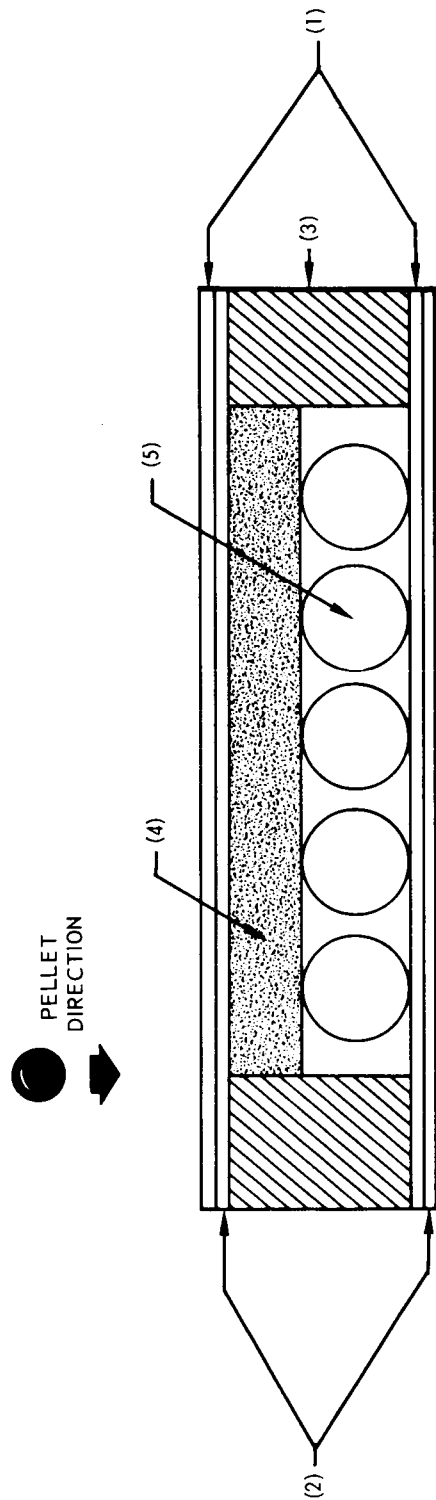
FIGURE 4-3 GUN FACILITY FOR BALLISTIC TESTING OF HEATED AND COOLED TARGETS IN A HIGH VACUUM

tion which has consistently demonstrated effective self-sealing action are shown in Figure 4-4. The dynamic action of a meteoroid while puncturing a pressurized compartment, causes the escaping fluid to set up a local dynamic imbalance across the hole. The working principle of this concept depends on the force generated by the pressure differential across the puncture in drawing a sphere to the hole and effecting a seal.

The sealing capability of the illustrated panel configuration has been experimentally demonstrated by puncturing the panel with a 1/8-inch diameter steel sphere at an impact velocity of 24,700 fps. Effective sealing action resulted with a residual air leakage rate (across a 14.7 psi pressure differential) of 1.3 lbs/day. Without the spheres to seal the 3/16-inch diameter hole in the pellet entry face, the air leakage rate would have been 595 lbs/day. The pellet exit face of the panel sustained an irregular hole approximately 7/16-inch in diameter. The punctured panel is shown in Figure 4-5.

From an evaluation of test results conducted with panel configurations using the elastomer sphere self-sealing technique, the following concluding statements may be made:

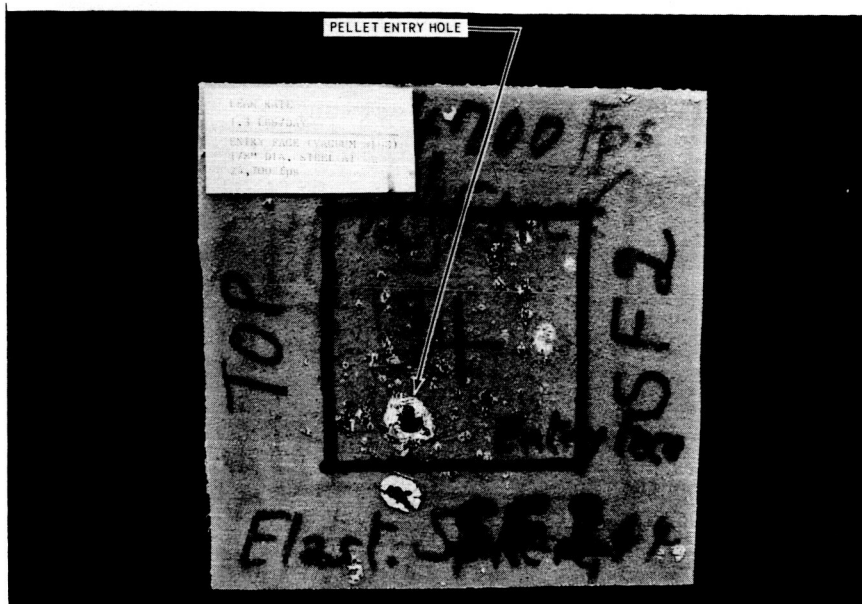
- The Elastomer Sphere Self-Sealing Concept is one of the simplest in design and can easily be incorporated into a double wall panel configuration.
- Of all the concepts evaluated, it is the lightest in weight since a weight addition of 0.31 lbs/ft² will give a double wall panel self-sealing capability.
- For successful sealing, a fairly clean punctured hole in the sealing face is required. For single thickness metallic or plastic pellet entry sheets, the inner face (sealing surface) of the punctured sheet must be free from radial cracks, petalling of the hole



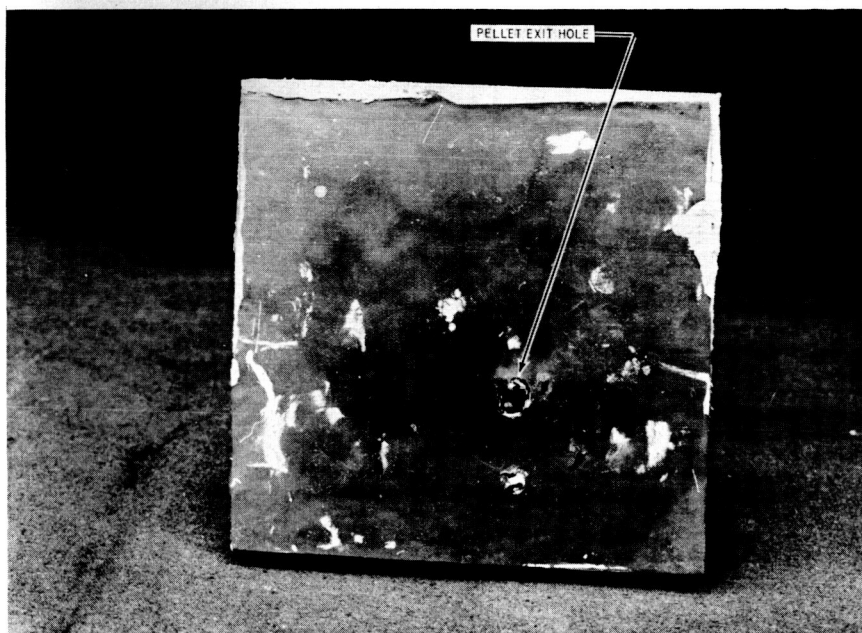
- (1) EPOXY LAMINATE (3-PLY FIBERGLASS; 60% VERSAMIDE 125; 40% EPON RESIN 828)
- (2) NITRILE RUBBERS SHEET (AMS3212J, 1/32" THICK)
- (3) HONEYCOMB CORE STRUCTURE, 5/8" THICK
- (4) SPONGE RUBBER (0.06#/FT²) 1/8" THICK
- (5) EXPANDED NATURAL RUBBER SPHERES (3M-EC1878), 3/8" DIAMETER

FIGURE 4-4 SELF-SEALING PANEL - ELASTOMER SPHERE CONCEPT

PROJECTILE: 1/8" DIA STEEL SPHERE
VELOCITY: 24,700 FPS



PELLET IMPACT FACE



PELLET EXIT FACE

FIGURE 4-5 PUNCTURED ELASTOMER SPHERE SELF-SEALING PANEL CONFIGURATION

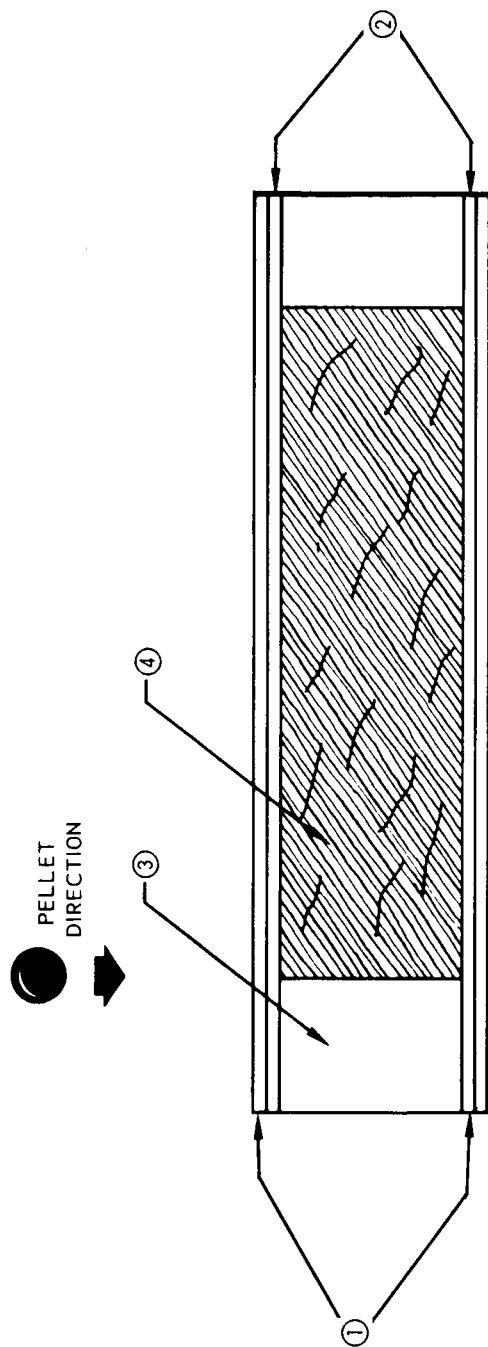
boundary and, in the case of laminated materials, free from delamination.

- The more pliable the sealing surface and/or elastomer spheres, the more effective will be the sealing action.
- In the panel configurations evaluated, sufficient spheres were used in the panel cavity (4 spheres/in²) to ensure that no sphere had to be moved an appreciable distance against the earth's gravitational attraction to seal the puncture. However, in the Zero-"G" conditions of space, the spheres would be "weightless" and the slightest imbalance, due to the escaping fluids, would cause them to move into the puncture. Therefore, it is expected that, for operation in a space environment, the number of spheres required to provide adequate protection could be reduced by a factor of at least two (i.e., 2 spheres/in²).
- A pertinent parameter that will affect the sealing effectiveness of this concept is the ratio of puncture diameter (D_p) at the sealing surface to the elastomer sphere diameter (D_s). For $\left(\frac{D_p}{D_s}\right) = 1$, the spheres would be drawn through the puncture without sealing or a bridging action by a few spheres might occur, in which case partial sealing will result. For very small holes, or $\left(\frac{D_p}{D_s}\right) \ll 1$, the sealing force may not be sufficient to properly seat the sphere in the puncture, in which case mechanical vibration may unseat the sphere from the hole. A possible solution would be to use a variety of sphere diameters so as to establish favorable $\left(\frac{D_p}{D_s}\right)$ ratios for the range of expected puncture sizes, whereby it would be expected that the smaller spheres would be more readily drawn to the smaller holes (since a smaller driving force would be required to move the smaller spheres). Another solution would be to incorporate into the panel configuration techniques for causing the sphere to adhere

to the sealing surface once it has been drawn to a puncture. This latter technique is described in detail in Section 4.3.5.

4.2.2 Fiber Mat Concept. The mechanism of this concept, whose configuration is given in Figure 4-6, depends upon the mobility of a fiber when subjected to a pressure differential, to flow or move into a low pressure area and become grossly entangled while attempting to pass through a small opening caused by the passage of a particle. Testing of this concept at low velocities ($\approx 7,000$ ft/sec.) yielded leak rates of about 5 lbs/day compared to a 260 lb/day leak rate for a 1/8-inch diameter hole. The testing program was continued at higher velocities ($> 15,000$ ft/sec.) with the Northrop light gas gun. Associated with the increased velocity of the particle, was the increased structural damage to both the entry and exit faces of the panel and increased material removal from the front face. Generally, the hole diameter of the front face increased from about an effective diameter of 1/32-inch at 7,000 ft/sec. to about 1/4-inch at higher velocities of 15,000 ft/sec. The major parameters affecting the sealing capabilities of the "Fiber Mat" concept at high velocities were examined and it was concluded that the concept, when tested at high velocities with a 1/8-inch diameter steel pellet, will not provide adequate sealing action against air leakage. The cause of this failure is the excessive material removal on the entry panel, creating a large 1/4-inch diameter hole and the shock waves, although attenuated by the fibers, which disperse the fibers sufficiently afar from the pellet entry path to prevent their being drawn to the hole in sufficient quantity to effect a seal. However, it has been shown that the Fiber Mat Concept does prevent catastrophic failures witnessed in the laboratory and, when combined with the chemical concepts, will enhance the sealing action.

Additional experimentation will be initiated to evaluate the effects of the thickness of the fiber mat compartment and also the leak rate of standard panels when penetrated by pellets 1/16-inch in diameter or smaller.



- (1) EPOXY LAMINATE (3-PLY FIBERGLASS; 55% VERSAMIDE 125, 45% EPON 128)
- (2) NITRILE RUBBER SHEET (AMS 3212J 1/32" THICK)
- (3) HONEYCOMB CORE STRUCTURE 1/2" THICK (USED AS EDGING MEMBER)
- (4) ASBESTOS FIBER (3R12)
(POLYSULFIDE 1221 USED FOR BONDING COMPOSITE MEMBERS)

FIGURE 4-6 FIBER MAT PANEL CONFIGURATION

4.3 COMBINED MECHANICAL AND CHEMICAL SELF-SEALING CONCEPTS

4.3.1 RTV Silicone Elastomer/Fiber Mat or Rubber Spheres or Air Gap Concept.

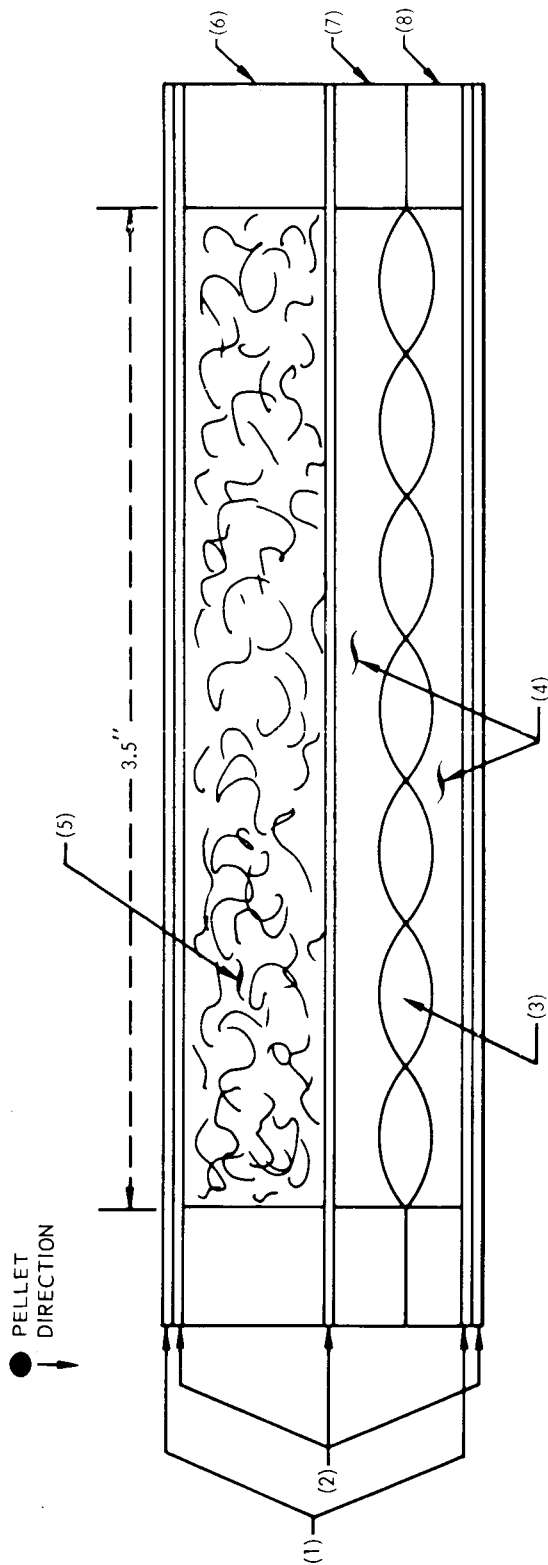
RTV Silicone Elastomer/Fiber Mat Concept

The self-sealing structure configuration for this concept is given in Figure 4-7. The principle of this concept is as follows:

Upon impact, the asbestos fibers attenuate the shock wave effects by dissipating the incident energy and, due to the existing pressure differential, some of the fibers are attracted to the puncture and effect a partial seal. At the same time, the penetrating pellet initiates a chemical reaction which effectuates a complete seal whereby the entry hole is completely sealed by the permanently adhering fibers and the cured material. Thus, the main functions of the fibers are to attenuate the shock wave effects, to minimize the damage to the structure face sheets, and to reduce the efflux of the sealing constituents through the puncture before the sealing process is completed.

Several self-sealing structures using this configuration were impacted with a 1/8-inch steel pellet projectile at medium velocities (10,000 to 15,000 fps) using the Northrop Light Gas Gun Facility and at higher velocities (up to 26,000 fps) using the McGill University Light Gas Gun. In each test, the self-sealing structure was mounted on a vacuum tank whereby one of the structure face sheets (impact face or entry face) was exposed to the vacuum and the back face (or exit face) was exposed to one atmosphere pressure. This was done to simulate the conditions in space.

The results obtained from these tests demonstrated excellent feasibility of this concept. Upon dissection of the self-sealing structures after



- (1) EPOXY LAMINATE (3-PLY FIBERGLASS; 55F VERSAMIDE 125, 45% EPON RESIN 828)
- (2) NITRILE RUBBER SHEET (AMS 2312J, 1/32" THICK)
- (3) CHAIN OF PLASTIC BAGS (MYLAR PLASTIC FILM) CONTAINING NUOCURE 28 AND BONDED TO THE SIDES OF THE HONEYCOMB STRUCTURE TO AVOID SLIPPAGE OF THE BAGS WHEN PANEL IS TESTED.
- (4) RTV 60 SILICONE
- (5) ASBESTOS FIBERS (3R 12)
- (6) HONEYCOMB CORE STRUCTURE, 1/2" THICK
- (7) HONEYCOMB CORE STRUCTURE, 1/4" THICK
- (8) HONEYCOMB CORE STRUCTURE, 3/16" THICK

FIGURE 4-7 COMBINED CONCEPT - RTV SILICONE ELASTOMER / FIBER MAT CONCEPT - CONFIGURATION

test, the inside of the structures showed clearly that the self-sealing mechanism had taken place as indicated above. The asbestos fibers, as an energy absorber, definitely assist in damage localization and self-sealing activity.

The only disadvantage with this concept is the high density of the uncured elastomer (RTV 60) used. It will appreciably affect the weight of the self-sealing structure and also it seems, as explained earlier in Section 3.3, that it contributes to the heavy cracking of the structure backup sheet when impacted at very high velocities (26,000 fps). But, due to the presence of the nitrile rubber sheet on the outside, the overall damage of the backup sheet is kept to a minimum.

To show the self-sealing capability of this concept at medium velocity (15,000 fps) and at higher velocity (26,000 fps), two test examples are given. The configuration of these two self-sealing structures is illustrated in Figure 4-7.

In the medium velocity case, the damage experienced on the face sheets was minor. A 3/16-inch hole was noted on both face sheets (entry and exit) and no cracking occurred. The fibers isolating the liquid constituents from the impact face responded very well to the shock wave effects. Upon dissection of the structure, it was noted that the mechanism of initiating the chemical reaction by the penetrating projectile performed very well.

This structure demonstrated good sealing capabilities. A leakage rate test after puncture showed a leakage of zero pounds of air per day at a pressure differential of one atmosphere (14.7 psi). This self-sealing structure was tested at the Northrop Light Gas Gun Facility using 1/8-inch steel pellets.

In the case of the higher velocity impact, the self-sealing structure was impacted at the McGill University Facility using 1/8-inch steel pellet at a velocity of 26,000 fps.

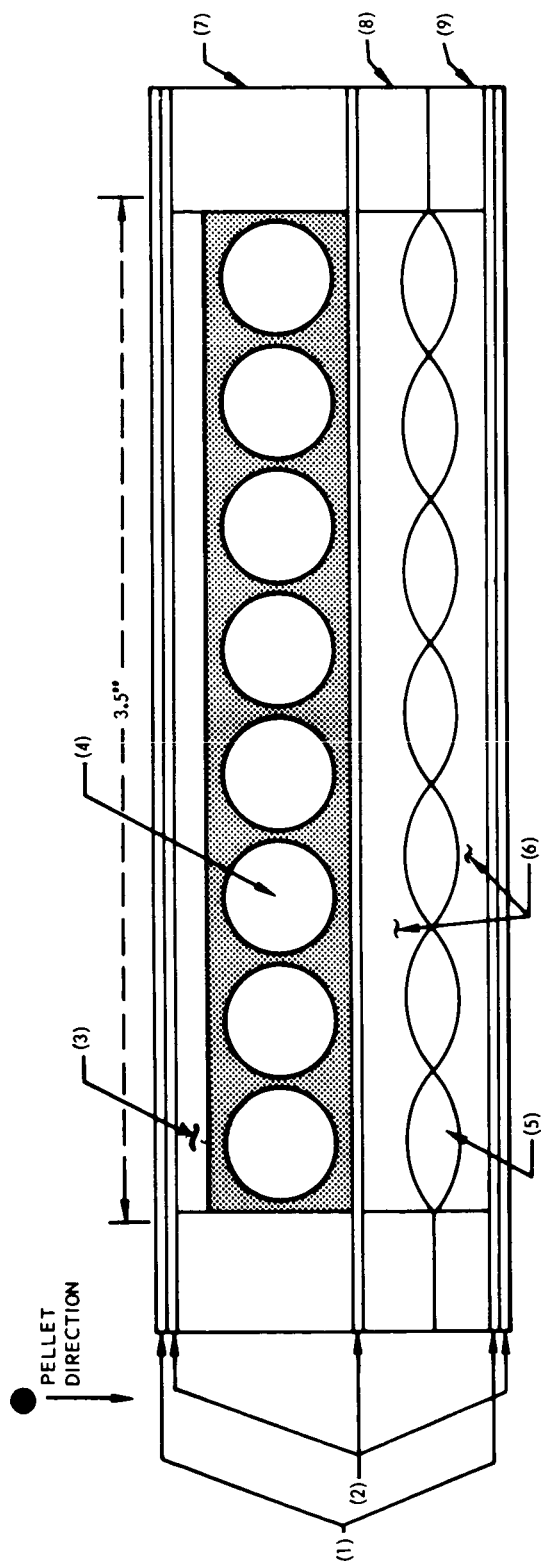
The damage provoked to the entry face was very similar to the case at medium velocity. However, the damage to the exit face was far more severe where heavy cracking of the epoxy laminate was obtained, but it was minimized due to the presence of the nitrile rubber sheet and the self-sealing structure was considered as successful. A leakage rate test showed, after puncture, a leakage of approximately 2 to 3 pounds of air per day at a pressure differential of one atmosphere (14.7 psi).

RTV Silicone Elastomer/Rubber Spheres Concept

The self-sealing structure configuration for this concept is given in Figure 4-8. The principle of this concept is very similar to the above concept with the only difference that here rubber balls are used as compressible material instead of fibers. The balls have the same functions; namely, to attenuate the shock wave effects, minimize the damage to the face sheets and to perform a partial or complete seal. The chemical reaction taking place in the chemical compartment upon penetration will form an elastomer which will complete the seal and adhere the balls permanently in the punctured hole.

Several self-sealing structures using this configuration were impacted with 1/8-inch steel pellets at medium and higher velocity. The details of the most successful configuration of this type are shown in Figure 4-8.

During some of the tests, simultaneous impacting of sabot, stripper and pellet debris occurred. However, in spite of multiple punctures in one shot, a structure in one instance sealed almost completely. Approximately three holes were hermetically sealed by the balls and a fourth hole (provoked by a big chunk of foreign material) almost sealed. Upon



- (1) EPOXY LAMINATE (3 PLY FIBERGLASS; 55% VERSAMIDE 125, 45% EPON RESIN 828)
- (2) NITRILE RUBBER SHEET (AMS 2312J, 1/32" THICK)
- (3) SOFT VINYL SPONGE, 1/8" THICK
- (4) RUBBER BALLS, 3/8" DIA. (EC 1878 NATURAL RUBBER)
- (5) CHAIN OF PLASTIC BAGS (MYLAR PLASTIC FILM) CONTAINING NUOCURE 28 AND BONDED TO THE SIDES OF THE HONEYCOMB STRUCTURE TO AVOID SLIPPAGE OF THE BAGS WHEN PANEL IS TESTED.
- (6) RTV 60 SILICONE
- (7) HONEYCOMB CORE STRUCTURE, 5/8" THICK
- (8) HONEYCOMB CORE STRUCTURE, 1/4" THICK
- (9) HONEYCOMB CORE STRUCTURE, 3/16" THICK

FIGURE 4-8 COMBINED CONCEPT - RTV SILICONE ELASTOMER/RUBBER SPHERES CONCEPT - CONFIGURATION

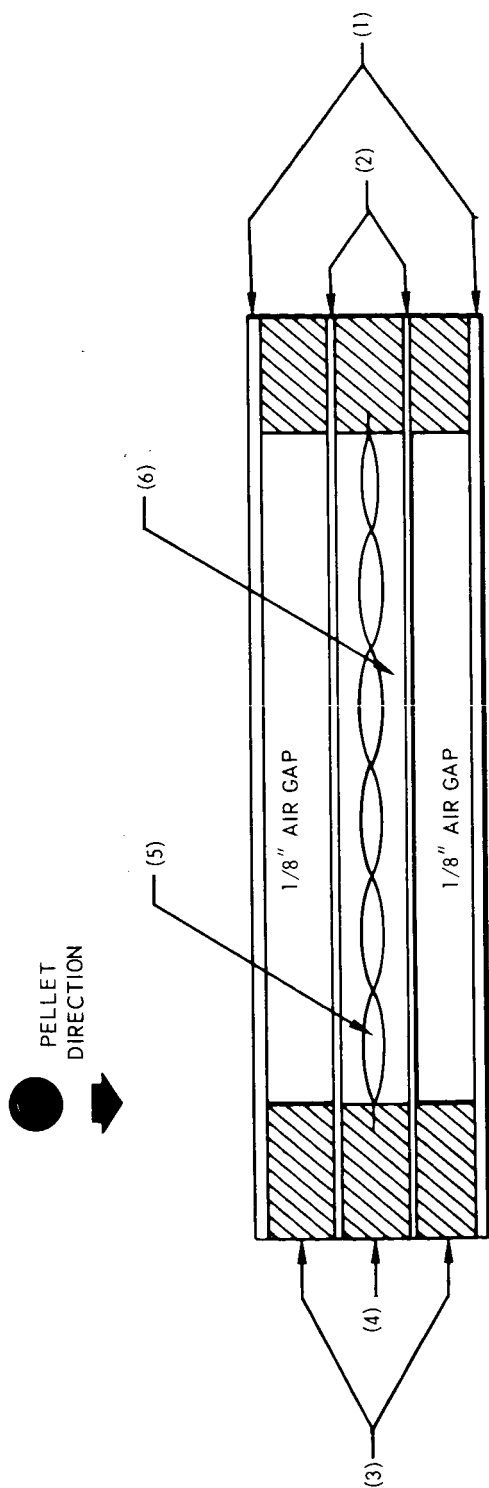
dissection of the panel, it was noted that the predicted mechanism had taken place. The three balls which sealed the three holes hermetically had adhered to the puncture with the help of the cured elastomer.

The exit face did not suffer any cracking of the laminate and the punctured holes were all sealed with the exception of one which was sealed almost completely by the cured material.

An attempt to penetrate a self-sealing structure with configuration shown in Figure 4-8, at higher velocity (19,000 fps) using 1/8-inch steel pellet and the McGill University Light Gas Gun, failed. Apparently, according to the after test analysis of the structure, the 1/8-inch steel pellet broke up after penetration of the entry face and, thus, penetration of the exit face did not occur. Upon dissection of the structure, it was observed that the chemical reaction had taken place at a slower rate (because of the non-existence of the pressure differential) and that the formed elastomer had sealed the approximately 1/4-inch hole provoked in the entry face. No seal was performed by the elastomeric balls due to the absence of any pressure differential from one side of the panel to the other after impact. The epoxy laminate on backup sheet cracked heavily, but the nitrile rubber sheet bonded to the outside of the laminate was untouched.

RTV Silicone Elastomer/Air Gap Concept

The panel configuration illustrated in Figure 4-9 was fabricated with aluminum face sheets instead of nonmetallic laminates as used in the other panel configurations. The purpose of this panel was to evaluate the extent of damage to metallic face sheets resulting from a high velocity particle penetration into the panel configuration. The panel was mounted on an air-filled tank pressurized to one atmosphere, and then impacted by a 1/8-inch diameter steel pellet at an impact velocity of approximately 18,500 fps. The result of this test is illustrated in Figure 4-10. The



- (1) 0.020 INCH ALUMINUM SHEET (2024-76)
- (2) NITRILE RUBBER SHEET (AMS 2312J, 1/32" THICK)
- (3) HONEYCOMB CORE STRUCTURE, 1/8" THICK
- (4) HONEYCOMB CORE STRUCTURE, 5/16" THICK
- (5) CHAIN OF PLASTIC BAGS (MYLAR PLASTIC FILM) CONTAINING NUOCURE 28
- (6) RTV 60 SILICONE FLUID (UNCURED)

FIGURE 4-9 RTV SILICONE ELASTOMER/AIR GAP CONCEPT

● 1/8" DIA. STEEL SPHERE
V = 18,500 FPS

PELLET IMPACT
FACE

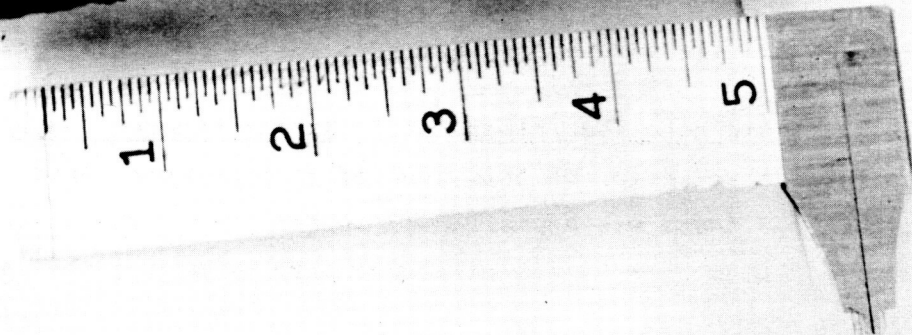


FIGURE 4-10 RUPTURED ALUMINUM FACED SELF-SEALING PANEL
(RTV SILICONE ELASTOMER/AIR GAP CONCEPT)

catastrophic failure of this panel resulted from a violent explosion occurring inside the tank. This phenomenon has been attributed to the spray of hot aluminum particles (from the panel face sheets) initiating a pyrophoric chemical reaction with the oxygen in the tank. Since the resulting reaction is exothermic, a large quantity of heat was released which generated localized and extremely high pressures at the panel interface. Since these pressures exceeded the dynamic rupture strength of the panel, explosive rupture occurred. For a further discussion of this phenomenon, and an analysis of the pertinent chemical reactions, see Part II of this report (Section 2.1.2).

Catastrophic rupture did not occur in any of the other self-sealing panel configurations in which nonmetallic face sheets were used, even though some of these panels were tested at impact velocities exceeding 18,500 fps (see Table 2-1). On the basis of this one test, in which an aluminum faced panel was catastrophically ruptured, one might conclude that aluminum walls should be avoided for air pressurized compartments. However, a further investigation of this phenomenon and related parameters will be required before a final assessment may be made on the extent of the magnitude of this potential hazard. An investigation of this phenomenon should consider the following pertinent parameters:

- Tank wall materials.
- Contained gas.
- Initial pressure in tank.
- Ballistic parameters (projectile size, material and velocity).

4.3.2 Rigid Silicone Foam/Fiber Mat or Rubber Spheres Concept. The reason for the selection of this type of foam (either rigid or flexible) over the other foams was explained in Section 3.3. The advantages of this type of foam over RTV 60 elastomer were primarily the density factor

(the foam is appreciably lighter) and the expansion of the material which occurs upon impact and improves significantly the self-sealing capability of this material in our self-sealing structures configuration.

Rigid Silicone Foam/Fiber Mat Concept

This concept in particular was evaluated very thoroughly during this year's program. The principle of this concept whose configuration is given in Figure 3-4 is as follows:

Upon penetration of the structure, the fibers attenuate the shock wave effects, minimize the structure damage and material removal and effectuates a partial seal. At the same time, while the fibers prevent the efflux of the chemical ingredients, chemical reaction is taking place upon penetration of the structure. A polymeric mass is formed which cures and expands at a very fast rate filling completely the chemical compartment and extruding into the fibers compartment mixing with the fibers and effectuating a complete seal along the pellet hole path.

A large number of structures were prepared and tested with either the Northrop Light Gas Gun or the McGill University Light Gas Gun, using 1/8-inch steel pellets as the projectile. Using the configuration shown in Figure 3-4, highly successful results were obtained as well at medium velocity (10,000 to 15,000 fps) impacts as at high velocity (up to 23,000 fps) penetrations. Two test examples are given below, one at medium velocity and one at higher velocity.

In the lower velocity (15,000 fps) test, the self-sealing configuration sealed immediately upon impact. The entry face showed a 1/4-inch diameter hole (in epoxy laminate) which was reduced to approximately 1/8-inch diameter by the 1/32-inch thick nitrile rubber sheet bonded in back of the epoxy laminate. This punctured hole was sealed immediately upon

impact by the foamed silicone mixed with some fibers. Upon dissection of the panel, it was observed that some of the fibers had been dispersed afar from the pellet entry path due to the shock wave effect. However, some of the fibers had been forced by the onflowing chemicals to mix and help to seal the puncture. The complete and tight seal was performed by the foamed material which sealed three holes, the entry hole, the 5/16-inch hole in the nitrile rubber sheet (which separates the chemical compartment from the fibers compartment) and the exit hole (3/8-inch). The chemical compartment itself was filled completely by the rigid silicone foam. An illustration of this effective sealing mechanism is given in Figure 4-11.

The high velocity test at 23,000 fps performed at the McGill University Facility, gave excellent results. The self-sealing structure sealed immediately upon impact and a leakage rate determination after test indicated a zero pound of air per day leakage. The degree of structural damage (see Figure 4-12) did not exceed appreciably the one at medium velocity. The entry face sheet showed a 3/16-inch diameter hole without cracking which was sealed tightly with the silicone foam intermixed with some fibers. The inside of the structure evidenced the sealing mechanism (very similar to the one shown in Figure 4-11) which had taken place upon impact and effecting a very successful seal. The 5/16-inch diameter hole in the exit face was also completely sealed.

To check the sealing capability consistency of this concept, seven self-sealing structures with configuration shown in Figure 3-4, were prepared. They were penetrated by 1/8-inch steel pellet at 7,000 fps using the Northrop Space Laboratories Particle Accelerator. The results obtained were excellent inasmuch as all seven structures sealed completely (which was determined with the leak detector) in a very short time. The leak rate in all cases was always very low (almost undetectable by ear) initially at impact and decreased, thereafter, very rapidly to zero

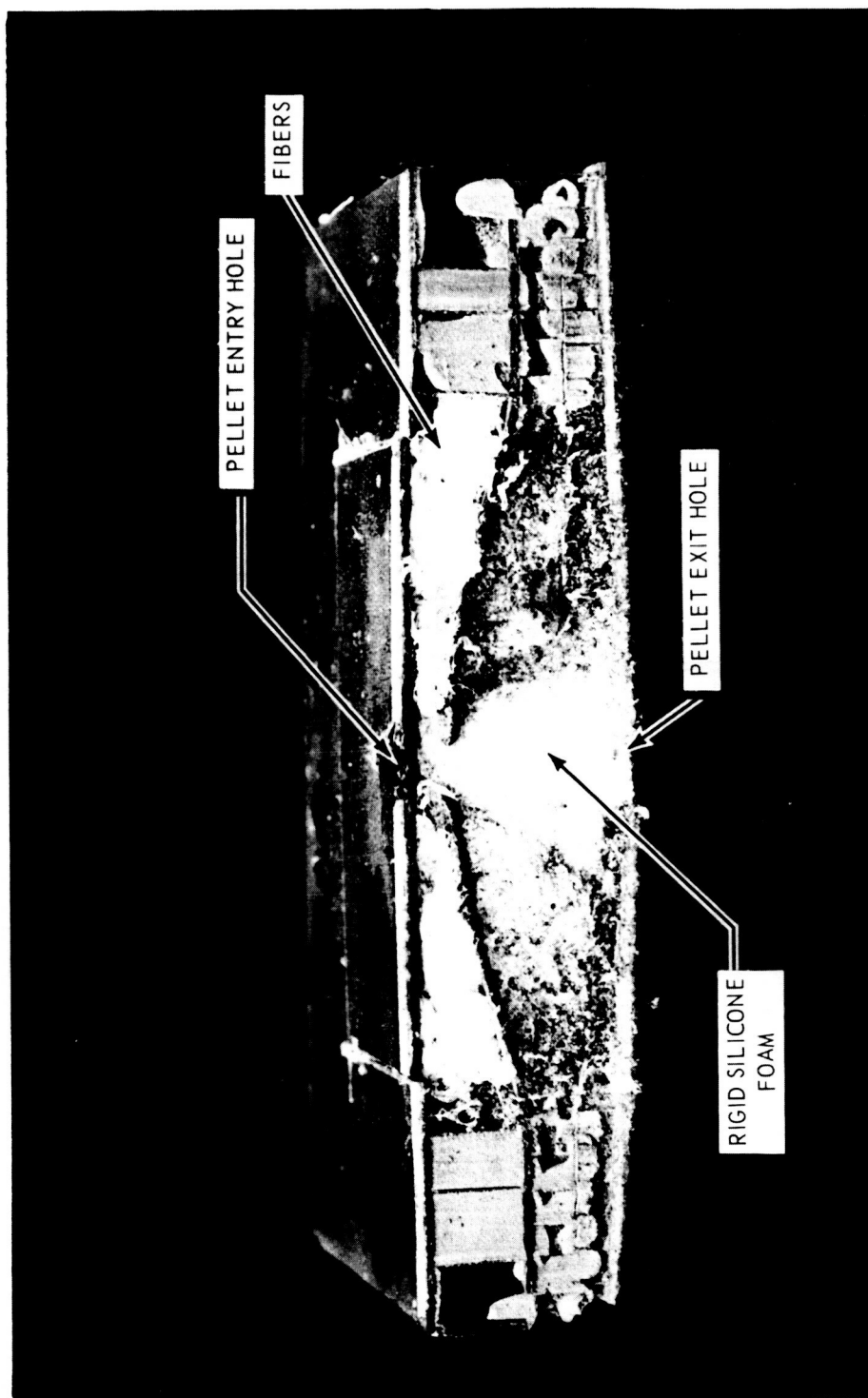
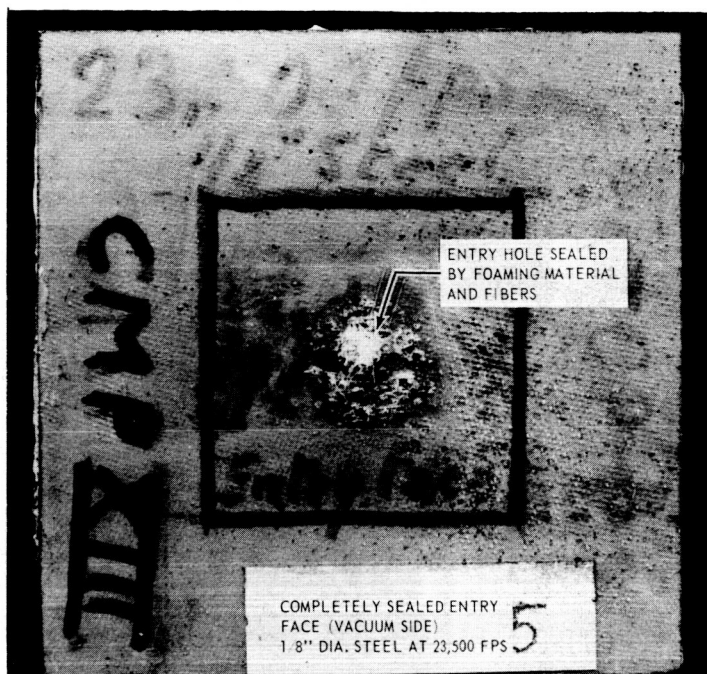


FIGURE 4-11 SELF-SEALING MECHANISM - RIGID SILICONE FOAM/FIBER MAT CONCEPT



IMPACT FACE



EXIT FACE

FIGURE 4-12 COMBINED CONCEPT – RIGID SILICONE FOAM/FIBER MAT CONCEPT

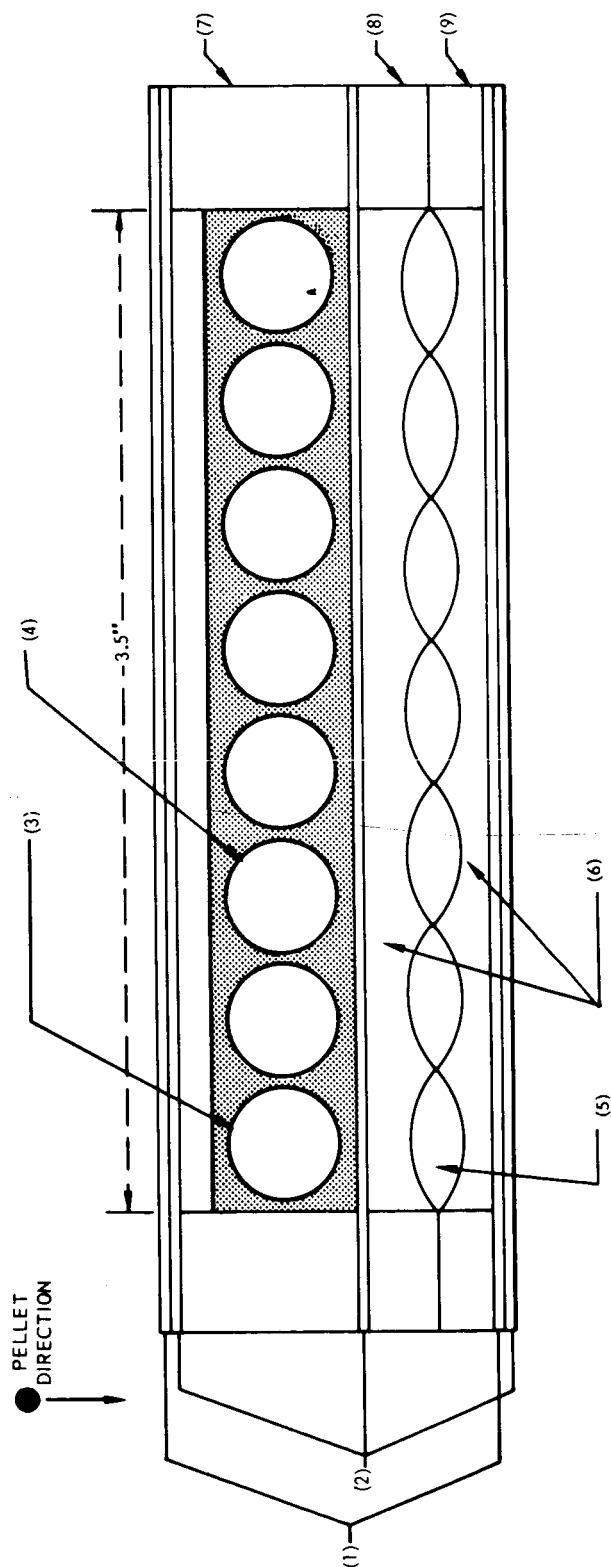
pound air per day until the structure sealed completely.

In a recently initiated new series of tests, further investigation of this highly successful self-sealing configuration will be performed. Three similar structures, using the same materials (but less) and the same configurations (but thinner) as above, have been prepared for testing at the McGill University Gun Facility. The following parameters are to be checked: (1) the continuous effective self-sealing capability of the structure after weight reduction by more than 25 per cent, (2) the self-sealing capability of this new structure when impacted with a 1/16-inch steel pellet at 25,000 fps, and, (3) the self-sealing capability when impacted with 1/8-inch steel pellets at a velocity in excess of 30,000 fps.

Rigid Silicone Foam/Rubber Spheres Concept

The efficiency of this concept is as great, or greater, as the one with the fibers. Because of the time factor, the number of structures tested was smaller for this concept. No structure was tested at the higher velocity, but several were at the medium velocities. Higher velocity shots are planned for the immediate future.

The medium velocity tests give a good indication of the self-sealing capabilities of such a structure at higher velocities. Most of the structures whose configuration is shown in Figure 4-13, gave excellent results at medium velocities. The principle of this concept is very similar to the one with the fibers. Upon penetration of the structure, one of the rubber spheres is drawn to the hole, due to the existing pressure differential across the structure faces, effectuating a partial or complete seal. At the same time, a chemical reaction is initiated, due to the penetrating projectile, releasing the two chemical constituents which mix and form a very fast curing and foaming silicone material. This foam expands into the chemical compartment, sealing the exit hole of the structure, sealing the hole provoked to the nitrile rubber sheet



- (1) EPOXY LAMINATE (3-PLY FIBERGLASS;
55% VERSAMIDE 125, 45% EPON RESIN 828)
- (2) NITRILE RUBBER SHEET (AMS2312J, 1/32" THICK)
- (3) SOFT VINYL SPONGE 1/8" THICK
- (4) RUBBER BALLS, 3/8" DIA (EC1878 NATURAL RUBBER)
- (5) CHAIN OF PLASTIC BAGS (MYLAR PLASTIC FILM)
CONTAINING NUOCURE 28 AND BONDED TO THE HONEYCOMB
STRUCTURE SIDES TO AVOID SLIPPAGE OF THE BAGS WHEN
PANEL IS TESTED
- (6) XR-6-3700 RIGID SILICONE FOAM RESIN
- (7) HONEYCOMB STRUCTURE, 5/8" THICK
- (8) HONEYCOMB STRUCTURE, 1/8" THICK
- (9) HONEYCOMB STRUCTURE, 3/16" THICK

**FIGURE 4-13 COMBINED CONCEPT - RIGID SILICONE FOAM/RUBBER
SPHERES CONCEPT - CONFIGURATION**

(membrane separating the chemicals from the balls), and extruding into the spheres compartment thus causing the rubber balls to adhere permanently.

When comparing this concept with the concept described above where fibers are used instead of balls, a very important difference was noted during the tests. As mentioned previously, upon impact of the structure using the concept "Rigid Foam/Fibers," the fibers are dispersed afar from the pellet due to the shock wave effect. However, some of the fibers (in sufficient amount) manage to mix with the onflowing chemicals and effectuate a partial seal, and prevent the liquid chemicals from extruding before the chemical process is completed. The amount of fibers and the degree of mixing with the chemicals will dictate the degree of partial seal of the entry face. Thus, with the fibers, the degree of the mechanical seal will vary more appreciably than with the balls. In the case of the concept where the balls are used, the shock wave pressure does not disperse the balls permanently from the pellet entry path. Once the shock wave is attenuated, one of the balls still can roll back into the punctured hole, mix with the foamed mass and help more effectively the self-sealing action. However, this statement does not minimize the self-sealing effectiveness of the "Rigid Foam/Fibers" concept, because highly successful results were obtained during the large series of tests performed at medium and high velocities.

One of the most successful self-sealing structures at medium velocity (15,500 fps) using the "Rigid Foam/Rubber Spheres" Concept and having the configuration shown in Figure 4-13, gave the following results:

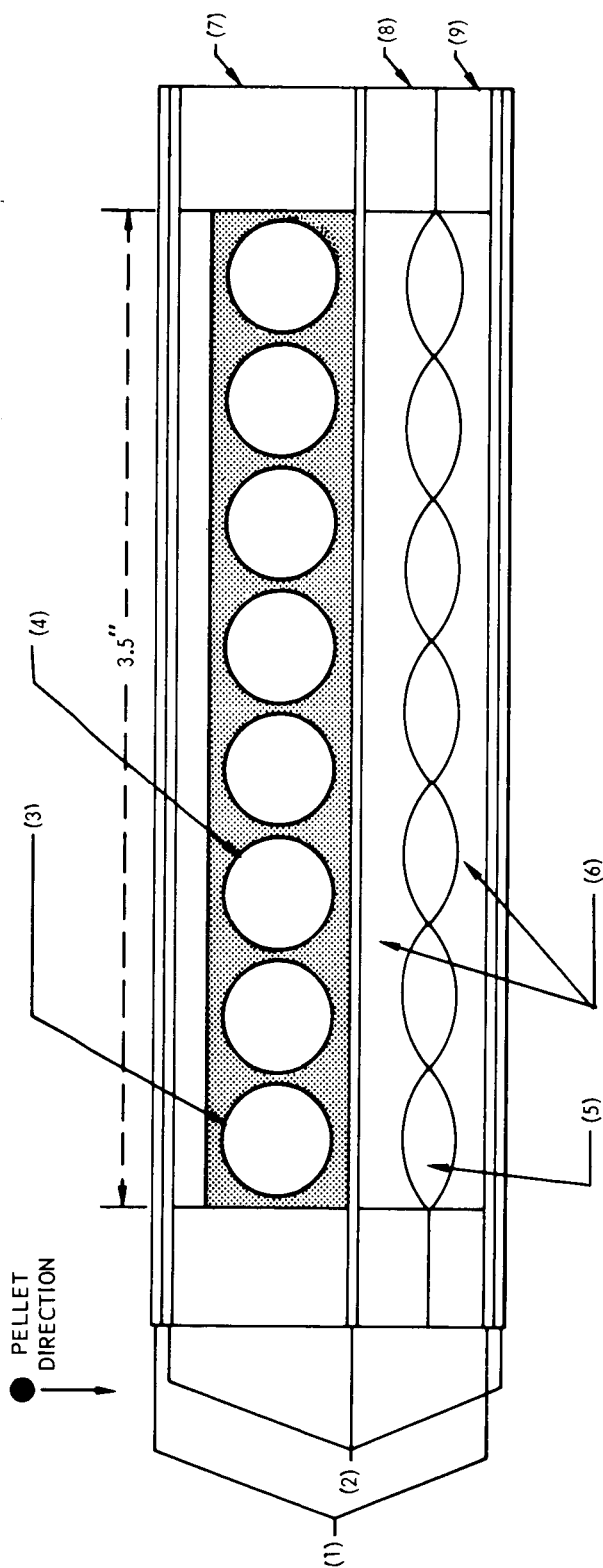
Minor damage occurred to the entry face (3/16-inch diameter hole). The exit face showed a 1/4-inch diameter hole. Both punctures sealed hermetically and immediately after impact. Upon dissection of the structure, it was noted that one of the rubber spheres had plugged the entry hole and other balls had gathered in the vicinity

of the pellet entry path. All the balls were held together by the foamed silicone rubber and had formed a permanent plug. Behind the balls in the chemical compartment all the free space had been filled completely by the foamed material which had sealed the structure completely.

4.3.3 Flexible Silicone Foam/Fiber Mat or Rubber Spheres Concept. This concept is very exciting and very promising inasmuch as a new catalyst (refer to Section 3.3 for more details) has been located which cures and foams the flexible silicone foam to a rate equivalent to the one for the rigid silicone foam. Both concepts, either the flexible foam with the fibers or with the rubber spheres were successfully tested at low velocities (up to 7,000 fps) during the last quarter. The tests at medium velocities have been initiated during this last quarter with the flexible foam/rubber spheres concept.

The principle of this concept is identical to the one with the rigid foam with the exception that, here, the end product is a flexible material which seals the holes and mixes with the elastomeric spheres. This was demonstrated by a self-sealing structure using the configuration shown in Figure 4-14. The structure was penetrated with a 1/8-inch steel pellet at a velocity of 15,200 fps and sealed immediately. The self-sealing mechanism worked perfectly as witnessed by the picture given in Figure 4-15. The structural damage was very similar to the one experienced by the other structures when impacted in that velocity range. The entry hole size was 3/16-inch in diameter and the exit hole approximately 1/4-inch.

Presently, a self-sealing structure with configuration given in Figure 4-16 is being tested at the McGill University Facility. This test consists of impacting the structure with a 1/8-inch steel pellet at a velocity of approximately 25,000 fps. This test is also the first step towards weight reduction (by more than 25 per cent) of the self-sealing structure.



- (1) EPOXY LAMINATE (3-PLY FIBERGLASS; 55% VERSAMIDE 125, 45% EPON RESIN 828)
- (2) NITRILE RUBBER SHEET (AMS2312J, 1/32" THICK)
- (3) SOFT VINYL SPONGE 1/8" THICK
- (4) RUBBER BALLS, 3/8" DIA (EC1878 NATURAL RUBBER)
- (5) CHAIN OF PLASTIC BAGS (MYLAR PLASTIC FILM) CONTAINING UNSTABILIZED STANNOUS OCTOATE CATALYST AND BONDED TO THE HONEYCOMB STRUCTURE SIDES TO AVOID SLIPPAGE OF THE BAGS WHEN PANEL IS TESTED.
- (6) FLEXIBLE FOAM RESIN (DC S-5370)
- (7) HONEYCOMB STRUCTURE, 5/8" THICK
- (8) HONEYCOMB STRUCTURE, 1/8" THICK
- (9) HONEYCOMB STRUCTURE, 3/16" THICK

FIGURE 4-14 COMBINED CONCEPT - FLEXIBLE SILICONE FOAM/RUBBER SPHERES CONCEPT - CONFIGURATION

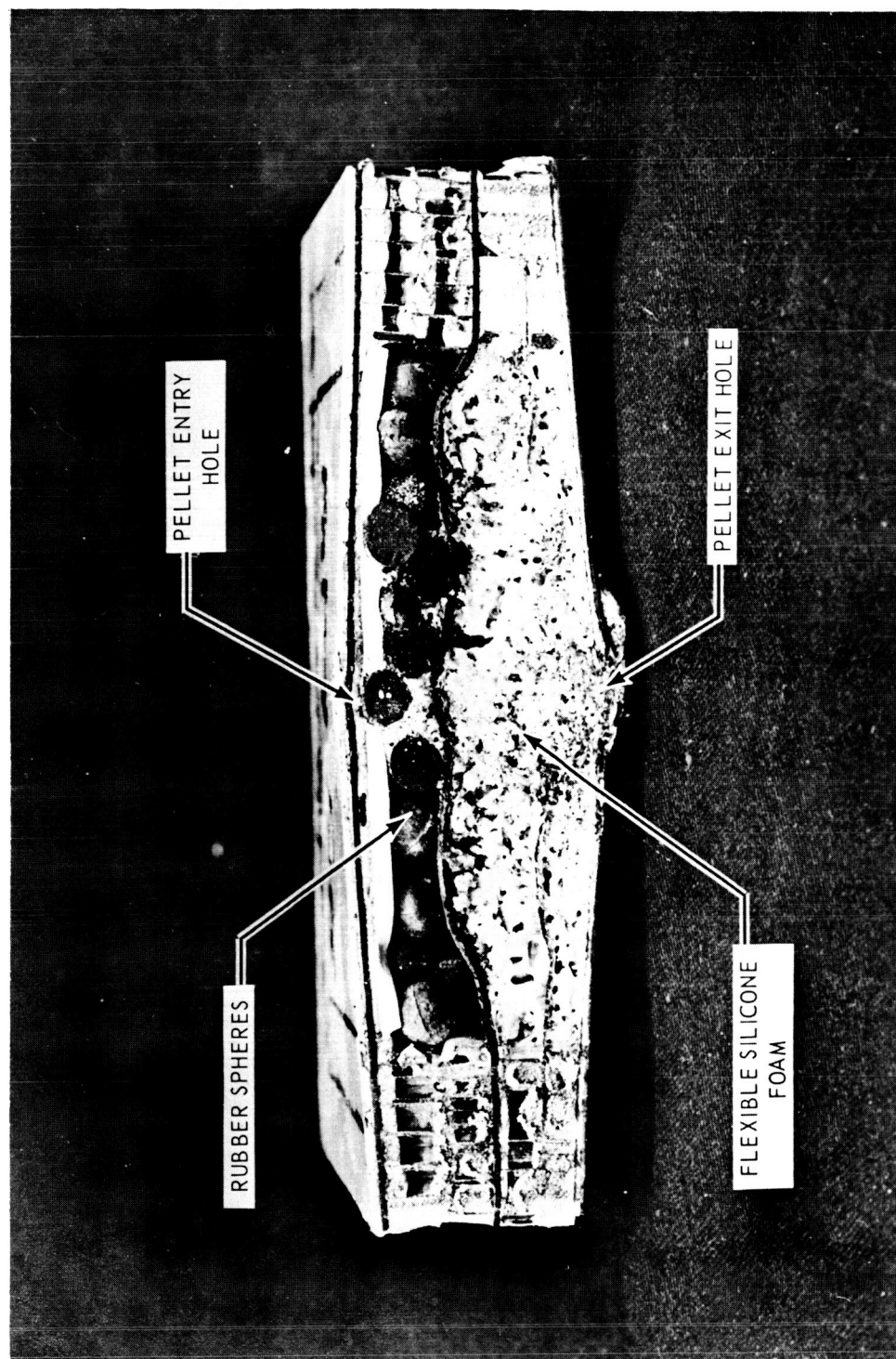


FIGURE 4-15 SELF-SEALING MECHANISM - FLEXIBLE SILICONE FOAM/RUBBER SPHERES CONCEPT

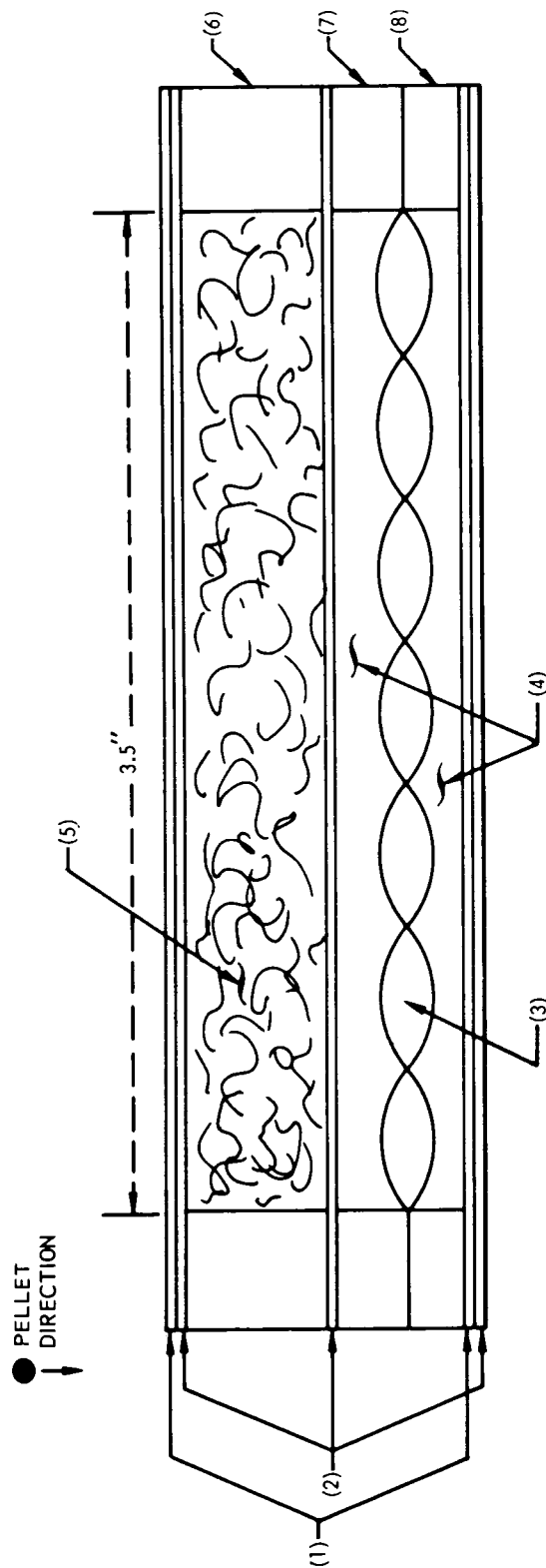
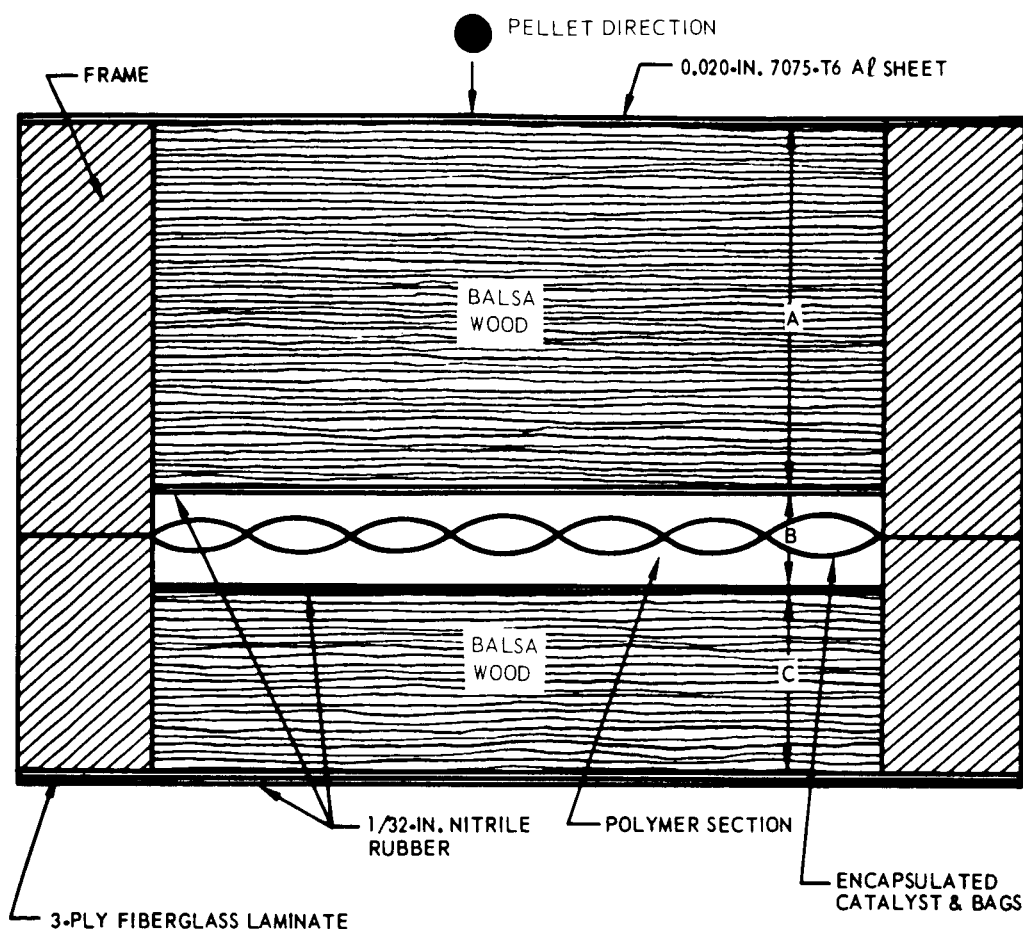


FIGURE 4-16 COMBINED CONCEPT - FLEXIBLE SILICONE FOAM/FIBER MAT CONCEPT - CONFIGURATION

4.3.4 Silicone Foam/Balsa Wood Concept. Past efforts in the use of fibers as a shock attenuator layer have shown some success. However, massive blow-out which results under conditions of projectile fragmentation, leaves large voids in this layer. The suggestion of the use of natural wood is considered an extension of the fiber concept with the application of a stronger attenuator layer. Since transmitted shock pressures are a function of material density (see Equation 2, Appendix A), balsa wood of 5 lb/ft³ density was selected. Rigid and flexible silicone foaming constituents were selected for the self-sealing layer. Panel geometries were selected not only for self-sealing capability, but also to complement the analysis discussed in Section 3.2 by entrapping the damage hole geometry observable upon post-shot dissection. Four shots were conducted using 1/8-inch diameter steel projectiles to a maximum impact velocity of 13,600 fps. After each shot, the pressure differential across the panel was released when external foaming subsided. Panel geometry and test conditions are shown in Figure 4-17, and results are discussed in the following paragraphs

Panel B-1

A 1/2-inch section for the liquid DC XR6-3700 constituents and encapsulated catalyst (yielding a rigid foam) was bounded by 2.0-inch and 1.0-inch Balsa layers on the entry and exit sides, respectively. A 0.020-inch 7075-T6 aluminum face sheet provided the simulated structural contribution as well as "bumper" activity in fragmenting the projectile. An interior view of the panel is shown in Figure 4-18. It can be seen that partial fragmentation of the projectile took place. Foaming and curing in the zone of displaced panel constituents was complete and of sufficient density to achieve total self-sealing nearly instantaneously. The presence of a confined volume in the polymer section inhibits internal expansion resulting in the formation of a dense layer plugging the projectile path. In the balsa layers, the characteristic foam was formed throughout. The presence of a partial vacuum assist in the acceleration of the foaming



PANEL NO.	DIMENSIONS INCHES			FOAM TYPE	AREA DENSITY [‡] LB/FT ²	IMPACT VEL-OCITY FPS	REMARKS
	A	B	C				
B-1	2	1/2	1	RIGID FOAM	4.0	10,000	PANEL COMPLETELY PERFORATED; FOAMING COMPLETE, NEARLY INSTANTANEOUS SELF-SEALING ACHIEVED.
B-2	2	1/2	1	FLEX. FOAM	4.5	10,500	PANEL COMPLETELY PERFORATED, FOAMING COMPLETE, PARTIAL SEAL ACHIEVED.
B-3	2	1/2	1	RIGID FOAM	4.0	11,600	PANEL <u>NOT</u> COMPLETELY PERFORATED; BALLISTIC LIMIT ACHIEVED.
B-4	3/4	1/4	3/4	RIGID FOAM	2.6	13,600	PANEL <u>NOT</u> COMPLETELY PERFORATED BY PROJECTILE. GOOD FOAMING ACTION IN DAMAGED ZONE.

[‡] DOES NOT INCLUDE CONTRIBUTION OF FACE SHEET $\approx 0.3\#/FT^2$

FIGURE 4-17 Balsa Wood/SILICONE FOAM CONCEPT

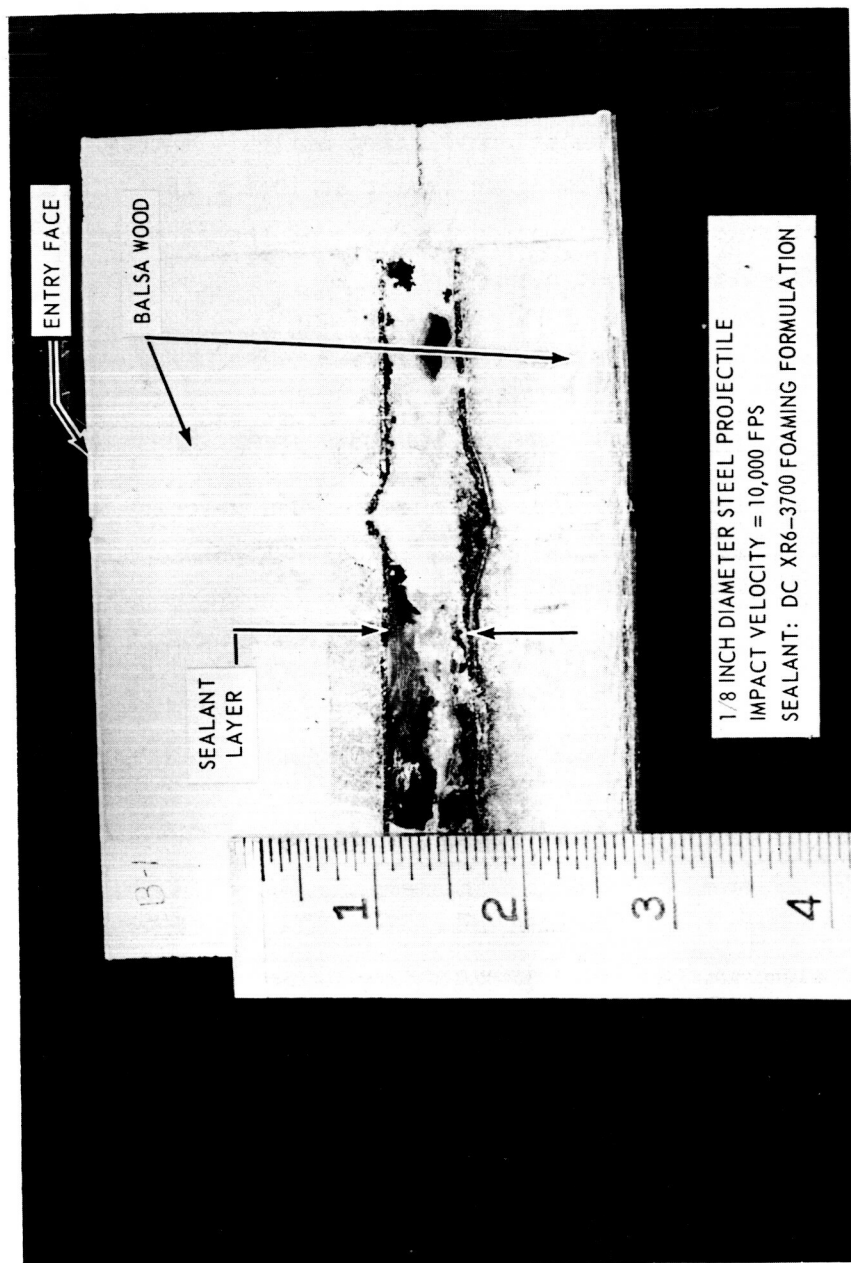


FIGURE 4-18 INTERNAL FOAMING IN PANEL B-1

action, which is literally "explosive" under the test conditions of 1.0 mm Hg (existing in the test chamber) with atmospheric conditions behind the panel.

Panel B-2

This panel was identical to B-1 except for the foaming constituent, which was the RTV S-5370 liquid formulation yielding a flexible foam. Partial self-sealing was achieved following an impact at 10,500 fps. This was attributed to the relatively slower curing rate of the formulation, since internal damage duplicated that of panel B-1.

Panel B-3

Panel B-1 was duplicated in this test, and an effort was made to achieve higher impact speeds. The test did not achieve this objective since the panel was not completely perforated and the recorded velocity was 11,600 fps. However, the ballistic limit of the configuration was fortuitously achieved. This permitted a calculation of the K-factor (panel strength factor in Watson's analysis, see Section 3.2) to be performed. This was calculated to be:

$$K = 1.66 \times 10^6 \text{ psf} = 7.96 \times 10^8 \text{ dynes/cm}^2$$

This compares with Watson's values from Reference 3 of

	<u>K-Factor</u>	<u>Brinell Hardness</u>
.2S-O aluminum	$3.37 \times 10^{10} \text{ dynes/cm}^2$	23
17S-O aluminum	4.86×10^{10}	45
2024-T3 aluminum	6.50×10^{10}	120
AZ 51X, B90-46T Mag alloy	4.92×10^{10}	

The comparison is favorable as one would expect the pseudo-strength factor to be lower for the Al/Balsa composite than for continuous metallic targets.

Panel B-4

This panel was identical to B-1 except for reduced thicknesses of the balsa and sealant layers. Panel B-4 was not completely perforated even though the impact velocity was increased over the previous three shots of this series. Foaming action, as in previous shots, was complete as the entire particle path was filled with cured material (see Figure 4-19). This was due to increased fragmentation of the projectile, observable in the balsa layer on the entry side. Again, however, the ballistic limit was achieved permitting a calculation of the panel K-factor. The results of this calculation are summarized in Table 4-1 for panel B-4.

$$K = 1.120 \times 10^8 \text{ psf} = 5.363 \times 10^8 \text{ dynes/cm}^2$$

This is a 48% decrease from that of panel B-3, possibly since the contribution of the aft sheet is absent. The comparison is considered highly favorable in view of the nearly identical variations of the K-factors presented above for the three aluminum alloys of successively increasing hardness.

In this series of tests, the performance of the balsa wood layer was satisfactory as no bulging of the face sheet was observed. Face sheet damage consisted only of a 3/16-inch diameter perforation. However, since impact speeds never exceeded 13,600 fps, complete fragmentation of the steel projectile was never achieved. Additional panels were fabricated for testing at speeds in excess of 20,000 fps for verification of the low speed calculations. These results will also verify the desired supposition that K is independent of impact velocity in the speed regime of the testing. The successful determination of K-factor will greatly

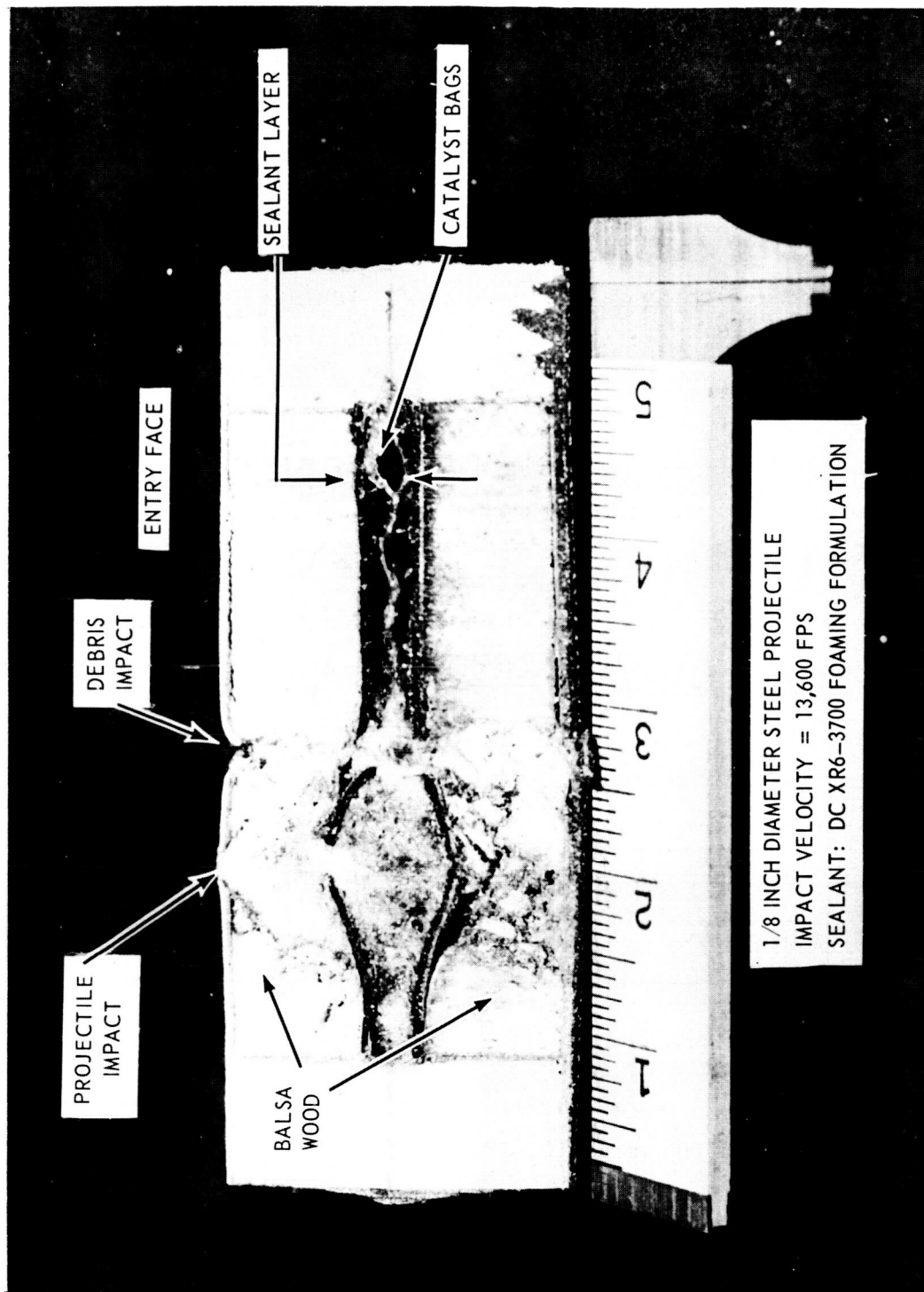


FIGURE 4-19 INTERNAL FOAMING IN PANEL B-4

TABLE 4-1 - SUMMARY OF CALCULATIONS

ANALYSIS OF PERFORATION OF COMPOSITE TARGETS:
DETERMINATION OF K-FACTOR FOR PANEL B-4

$$K = \frac{m_p}{2} V_i^2 \left[\int_0^P e^{R A_0 / m_p} A_r dz - \int_0^P A_r dz \right]^{-1}$$

	$\int_0^P e^{R A_0 / m_p} A_r dz$ (ft^3)	$\int_0^P A_r dz$ (ft^3)
0.020-inch Al sheet	3.333×10^{-7}	3.194×10^{-7}
3/4-inch balsa	3.777×10^{-4}	3.565×10^{-4}
1/32-inch nitrile	2.537×10^{-4}	8.875×10^{-7}
Sealant layer	5.155×10^{-3}	2.997×10^{-4}
1/32-inch nitrile	9.230×10^{-7}	2.218×10^{-7}
3/4-inch balsa	2.485×10^{-3}	3.740×10^{-4}
1/32-inch fiberglass	not perforated	
1/32-inch nitrile	not perforated	

$$\Sigma = 8.272 \times 10^{-3} \quad \Sigma = 1.031 \times 10^{-3}$$

1/8-inch diameter steel projectile:

$$m_p = 2.863 \times 10^{-4} \text{ lb.}$$

$$A_p = 8.550 \times 10^{-5} \text{ ft}^2$$

$$V_i = 13,600 \text{ fps}$$

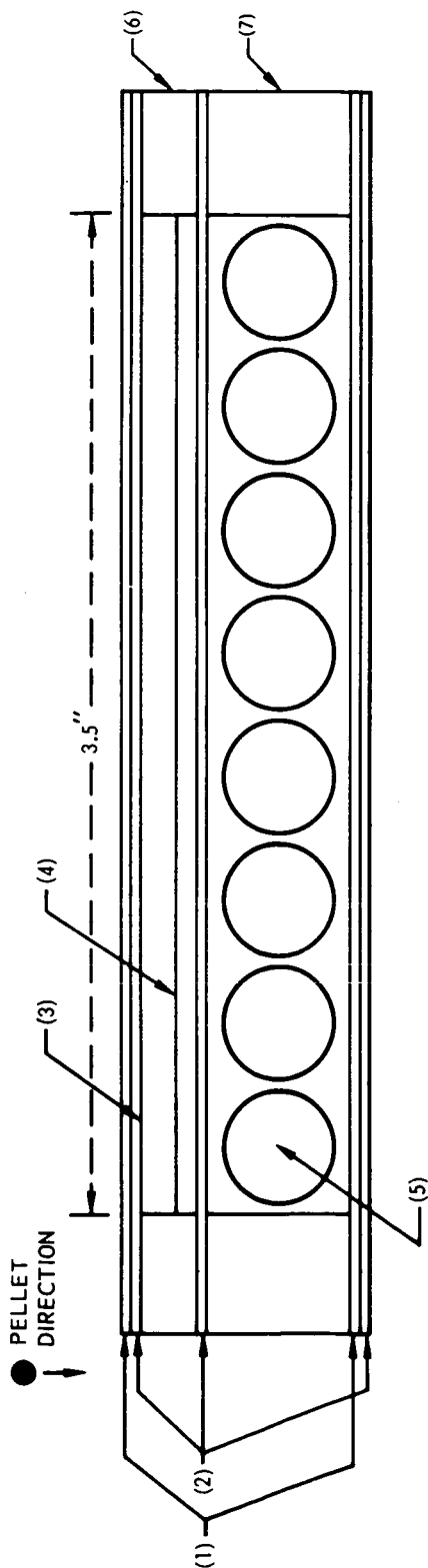
$$K = \frac{2.863 \times 10^{-4}}{2(32.2)} (1.849 \times 10^8) \left[(8.272 - 1.031) \times 10^{-3} \right]^{-1} = 1.120 \times 10^6 \text{ psf} = 5.363 \times 10^8 \text{ dynes/cm}^2$$

assist in the scaling of panel weights and thicknesses to realistic meteoroid environment conditions. However, these latest results are not available for reporting at this time. The test results and analysis of four remaining panels will be presented in succeeding reports, and will permit a better assessment of the performance of realistic panel geometries in subsequent applied design efforts.

4.3.5 Elastomeric Spheres/Viscous Face Concepts. Figure 4-20 gives the self-sealing structure configuration of this concept. The principle is as follows:

Upon penetration, one of the spheres sets itself in the punctured hole to effect either a partial or complete seal. At the same time, the rubber sphere contacts the viscous fluid which initiates a curing action due to the presence of an excess of catalyst remaining on the surface of the rubber sphere. This mechanism permits the punctured hole to be sealed completely (in the case where the sealing was only partial with the sphere alone) and to give a permanent adhesion of the sphere to the sealing surface. This prevents the sphere from being shaken loose (due to vibration or other mechanical loads) from the sealing surfaces and from unsealing the hole.

Several structures, using this concept, were tested at 7,000 fps and results obtained were very encouraging. Structures were then fabricated for higher velocities. Two structures with configuration shown in Figure 4-20 were tested at 18,000 fps and 17,000 fps and gave very interesting results. For example, the tank effect (that is, the effect experienced when a tank containing a liquid is impacted by a projectile at high velocities) was clearly demonstrated here. One of these structures was impacted with the viscous face on the side of the entry face and the other with the viscous face on the exit face side. In the first case, the damage to the entry face was heavy (large cracks across the structure surface and a



- (1) EPOXY LAMINATE (3-PLY FIBERGLASS; 55%VERSAMIDE 125, 45% EPON RESIN 828)
- (2) NITRILE RUBBER SHEET (AMS2312J, 1/32" THICK)
- (3) SOFT VINYL SPONGE, 1/8" THICK
- (4) RTV SILICONE LAYER
- (5) RTV SILICONE BALLS, 3/8" DIAMETER
- (6) HONEYCOMB STRUCTURE, 3/16" THICK
- (7) HONEYCOMB STRUCTURE, 1/2" THICK

FIGURE 4-20 ELASTOMER SPHERES/VISCOUS FACE CONCEPT - CONFIGURATION I

3/8-inch hole) and in the second case, the damage to the entry face was minor (3/16-inch hole). This test indicates that the increased damage was principally due to the tank effect.

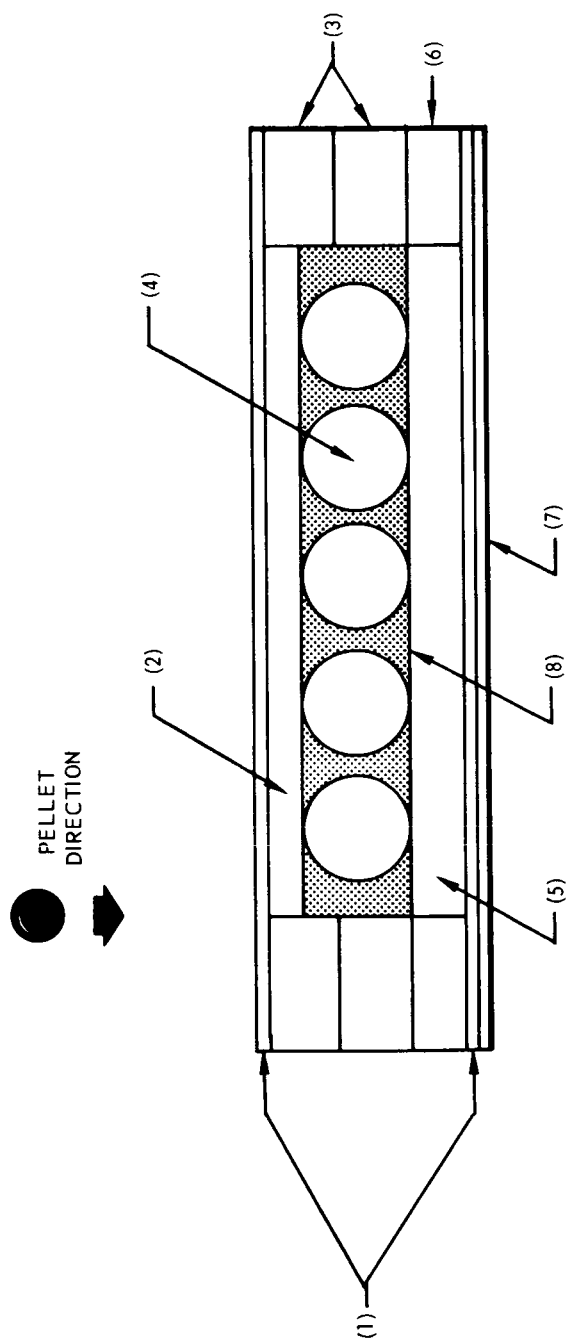
Upon dissection of the structure from the second case, it was noted that the predicted mechanism had taken place. One of the balls had set itself in the punctured hole and was permanently adhered to the sealing surface. A leakage rate determination indicated a small leak.

To make this concept work more reliably, the following new refinements were added to the above structure:

Instead of using RTV 60 uncured elastomer as the viscous fluid, a silicone foam (either rigid or flexible) rubber base was used. To speed up the curing and foaming action of the foam rubber base, the elastomeric spheres were coated with a fast curing and foaming catalyst. The new configuration with the added refinements is given in Figure 4-21.

Preliminary tests of this new configuration at low velocities (up to 7,000 fps) showed very promising results. To obtain data at higher velocities ($\approx 25,000$ fps), a similar self-sealing structure was prepared and sent to McGill University where the test should be performed very shortly.

4.3.6 Rigid Silicone Foam/Air Gaps Concept. For weight reduction purposes, this concept would be ideal. Instead of using rubber balls or fibers, air would be used as the energy absorber. Such a concept was evaluated in the laboratory and Figure 4-22 shows its configuration. This self-sealing structure was impacted with a 1/8-inch steel pellet at a velocity of 13,500 fps with the Northrop Light Gas Gun Facility. After penetration of the structure, the entry face showed a 5/16-inch hole and a 1/2-inch hole on the exit face was recorded. Upon dissection of the structure, the gap between the entry face and the chemical compartment was half



- (1) EPOXY LAMINATE (3-PLY FIBERGLASS; 55% VERSAMIDE 125, 45% EPQN RESIN 828)
- (2) SOFT VINYL SPONGE, 1/8" THICK
- (3) HONEYCOMB STRUCTURE, 5/16" THICK (EACH)
- (4) RTV SILICONE BALLS (3/8" DIAMETER) COATED WITH STANNOUS OCTOATE (CATALYST)
- (5) RIGID SILICONE FOAM RESIN (DC XR-6-3700)
- (6) HONEYCOMB STRUCTURE, 1/16" THICK
- (7) NITRILE RUBBER SHEET (AMS 2312J, 1/32" THICK)
- (8) THIN PLASTIC FILM

FIGURE 4-21 ELASTOMER SPHERES/VISCOUS FACE CONCEPT - CONFIGURATION II

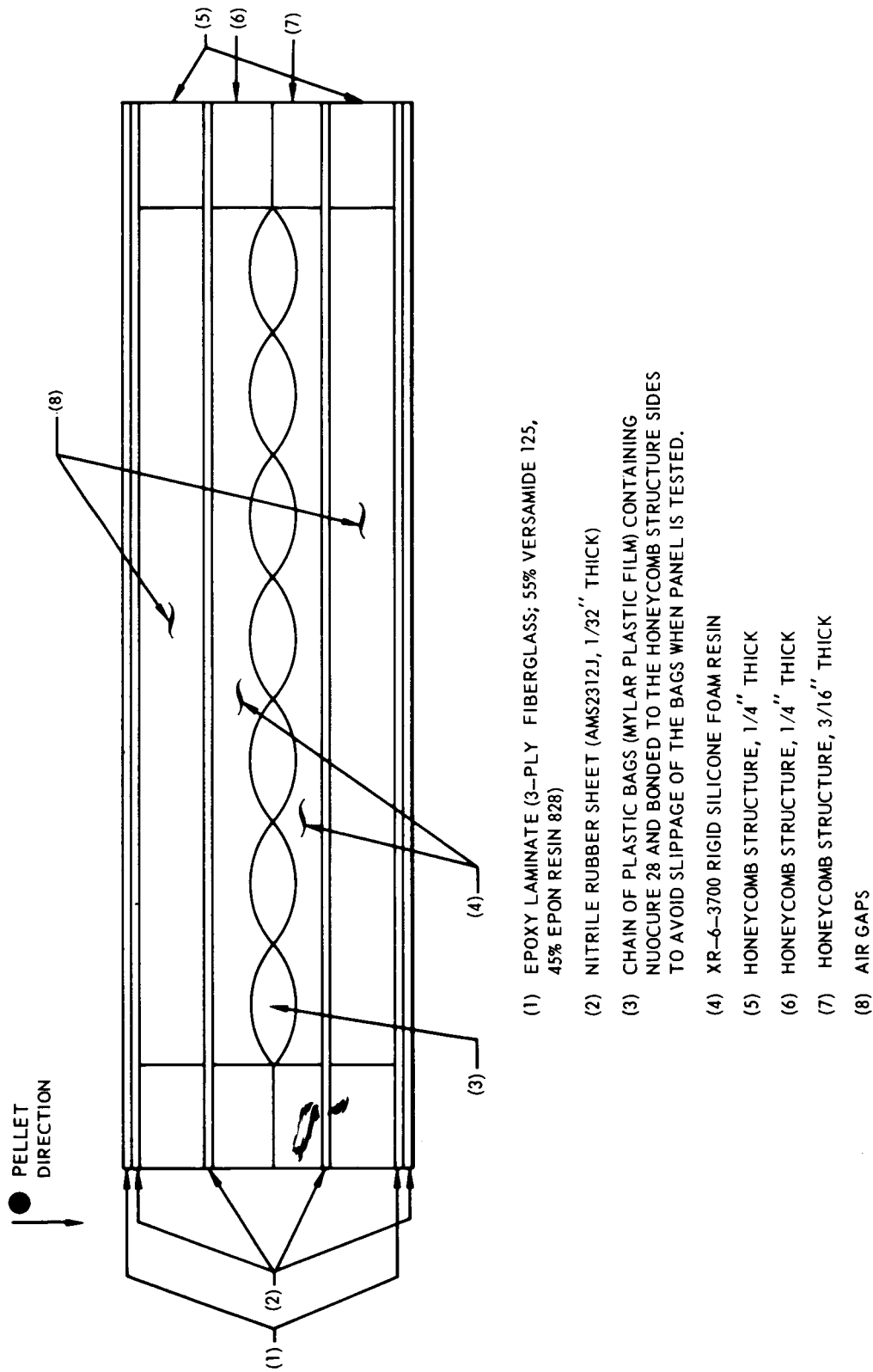


FIGURE 4-22 RIGID SILICONE FOAM/AIR GAPS CONCEPT - CONFIGURATION

filled, particularly in the vicinity of the punctured hole. The holes in the nitrile rubber sheets separating the chemicals from the air gaps were tightly sealed. Practically no foaming material had extruded into the gap between the chemical compartment and the exit face. No immediate seal was obtained, but complete seal was recorded a few minutes later.

It is interesting to note here, that, with a similar self-sealing structure whereby metal facings were used instead of nonmetallic facings, an explosive rupturing and heavy damage to the entry and exit faces had been experienced. The explanation of this phenomenon has not been attempted as yet but will be done in the very near future.

4.3.7 Rigid Silicone Foam/Rubber Spheres/Air Gap Concept. This concept is the regular "Rigid Silicone Foam/Rubber Spheres" concept with the exception that here, an air gap has been added to the back side of the structure. The configuration of this concept is given in Figure 4-23. The air gap at the back side of the structure is there to give more protection to the chemical compartment. Up to now, this configuration has not been necessary to protect the chemical compartment when the proper materials are being used. The self-sealing structure using the "Rigid Silicone Foam/Rubber Spheres or Fibers" concept does not need this air gap to seal successfully when impacted with 1/8-inch steel pellets at velocities up to 26,000 fps as was experienced experimentally. However, it might be necessary at higher velocities (above 30,000 fps). This will be shown in future tests.

Nevertheless, such a self-sealing structure with configuration shown in Figure 4-23 was tested at McGill University Gun Facility. This structure was highly successful inasmuch as it sealed immediately upon being impacted with a 1/8-inch steel pellet at a velocity of 26,000 fps. A leakage rate determination indicated a zero pound of air per day leak rate. The self-sealing mechanism worked perfectly as the analysis of the dissected structure indicated.

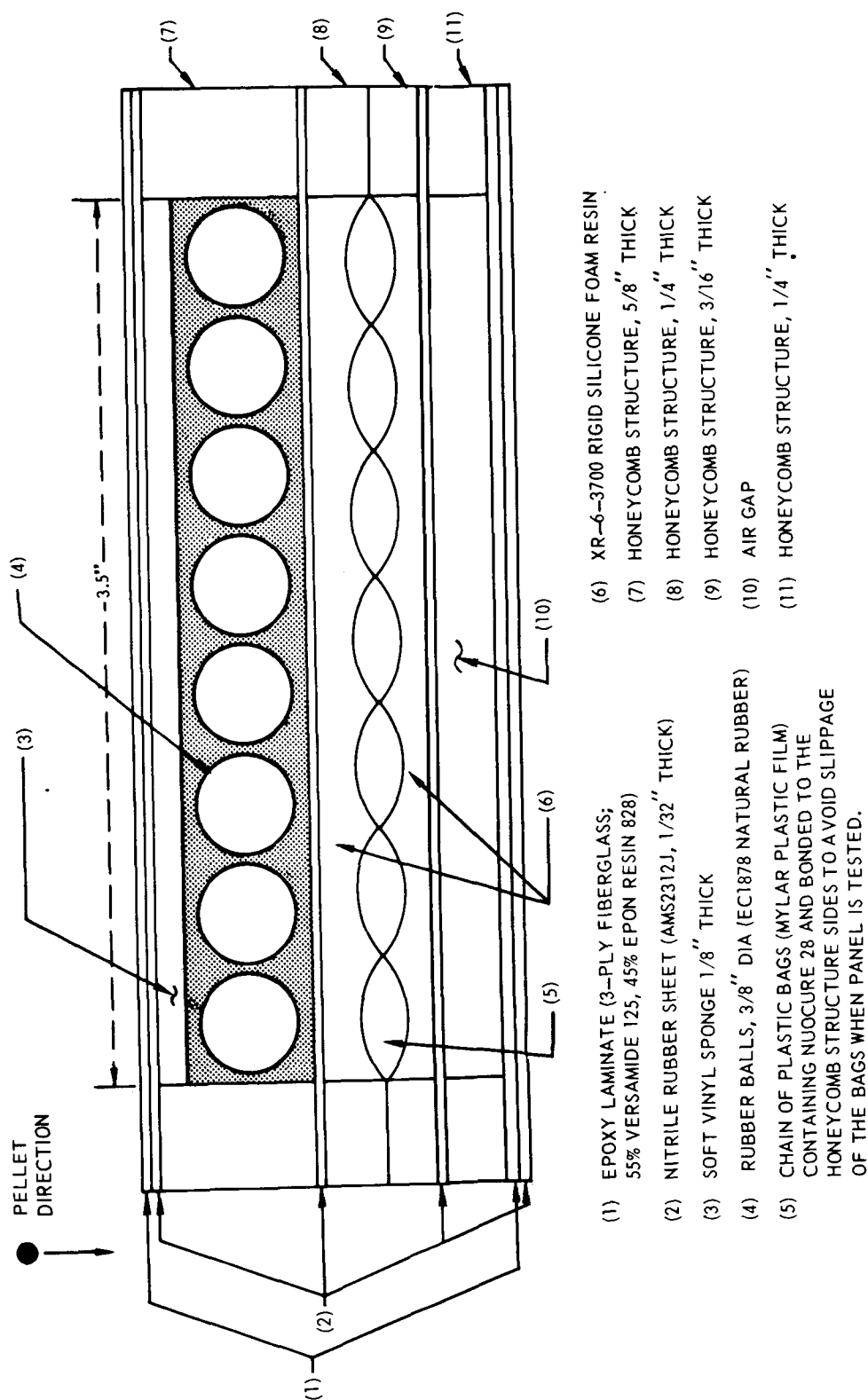


FIGURE 4-23 COMBINED CONCEPT - RIGID SILICONE FOAM/RUBBER SPHERES/AIR GAP - CONFIGURATION

5.0 REFERENCES

1. "Self-Sealing Structures for Control of the Meteoroid Hazard to Space Vehicles," Fourth Quarterly Summary Report, NASA Contract NASr-102, March 1963 (Northrop Technical Memorandum NSL 62-132-3).
2. "Self Sealing Structures for Control of the Meteoroid Hazard to Space Vehicles," Fifth Quarterly Report, NASA Contract NASr-102, June 1963 (Northrop Technical Memorandum NSL 62-132-4).
3. Watson, R. W., "The Perforation of Thin Plates by High Velocity Fragments," Proceedings of Fifth Symposium on Hypervelocity Impact, Vol. I, Part 2, April 1962.

APPENDIX A

STATE OF MATERIAL SUBJECTED TO IMPACT SHOCK

When two surfaces collide with sufficient speed, portions of both the projectile and target local to the interface are compressed to a great degree. Shock waves are generated in both target and projectile, radiating outward from the point of contact. A most simple description of this incident condition can be visualized by considering the one-dimensional impact situation wherein all motion is unidirectional and normal to the plane of the disturbance. For purposes of determining the severity of impact, it is of interest to know the pressures and associated velocities. Referring to Figure A-1, incident conditions are shown for a target material, initially at rest, impacted by a projectile moving to the right at a speed of V_i . The description of the target material in the shocked state can be defined by the classical Rankine-Hugoniot equations:¹

$$\left(\frac{\rho}{\rho_{o_t}}\right) = \frac{U_{s_t}}{U_{s_t} - U_{p_t}} \quad \text{(conservation of mass)} \quad (1)$$

$$P_t - P_{o_t} = \rho_{o_t} U_{s_t} U_{p_t} \quad \text{(conservation of momentum)} \quad (2)$$

$$E_t - E_{o_t} = \frac{1}{2} (P_t + P_{o_t}) (v_{o_t} - v_t) \quad \text{(conservation of energy)} \quad (3)$$

where

P = pressure

ρ = density

U_s = shock wave front velocity of propagation

U_p = material particle velocity in the shocked region

E = specific internal energy
 v = specific volume ($= 1/\rho$)

subscripts:

$_o$ refers to initial (unshocked) state
 $_t$ refers to target material

The above three equations in five unknowns (assuming that the unshocked state is defined) are augmented by the equation of state of the material,

$$P = f(\rho, E) \quad (4)$$

Equation (4) is often replaced by an empirical relation found by experiment to be very accurate for most metals, viz.,²

$$U_{s,t} = Co_t + \lambda_t U_{p,t} \quad (5)$$

where

Co_t = adiabatic bulk sonic velocity
 λ_t = empirical constant

This system of equations (1), (2), and (5) with four unknowns, $(U_s, U_p, P, \rho)_t$, is conventionally solved by considering similar conditions applicable to the projectile material, viz.,

$$\frac{\rho_p}{\rho_{op}} = \frac{V_i - U_{s,p}}{V_i - U_{s,p} - U_{p,p}} \quad (6)$$

$$P_p - P_{op} = \rho_{op} (V_i - U_{s,p}) (V_i - U_{p,p}) \quad (7)$$

$$U_{s,p} = Co_p + \lambda_p (V_i - U_{s,p}) \quad (8)$$

where the subscript p refers to projectile properties. Two additional stipulations are necessary to make the system determinant. These are the conditions that insure that both surfaces remain in contact, viz.,

$$P_p = P_t = P \quad (9)$$

$$U_{p_p} = U_{p_t} = U_p \quad (10)$$

The solution for impact pressure, P , is of greatest interest from the standpoint of target damage and will now be discussed. From equations (2), (5), (7), (8), one may write

$$P = \rho_{o_t} C_{o_t} U_p + \lambda_t \rho_{o_t} U_p^2 \quad (11)$$

$$P = \rho_{o_p} C_{o_p} (V_i - U_p) + \lambda_p \rho_{o_p} (V_i - U_p)^2 \quad (12)$$

Explicit solutions for P and U_p from equations (11) and (12) result in cumbersome expressions. For this reason, a graphical solution in the P - U_p plane is employed. This simple solution is executed as shown in Figure A-2. It can be seen that one merely offsets the projectile material curve on the horizontal scale by an amount equal to V_i , reflecting it about the vertical scale. (It can be seen that for impact of identical materials, the target material is accelerated to one-half the impact velocity due to the symmetry of the problem.) This graphical method of solution is used by experimenters for determining previously undefined Hugoniot properties of solids^{3,4} and liquids.⁵

The same procedure may be used for shocks traversing layered media. The problem is merely "re-started" when an additional interface is encountered, using as initial conditions the results from the previous cycle. To extend the previously cited example, the pressure of a second layer of

target material behind the first requires that we "start" the solution for this next interface at the intersection point shown in Figure A-2. This is done by reflecting the initial target layer material curve about a vertical line through (P_1, U_{p1}) , since the initial target layer now is effectively a "projectile" impacting the sublayer. The intersection of this reflected curve with the Hugoniot for the sublayer defines the new values of P_2 and U_{p2} for this interface. This procedure is outlined in Figure A-3.

For the condition, $P_2 > P_1$, the first target layer is additionally compressed by a shock pressure jump $(P_2 - P_1)$. In this instance, the compression follows the Hugoniot curve as presented. It is in the existence of the alternative, $P_2 < P_1$, that questions arise concerning the accuracy of the reflection method. In this case, the incident target layer expands upon rarefaction along approximately the adiabatic curve rather than the Hugoniot as assumed here. However, this inconsistency is disregarded for the calculations used in this study. In all instances, shock attenuation is neglected and, accordingly, results apply only to incident conditions. Factors of geometry which affect the one-dimensional motion assumption have been similarly disregarded, and the usual conditions of isotropy have been assumed.

This calculation method was used in this study for the determination of impact and interfacial pressures. Hugoniot data are available for approximately 27 basic metals, some common alloys, and a few organic and inorganic solids and liquids. In general, no Hugoniot data exist for the class of polymers used in the self-sealing program. However, it is still possible to utilize the analysis with polymers in the configurations (e.g., for the metal/polymer/liquid interface problem). This particular problem is discussed and illustrated in Part II of this report.

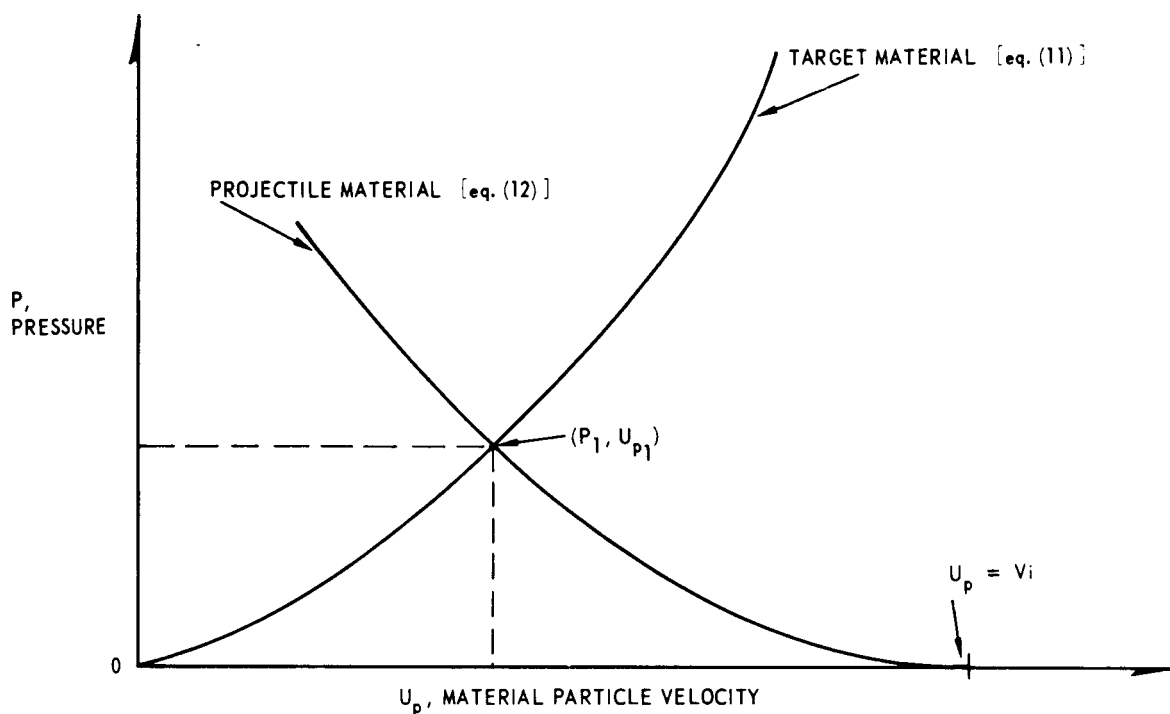


FIGURE A-2 GRAPHICAL SOLUTION TO IMPACT PROBLEM

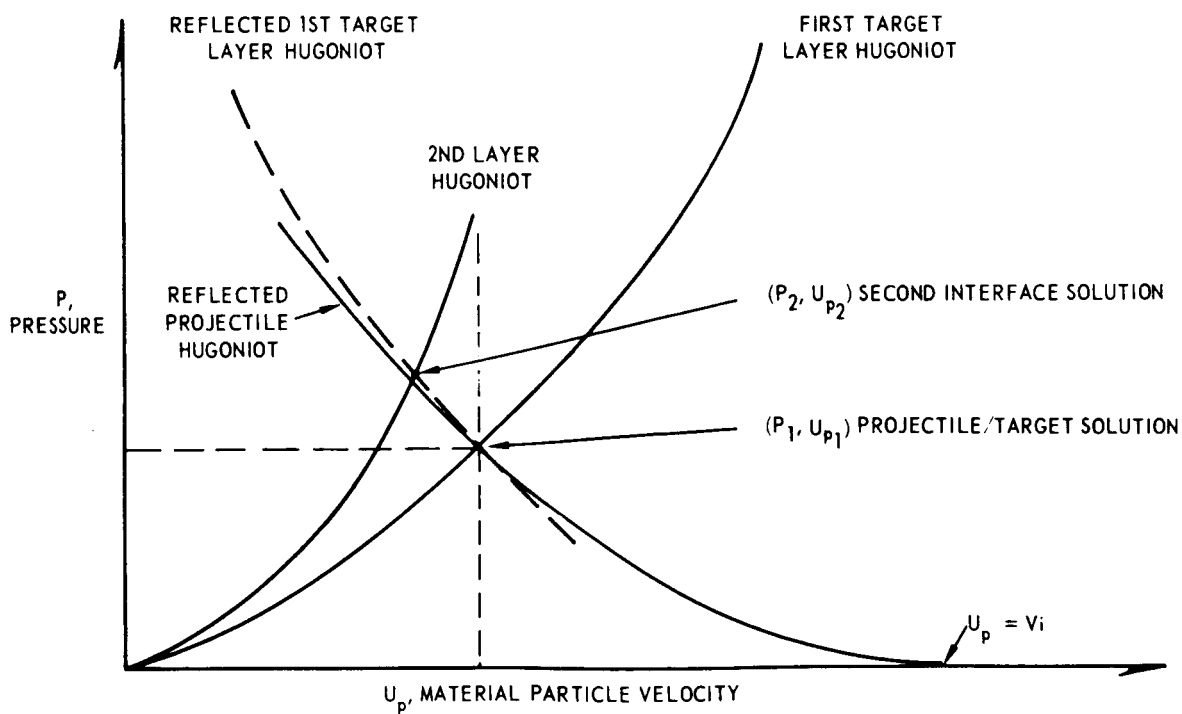


FIGURE A-3 SHOCK SOLUTION: TWO-LAYERED TARGET

REFERENCES FOR APPENDIX A

1. Courant, R. and Friedrichs, K. O., "Supersonic Flow and Shock Waves, Vol. I," Interscience Publishers, Inc., New York, 1948.
2. Herrmann, W. and Jones, A. H., "Survey of Hypervelocity Impact Information," A.S.R.L. Report No. 99-1, Aeroelastic and Structures Research Laboratory, MIT, September (1961).
3. Walsh, J. M., et al., Phys. Rev., 108, 196-216 (1957).
4. McQueen, R. G. and Marsh, S. P., J. Appl. Phys., 31, 1253-1269 (1960).
5. Walsh, J. M. and Rice, M. H., J. Chem. Phys., 26, 815-823 (1957).